

CHROMATIN-TARGETING DOMAINS AND THE DIVERGENCE OF HISTONE H3

by

KRISTINA LILLIAN MCBURNEY

B.Sc., The University of British Columbia, 2008

A THESIS SUBMITTED IN PARTIAL FULFILLMENT OF
THE REQUIREMENTS FOR THE DEGREE OF

DOCTOR OF PHILOSOPHY

in

THE FACULTY OF GRADUATE AND POSTDOCTORAL STUDIES
(Biochemistry and Molecular Biology)

THE UNIVERSITY OF BRITISH COLUMBIA
(Vancouver)

February 2016

© Kristina Lillian McBurney, 2016

ABSTRACT

NuA3 is one of the major histone H3 HATs in yeast, as its catalytic subunit, Sas3, is responsible for acetylation of K14 and 23. The only characterized chromatin-targeting domain within the HAT is the PHD finger of Yng1, which associates with H3K4me3 and directs NuA3 to the 5' ends of genes. We examined the genome-wide localization of Sas3, and found that it strongly correlates with H3K36me3. We demonstrated that recruitment of NuA3 to chromatin is dependent on methylation of both H3K4 and K36, and have implicated a novel member of the NuA3 complex – Pdp3 – as being responsible for this interaction. This likely occurs through its PWWP domain, which is a known H3K36me3-interactor in other proteins. In combination with the PHD finger of Yng1, this provides a mechanism by which NuA3 is recruited across the entirety of transcribed genes.

In addition to its PHD finger and PWWP domain, NuA3 also contains the YEATS domain of Taf14. This is a conserved eukaryotic domain of unknown function present exclusively in transcription-related complexes. Although evidence exists suggesting that YEATS domains in other proteins interact directly with histones, its role in the NuA3 complex has remained elusive. We confirmed that the YEATS domain functions in chromatin-targeting of NuA3, and that it interacts directly with H3K9, 18, and 27 acetylated peptides. Finally we showed that NuA3 recruitment is dependent on Gcn5. This work describes a novel mechanism by which acetylation by one HAT targets further acetylation by another, and provides an additional mechanism for recruitment of NuA3.

Finally, we explored the functional divergence of residues within histone H3 in yeast and humans. We showed that, while amino acids that define histone H3.3 are dispensable for yeast growth, substitution of residues within the histone H3 α 3 helix with their human counterparts resulted in a severe growth defect. Furthermore, these mutations resulted in altered nucleosome positioning, both *in vivo* and *in vitro*, which was accompanied by an increased preference for nucleosome positioning sequences. Taken together, this suggests that divergent residues within the histone H3 α 3 helix play differing roles in chromatin regulation between yeast and metazoans.

PREFACE

Chapter 2: This chapter is based on a first author manuscript currently in preparation. All experiments were designed by Dr. LeAnn Howe and Kristina McBurney. All experiments were performed by Kristina McBurney with the exception of those shown in Figures 2.8A and 2.8C which were performed by Julia Gomez Camblor and Dr. Vicki Maltby, respectively. Dr. Julie Brind'Amour helped in the construction of libraries for sequencing.

Chapter 3: This chapter is based on ongoing research to be made into a first author publication. All experiments were designed by Dr. LeAnn Howe and Kristina McBurney, and all experiments carried out by Kristina McBurney.

Chapter 4: This chapter is based on a first author manuscript published in the journal *Genetics* (McBurney, K., Leung, A., Choi, J.K., Martin, B.J., Irwin, N.A., Bartke, T., Nelson, C.J., and Howe, L.J. 2015. Divergent residues within histone H3 dictate a unique chromatin structure in *Saccharomyces cerevisiae*. *Genetics*. PMID 26534951). Experiments were designed by Dr. LeAnn Howe, Dr. Chris Nelson, Kristina McBurney, and Andrew Leung. Kristina McBurney conducted the majority of the experiments (Figures 4.1-4.4), while Andrew Leung of Dr. Chris Nelson's lab completed the *in vitro* analysis of nucleosome positioning (Figure 4.5). The dilution plates in Figures 4.1C and 4.1D were spotted by Nicholas Irwin and Jennifer Choi, respectively.

TABLE OF CONTENTS

ABSTRACT	ii
PREFACE	iii
TABLE OF CONTENTS	iv
LIST OF TABLES	vii
LIST OF FIGURES	viii
LIST OF ABBREVIATIONS	x
ACKNOWLEDGEMENTS	xiv
DEDICATION	xv
CHAPTER 1 – INTRODUCTION	1
1.1 CHROMATIN	1
1.2 HISTONE POST-TRANSLATIONAL MODIFICATIONS	3
1.3 HISTONE ACETYLATION	7
1.4 HISTONE METHYLATION.....	10
1.5 CHROMATIN-TARGETING DOMAINS.....	12
1.6 THE NUA3 HISTONE ACETYLTRANSFERASE COMPLEX	13
1.7 HISTONE VARIANTS	14
1.8 CHAPTER SUMMARIES	17
CHAPTER 2 – RECRUITMENT OF NUA3 TO CHROMATIN IS DEPENDENT ON H3K36ME3 AND THE PWWP PROTEIN PDP3	20
2.1 INTRODUCTION	20
2.2 MATERIALS AND METHODS	23
2.2.1 Yeast strains and plasmids.....	23
2.2.2 Chromatin immunoprecipitation (ChIP) for sequencing	25
2.2.3 Library preparation, Illumina sequencing, and data analysis	27
2.2.4 Immunoblot analysis.....	28
2.2.5 Modified chromatin immunoprecipitation (mChIP)	28
2.2.6 Chromatin immunoprecipitation and quantitative PCR (ChIP-qPCR).....	28
2.3 RESULTS.....	30
2.3.1 NuA3 preferentially binds di-nucleosomes	30
2.3.2 Sas3 occupancy peaks at +5 and +6 nucleosomes.....	32
2.3.3 Sas3 occupancy correlates with transcription and H3K4me3, but not H3K14ac or H3K23ac.....	35
2.3.4 Meta-analysis of Sas3 occupancy reveals strong correlation with H3K36me3.....	39
2.3.5 H3K4me3 and H3K36me3 are both required for efficient recruitment of NuA3	42
2.3.6 Identification of Pdp3 as a novel subunit of the NuA3 complex	45
2.3.7 Pdp3 and Yng1 function together to recruit NuA3 to chromatin	46

2.4 DISCUSSION AND CONCLUSIONS	50
CHAPTER 3 – THE YEATS DOMAIN OF TAF14 RECRUITS NUA3 TO CHROMATIN THROUGH INTERACTION WITH GCN5-TARGETED ACETYLATION	57
3.1 INTRODUCTION	57
3.2 MATERIALS AND METHODS	59
3.2.1 Yeast strains and plasmids.....	59
3.2.2 Immunoblot analysis.....	62
3.2.3 Peptide pulldowns	63
3.2.4 MODified histone peptide array	63
3.2.5 Chromatin immunoprecipitation and quantitative PCR (ChIP-qPCR).....	63
3.3 RESULTS.....	65
3.3.1 The YEATS domain of Taf14 mediates the interaction between NuA3 and histone H3.....	65
3.3.2 The YEATS domain of Taf14 interacts with acetylated H3K9, 18, and 27 <i>in vitro</i>	71
3.3.3 Sas3 occupancy shows weak but positive correlations with H3K9ac, H3K18ac, and H3K27ac.....	77
3.3.4 The YEATS domain of Taf14 recruits NuA3 to chromatin through interaction with Gcn5-deposited acetylation.....	79
3.3.5 Taf14 YEATS domain mutants do not show phenotypes indicative of loss of SWI/SNF or INO80 function	82
3.4 DISCUSSION AND CONCLUSIONS	84
CHAPTER 4 – DIVERGENT RESIDUES WITHIN HISTONE H3 DEFINE A UNIQUE CHROMATIN STRUCTURE IN <i>S. CEREVISIAE</i>	89
4.1 INTRODUCTION.....	89
4.2 MATERIALS AND METHODS	91
4.2.1 Yeast strains and plasmids.....	91
4.2.2 Chromatin association assay.....	92
4.2.3 Immunoblot Analysis	93
4.2.4 Micrococcal nuclease sequencing (MNase-seq).....	93
4.2.5 Analysis of MNase-seq data.....	94
4.2.6 In vitro analysis of nucleosome positioning	95
4.3 RESULTS.....	95
4.3.1 Histone H3.3-defining amino acids are dispensable for growth of <i>S. cerevisiae</i>	95
4.3.2 The α 3 helix of yeast histone H3 mediates nucleosome positioning <i>in vivo</i>	98
4.3.3 The human histone H3 α 3 helix enhances preference for nucleosome positioning sequences in <i>S. cerevisiae</i>	103
4.3.4 The α 3 helix of histone H3 influences nucleosome positioning <i>in vitro</i>	106
4.4 DISCUSSION AND CONCLUSIONS	108
CHAPTER 5 – CONCLUSIONS AND DISCUSSION	111
5.1 CHAPTER SUMMARY	111

5.2 GENERAL DISCUSSION.....	113
5.3 FUTURE DIRECTIONS.....	117
REFERENCES	120

LIST OF TABLES

Table 2.1: Yeast strains used in this study	23
Table 2.2: Plasmids used in this study	25
Table 2.3: Antibodies used in this study	26
Table 2.4: Primers used in this study.....	30
Table 3.1: Yeast strains used in this study	60
Table 3.2: Plasmids used in this study	61
Table 3.3: Antibodies used in this study	62
Table 3.4: Primers used in this study.....	65
Table 4.1: Yeast strains used in this study	91
Table 4.2: Plasmids used in this study	91
Table 4.3: Antibodies used in this study	93

LIST OF FIGURES

Figure 1.1: Histone post-translational modifications in <i>S. cerevisiae</i>	5
Figure 1.2: Yeast histone H3 is more closely related to the human histone H3 variant H3.3, than to H3.1 or H3.2	17
Figure 2.1: Sas3 preferentially binds di-nucleosomes	32
Figure 2.2: Sas3 occupancy peaks at +5 and +6 nucleosomes	34
Figure 2.3: Sas3 occupancy does not correlate with H3K14 or K23 acetylation	37
Figure 2.4: Sas3 occupancy correlates with H3K4me3 and RNAPII occupancy	38
Figure 2.5: Meta-analysis of Sas3 occupancy reveals strong positive correlation with H3K36me3 ..	40
Figure 2.6: Meta-analysis of Sas3 occupancy reveals strong positive correlation with H3K36me3 ..	41
Figure 2.7: Sas3 occupancy is highly positively correlated with H3K36me3.....	42
Figure 2.8: H3K4 and K36 methylation are both required for efficient recruitment of Sas3 to chromatin.....	44
Figure 2.9: The association of Pdp3 with NuA3 is dependent on Eaf6 and Yng1	45
Figure 2.10: Deletion of <i>PDP3</i> results in a synthetic growth defect in combination with deletion of <i>GCN5</i> and loss of the PHD finger of <i>YNG1</i>	47
Figure 2.11: The PWWP domain of Pdp3 possesses the conserved residues that make up the H3K36me3-binding pocket of other PWWP domain proteins.....	49
Figure 2.12: Pdp3 mutants with mutations in the residues making up the methyl-binding pocket are not toxic in a <i>gcn5Δ yng1ΔPHD</i> strain	50
Figure 3.1: Deletion of <i>TAF14</i> results in a synthetic lethal phenotype in combination with deletion of <i>GCN5</i> and the PHD finger of <i>YNG1</i>	66
Figure 3.2: Conserved residues within the YEATS domain of Taf14.....	68
Figure 3.3: Taf14 YEATS domain mutants have no growth defects on their own or in a <i>gcn5Δ yng1ΔPHD</i> strain under regular growth conditions	69
Figure 3.4: Taf14 YEATS domain mutants impair the interaction between Sas3 and histone H3	71
Figure 3.5: The YEATS domain of Taf14 interacts with H3K9, 18, and 27 acetylated peptides	74
Figure 3.6: The YEATS domain of Taf14 interacts with a common R-Kac motif unique to H3K9, 18, and 27	76
Figure 3.7: Sas3 occupancy shows weak but positive correlations with H3K9, 18, and 27 acetylation.	78
Figure 3.8: Gcn5 is required for efficient recruitment of NuA3 to <i>COX10</i>	80

Figure 3.9: H3K14 and K23 are targets of Sas3 HAT activity.....	82
Figure 3.10: The YEATS domain of Taf14 is not essential for SWI/SNF or INO80 function	83
Figure 4.1: Histone H3.3-defining amino acids are dispensable for growth in <i>S. cerevisiae</i>	97
Figure 4.2: Mutation of the histone H3 α 3 helix confers a growth defect in yeast that is not due to impaired histone deposition.....	99
Figure 4.3: The α 3 helix of yeast histone H3 mediates nucleosome positioning	102
Figure 4.4: The human histone H3 α 3 helix enhances preference for nucleosome positioning sequences in <i>S. cerevisiae</i>	105
Figure 4.5: The α 3 helix of histone H3 affects nucleosome positioning <i>in vitro</i>	107

LIST OF ABBREVIATIONS

α	Alpha – signifies anti
Δ	Delta – signifies deletion
$^{\circ}\text{C}$	Degree celcius
5-FOA	5-Fluoroorotic acid
6-AU	6-Azaauracil
Ac	Acetylated
Acetyl-CoA	Acetyl coenzyme A
ATP	Adenosine triphosphate
bp	Base pair
BWA	Burrows-Wheeler aligner
ChIP	Chromatin immunoprecipitation
ChIP-chip	Chromatin immunoprecipitation followed by microarray
ChIP-qPCR	Chromatin immunoprecipitation followed by quantitative PCR
ChIP-seq	Chromatin immunoprecipitation followed by sequencing
Chr	Chromosome
COMPASS	Complex proteins associated with Set1
CTD	C-terminal domain
C-terminal	Carboxy-terminal
DNA	Deoxyribonucleic acid
DNase	Deoxyribonuclease
dNTP	Deoxynucleoside triphosphate
g	Gravity
GST	Glutathione S-transferase
H2BK123	Histone H2B lysine 123
H3K4	Histone H3 lysine 4
H3K9	Histone H3 lysine 9
H3K14	Histone H3 lysine 14
H3K18	Histone H3 lysine 18

H3K23	Histone H3 lysine 23
H3K27	Histone H3 lysine 27
H3K36	Histone H3 lysine 36
H3S10	Histone H3 serine 10
<i>H. sapien</i>	Homo sapien
HAT	Histone acetyltransferase
HDAC	Histone deacetylase
HDM	Histone demethylase
HMT	Histone methyltransferase
HU	Hydroxyurea
IgG	Immunoglobulin G
mChIP	Modified chromatin immunoprecipitation
me	Methylated
me3	Tri-methylated
mg	Milligram
mL	Millilitre
mM	Millimolar
MMS	Methyl methanesulfonate
MNase	Micrococcal nuclease
MORF	MOZ related factor
MOZ	Monocytic leukemic zinc finger protein
MYST	MOZ-YBF2(SAS3)-SAS2-TIP60
NDR	Nucleosome depleted region
Nm	Nanometre
NMR	Nuclear magnetic resonance
N-terminal	Amino-terminal
NuA3	Nucleosome acetyltransferase for histone H3
NuA4	Nucleosome acetyltransferase for histone H4
OD ₆₀₀	Optical density at 600 nm
PBS	Phosphate-buffered saline

PCR	Polymerase chain reaction
PHD	Plant homeodomain
PIC	Pre-initiation complex
Poly(A)	Poly-adenylated
PTM	Post-transcriptional modification
PWWP	Proline-Tryptophan-Tryptophan-Proline
RC	Replication-coupled
rDNA	Ribosomal DNA
RI	Replication-independent
RNA	Ribonucleic acid
RNAPII	RNA polymerase II
RNase	Ribonuclease
rpm	Rotations per minute
rRNA	Ribosomal RNA
r_s	Spearman correlation
RSC	Remodels structure of chromatin
<i>S. cerevisiae</i>	Saccharomyces cerevisiae
<i>S. pombe</i>	Saccharomyces pombe
SAGA	Spt-Ada-Gcn5-acetyltransferase
SANT	Swi3-Ada2-N-cor-TFIIB
SDS-PAGE	Sodium dodecyl sulfate polyacrylamide gel electrophoresis
SWI/SNF	Mating type switching/Sucrose non-fermenting
TAP	Tandem affinity purification
TBP	TATA-binding protein
TE	Tris-EDTA
TSA	Trichostatin A
TSS	Transcription start site
U	Unit
WCE	Whole cell extract
YEATS	Yaf9-ENL-AF9-Taf14-Sas5

YPD	Yeast extract-peptone-dextrose
μL	Microliter
μM	Micromolar

ACKNOWLEDGMENTS

First and foremost, I would like to thank my supervisor, Dr. LeAnn Howe, for her guidance and support throughout the course of my graduate studies. In many ways I was not the ideal graduate student, but your faith and reassurance in my abilities provided me with the determination to succeed. I am especially grateful for the encouragement and support you have shown towards my future pursuits in teaching; the opportunities you have provided in this regard will always be greatly appreciated.

I would like to thank past and present members of my laboratory: Jennifer Choi, Adam Chruscicki, Nicolas Coutin, and Vicki Maltby. I wouldn't have been able to complete this degree without your shared knowledge and support. I would also like to extend a special thanks to Benjamin Martin for the many hours he invested in attempting to teach me how to analyse my sequencing data, and the subsequent hours he then spent analysing it for me. Ben, without your help I would still be stuck in my office trying to figure out the difference between and bed and bam file. I would also like to extend my gratitude to my supervisory committee, Dr. Ivan Sadowski and Dr. Michael Kobor, for the mentorship and scientific insights they have provided throughout my time here.

I would like to thank my family and friends. To my parents, Allan and Sandra McBurney: I could never have completed this degree without your endless emotional support. Thank you for challenging me during the highs and encouraging me during the lows. I would also like to extend my gratitude to my colleagues Wendy Barretto, Nathan Belliveau, Julien Bergeron, Carol Chen, Julienne Jagdeo, Stuart Malcolm, Aym Moosa, and Jenna Riffel for their perpetual willingness to accompany me to Mahony's. Lastly I would like to extend an extra special thank you to Elizabeth Donohue who supported me through both the laughter and the tears. These are the memories of graduate school that I will keep with me forever.

DEDICATION

I would like to dedicate this thesis to my mother, Sandra McBurney, for her endless support and encouragement throughout my entire education. Mom, you've had to deal with my frustration, my disappointments, and my psychosis. There is no way I could have done it without you.

CHAPTER 1:

Introduction

1.1 Chromatin

DNA is a complex cellular molecule that encodes the genetic information necessary for the development and functioning of all living organisms. Each molecule of DNA consists of two nucleotide polymers (composed of repeating units of a nitrogenous base, a deoxyribose sugar, and a phosphate group) wound around one another to form a double helix. Although eukaryotic DNA is segmented into chromosomes, genomes can range in size from 2.3 million base pairs to 1400 billion base pairs of DNA (Vivarès and Méténier 2000; Corradi *et al.* 2010). Given that an average nucleotide measures approximately 0.6 nm, this means that if all chromosomes were to be placed end to end, the DNA of some organisms would measure upwards of 800 meters (Smith *et al.* 1996). Consequently, the cell requires an efficient means of packaging DNA into the microscopic space of the nucleus.

In order to facilitate such a high degree of packaging, DNA is organised into an ordered structure known as chromatin – a nucleoprotein structure consisting of DNA, histones, and non-histone proteins. The basic repeating unit of chromatin is the nucleosome which is composed of 147 base pairs of DNA wound around two copies each of histones H2A, H2B, H3, and H4 (Luger *et al.* 1997). Nucleosomes are separated by varying lengths of linker DNA, producing a “beads on a string” structure that is 10 nm in diameter. In addition to the core histones, histone H1 – known as the linker histone – contacts the entry and exit points of nucleosomal DNA, resulting in further compaction (Zhou *et al.* 1998). The combination of a nucleosome with a linker histone, known as a chromatosome, was originally thought to form a helical 30 nm diameter structure known as the 30 nm fibre (Finch and Klug 1976). In addition to histone-DNA interactions, internucleosomal contacts are also thought to contribute to chromatin compaction. Perhaps one of the best examples of this is interaction of the positively charged N-terminal tail of histone H4 with an acidic patch of H2A on a neighbouring nucleosome (Dorigo *et al.* 2003; Kan *et al.* 2009; Sinha and

Shogren-Knaak 2010). This interaction between the H4 tail of one nucleosome and the globular domain of H2A on the next is thought to contribute to the formation of the 30 nm fibre. Nevertheless, despite the myriad of data supporting the existence of higher order levels of chromatin structure such as the 30 nm fibre, there is still debate as to whether they truly exist as organized, distinct states, or whether their organization is more dynamic (Woodcock and Ghosh 2010; Maeshima *et al.* 2010).

Traditionally, regions of chromatin in a highly condensed state were referred to as heterochromatin, and were identified based on their tendency to stain darkly under the microscope (Angell and Jacobs 1975). Conversely, less compact regions were referred to as euchromatin, and identified based on their tendency to stain lightly. More recently the definitions of heterochromatin and euchromatin have been modified to describe transcriptionally repressive or transcriptionally active regions of the genome, respectively. In the budding yeast, *Saccharomyces cerevisiae*, euchromatin makes up the vast majority of the genome, while heterochromatin is restricted to the two silent mating type loci (*HMR* and *HML*), the telomeres, and the rRNA-encoding DNA (Rusche *et al.* 2003). The increased nucleosome occupancy and higher degree of compaction found within heterochromatin directly influence the repressive state of these regions, as they create barriers to transcription, replication, and other DNA-related processes. In order to overcome nucleosome obstructions during these processes, the cell requires a mechanism by which these obstacles can be temporarily displaced. Fortunately, several of these mechanisms exist. One known system by which chromatin structure is regulated is through the post-translational modification of histones which can modify chromatin structure directly or indirectly by acting as docking sites for chromatin-modifying complexes (Peterson and Laniel 2004). Some of these chromatin-modifying complexes include chromatin remodelers, which use the energy derived from ATP hydrolysis to physically slide or evict nucleosomes (Hargreaves and Crabtree 2011). Other chromatin-modifying complexes are involved in the deposition of histone variants which alter the stability of the nucleosome (Weber and Henikoff 2014). In more complex eukaryotes, DNA methylation also acts to regulate chromatin structure

either by physically preventing the binding of chromatin-modifying complexes or recruiting other chromatin-modifying complexes (Bird and Macleod 2004). Together these mechanisms tightly regulate the accessibility of DNA to the transcriptional and replicational machinery.

The budding yeast, *Saccharomyces cerevisiae*, is an ideal model organism for the study of chromatin and chromatin-related processes. Although it is considered a simple eukaryote, many essential cellular processes are conserved between yeast and humans. Indeed, it is estimated that about one-third of its genes encode proteins with homologues in humans, making it ideal for the study of cellular processes in higher eukaryotes (Botstein *et al.* 1997). Yeast also have the advantage of possessing genomes that are easily manipulated, allowing for greater flexibility in experimental design. As an example, two independent genetic screens in yeast led to the identification of the chromatin remodeler Swi/Snf long before the discovery of its human counterpart, the Brg1-Associated Factors (BAF) (Carlson *et al.* 1981; Stern *et al.* 1984; Wang *et al.* 1996).

1.2 Histone Post-Translational Modifications

Early work exploring the function of histones led to the discovery that these proteins can be acetylated and methylated (Allfrey, Faulkner, and Mirsky 1964). Since these initial experiments, numerous other histone post-translational modifications (PTMs) have been identified, including but not limited to phosphorylation, ubiquitination, citrullination, and sumoylation (Goldknopf and Busch 1977; Mahadevan *et al.* 1991; Shiio and Eisenman 2003; Thompson and Fast 2006). The majority of these modifications occur on the unstructured N-terminal tails of histones which make up 25-30% of the mass of the proteins (Figure 1.1) (Strahl and Allis 2000). Acetylation of histone H4, for example, occurs solely at lysines 5, 8, 12, and 16, all of which are found on its N-terminal tail. Nevertheless, PTMs can also be found within the globular domain of histone H3, and within the C-terminal tails of histones H2A and H2B. Early models suggested

that these modifications alter chromatin structure by influencing histone-DNA and histone-histone contacts, while more recent research suggests that their ability to recruit various chromatin-modifying complexes may play a larger role in this function (Strahl and Allis 2000).

The histone code hypothesis was first published in 2000, and posits that histone PTMs act in combination to elicit specific downstream functions (Strahl and Allis 2000). If correct, the code has the potential to be incredibly complex, as each copy of the four core histones can simultaneously be modified at multiple sites with multiple different modifications. As an example, in *S. cerevisiae* there are 14 lysines that can be acetylated and 3 lysines that can be methylated across histones H2A, H2B, H3, and H4 (excluding acetylation of H3K4 and K36). As each of the acetylated residues can be acetylated or unmodified, and each of the methylated residues can be un-, mono-, di-, or tri-methylated, there is the potential for $4^3 \times 2^{14}$ - or over 1 million – independent combinations of acetylation and methylation on these histones. This far outnumbers the approximately 60,000 nucleosomes in yeast, and doesn't even take into consideration the second copy of each histone or the numerous other histone PTMs that exist. Because of this complexity, the extent to which combinatorial patterns of histone modifications exist throughout the genome has been explored. A study examining the patterns of 39 different histone modifications across the genome of human CDC4+ T cells established that of just over 4300 different patterns identified at promoters, approximately 1100 are associated with multiple genes (Wang *et al.* 2008). Furthermore, a set of 17 modifications was found at the promoters of 3,286 genes, while less than 400 promoters possessed only 16 of the modifications. This suggests that combinatorial patterns of histone modifications are common and widespread.

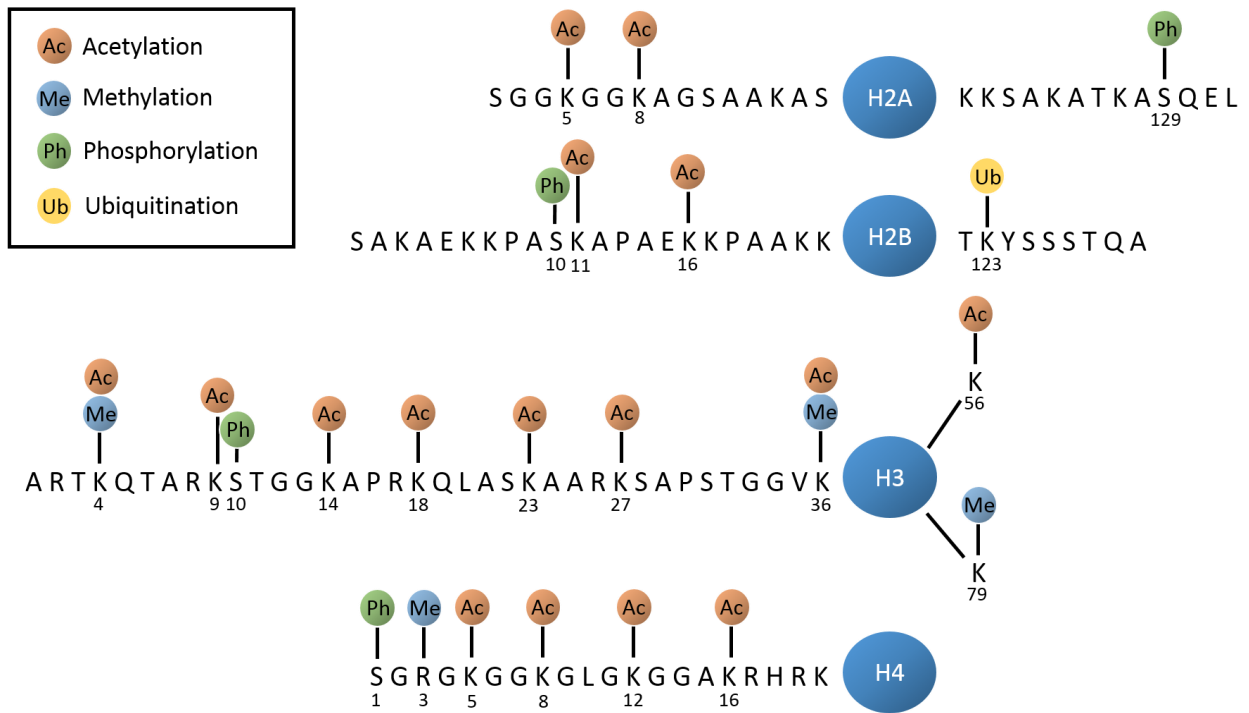


Figure 1.1: Histone post-translational modifications in *S. cerevisiae*. Schematic representation of modified residues within the four core histones. Note that the conventional numbering system differs for H2A, in which residue “1” refers to the post-translationally cleaved methionine, whereas all other histones are numbered with residue “1” referring to the first residue after the cleaved methionine. The presence of two modifications on a single residue implies that the residue can be modified in either way.

Even so, in order for the histone code hypothesis to be correct, histone PTMs need to function in combination. More precisely, recognition of a given combination of modifications by a chromatin-modifying or other transcription related complex must lead to a distinct outcome from that which would occur for either modification alone; however ambiguity exists even within this definition. If a complex is able to bind to either of two histone PTMs on its own, but binding to both results in an additive affinity, is this a code? Or must the effect be “all or nothing”, where binding is only observed in the presence of both modifications? This issue remains hotly debated in the field of chromatin biology, as examples of both

exist. For example, the human chromatin-remodeling factor BPTF contains a bromodomain and PHD finger that independently bind to H4K16ac and H3K4me3 respectively, but which bind with a two-fold increased affinity to a H3K4me3/H3K16ac peptide over the H3K4me3 peptide alone (Ruthenburg *et al.* 2011). Conversely, mouse Brdt - a homolog of the TFIID subunit Taf1 – binds strongly to H4K5ac/K8ac peptides, but shows no affinity for either individually modified peptide (Morinière *et al.* 2009). Similarly, the Arabidopsis CMT3 methyltransferase specifically binds H3K9me3/K27me3, but not to either individually methylated lysine (Lindroth *et al.* 2004). Certainly then, an increasing body of evidence supports the idea that combinations of histone PTMs can function additively *or* absolutely to recruit a variety of chromatin-modifying complexes. Thus, although the exact definition of the code remains controversial, evidence supports the basic hypothesis that histone modifications are capable of functioning in combination to recruit proteins through multivalent binding (Rando 2012).

The real debate concerning the histone code surrounds the final claim of the hypothesis – that PTMs act in combination to produce a specific downstream *function*. Functional studies examining transcriptional output in strains lacking specific histone PTMs, or combinations thereof, show little effect on gene expression (Martin 2004; Dion *et al.* 2005). For example, despite the universal targeting of H3K4me3 to the 5' ends of actively transcribed genes, mutation of H3K4 or its methyltransferase results in transcription profiles that are almost indistinguishable from wild type (Lenstra *et al.* 2011). Furthermore, the transcriptional responses that are observed for one PTM mutant are generally little different from that of other PTMs or combinations of PTMs (Martin 2004; Dion *et al.* 2005). Similar results have also been observed in strains harbouring deletions of genes encoding chromatin-modifying factors (Lindstrom *et al.* 2006). For example, although Polycomb group proteins are found at the promoters of key developmental regulators in embryonic stem cells, knockdown of Polycomb proteins do not result in upregulation of these genes (Rando 2012). Numerous arguments defending these behaviours have been proposed, including the possibility that transcription is not the relevant downstream function, or that

certain modifications may “poise” genes for future activation or repression and thus an immediate transcriptional response would not be expected (Rando 2012). Nonetheless, the link between the binding of chromatin regulatory complexes and downstream function remains a much debated issue surrounding the validity of the histone code.

1.3 Histone Acetylation

As early as 1964, Allfrey, Faulkner, and Mirsky demonstrated a link between histone acetylation and transcription, suggesting that acetylation functions as a “a dynamic and reversible mechanism for activation as well as repression of RNA synthesis” (Allfrey, Faulkner, and Mirsky 1964). More than three decades later, two breakthrough articles revealed that Gcn5 and Rpd3 – a known transcriptional co-activator and co-repressor, respectively – were in fact a histone acetyltransferase and histone deacetylase (Brownell *et al.* 1996; Taunton *et al.* 1996). This provided the first clear connection between histone acetylation and transcriptional regulation. Much work has gone into elucidating the mechanism by which this occurs, leading to the discovery that acetylation prevents the formation of higher order chromatin structures *in vitro*, and contributes to increased accessibility of DNA *in vivo* (Hebbes *et al.* 1994; Garcia-Ramirez *et al.* 1995; Krajewski and Becker 1998; Tse *et al.* 1998). Histone acetylation is thought to contribute to this opening of chromatin structure through two independent mechanisms. First, it’s thought to destabilize nucleosome structure by weakening contacts between the negatively charged phosphate backbone of DNA and the positively charged N-terminal tails of histones by neutralizing the positive charge of lysine residues. (Hong *et al.* 1993; Lee *et al.* 1993). Secondly, it can act as a docking site for chromatin-modifying complexes. One well characterized example of this is H3K14ac which recruits the RSC chromatin remodelling complex to genes through association with one of the two bromodomains of

Rsc4 (Ferreira *et al.* 2007). Both of these mechanisms contribute to an altered chromatin structure that increases the accessibility of DNA to the transcriptional machinery.

Histone acetylation occurs primarily at promoters, where it functions in transcription initiation. (Schübeler *et al.* 2004; Kurdistani *et al.* 2004; Pokholok *et al.* 2005; Barski *et al.* 2007; Wang *et al.* 2008). Promoter acetylation generally occurs through recruitment of histone acetyltransferase (HAT) complexes by transcriptional activators. One of the first discovered examples of this is recruitment of the Gcn5 HAT complex to promoters by the transcriptional activator Gcn4, which has been shown to be required for gene activation (Kuo *et al.* 1998, 2000). A similar mechanism exists for recruitment of the NuA4 HAT complex (Robert *et al.* 2004). In addition to promoters, acetylation is also targeted to gene bodies through several different mechanisms (Schübeler *et al.* 2004; Kurdistani *et al.* 2004; Pokholok *et al.* 2005; Barski *et al.* 2007; Wang *et al.* 2008). Independent of their recruitment to promoters, Gcn5 and NuA4 are also localized to transcribed regions through physical interaction with transcription-dependent phosphorylation of serine 5 on the CTD of elongating RNAPII (Govind *et al.* 2007; Ginsburg *et al.* 2009). Recruitment of HATs through the phosphorylated CTD of RNAPII has also been shown in humans for the PCAF histone acetyltransferase complex (Obrdlik *et al.* 2008). A second potential mechanism for the recruitment of HATs to transcribed regions of the genome is through H3K4 and H3K36 methylation. The methyltransferases responsible for these modifications, Set1 and Set2, associate with the elongating RNAPII CTD through phosphorylation of serine 5 and serine 2, respectively (Krogan *et al.* 2003a). This results in a trail of methylation in the wake of elongating RNAPII, which can act as docking sites for a number of different HAT complexes (Shi *et al.* 2006a; b; Martin *et al.* 2006b; Taverna *et al.* 2006; Bian *et al.* 2011). One example of this is H3K4me₃, which has been shown to interact with a PHD finger domain within the NuA3 complex, resulting in its recruitment to - and activity at - actively transcribed genes (Martin *et al.* 2006b; Taverna *et al.* 2006). Finally, histone acetylation can be targeted to both promoters and transcribed regions through histone turnover (Rufiange *et al.* 2007).

Histone acetyltransferases are generally conserved complexes that consist of a catalytic subunit and auxiliary proteins required for enzymatic activity and targeting. In *S. cerevisiae*, seven proteins with HAT activity exist, four of which acetylate H3 as a substrate (Gcn5, Sas3, Rtt109, and Elp3) (Grant *et al.* 1997; Howe *et al.* 2001; Winkler *et al.* 2002; Han *et al.* 2007). The majority of HATs acetylate multiple sites, often with targets overlapping those of other HAT complexes. As an example, Gcn5, the catalytic subunit of SAGA, SLIK/SALSA, and ADA, has been shown to acetylate H3K14, as well as a number of other H3, H2A, and H2B targets (Kuo *et al.* 1996; Grant *et al.* 1997). However, Sas3, the catalytic subunit of the NuA3 histone acetyltransferase complex also targets this residue in addition to H3K23 (Howe *et al.* 2001). Clearly then, HATs function in a complex dance, working together to regulate chromatin structure and transcription.

Histone acetylation is a dynamic mark with a relatively short half-life due to the existence of histone deacetylase complexes (HDACs). Similar to HATs, HDACs are also multi-protein complexes with catalytic subunits that can deacetylate multiple targets. In *S. cerevisiae*, ten HDACs exist (Hda1, Rpd3, Hos1, Hos2, Hos3, Sir2, Hst1, Hst2, Hst3, and Hst4) all of which deacetylate specific sets of genes and regions of the genome (Kurdistani and Grunstein 2003; Li *et al.* 2013a). Some of these are recruited specifically to promoters, presumably to help shut down transcription. A well characterized example of this is the Rpd3L HDAC, which is recruited to promoters through association with the DNA-binding protein Ume6 (Rundlett *et al.* 1998; Kadosh and Struhl 1998). Nonetheless, HDACs are also found throughout coding regions, often functioning in an effort to repress transcription from cryptic promoters. For example, in addition to its role at promoters, Rpd3 also functions within transcribed regions as part of the Rpd3S complex. This complex is recruited through phosphorylation of the CTD of elongating RNAPII and its activity stimulated by H3K36me₃, resulting in rapid removal of acetylation towards the mid to 3' ends of genes (Li *et al.* 2009a; Drouin *et al.* 2010).

1.4 Histone Methylation

It was in the same landmark work demonstrating histone acetylation in 1964 that histones were also discovered to be methylated (Allfrey, Faulkner, and Mirsky 1964). This modification can occur in mono-, di-, or tri-states on the ϵ -amino group of lysine, or in mono- or di-states on the guanidino group of arginine. In *S. cerevisiae*, lysine methylation occurs only at K4, K36, and K79 of histone H3, and is catalyzed by the histone methyltransferases (HMTs) Set1, Set2, and Dot1, respectively. Although in more complex eukaryotes histone methylation is associated with both transcription and repression, in yeast this modification is a marker of active transcription.

Although Set1 is the catalytic HMT responsible for H3K4 methylation, it functions as part of the larger COMPASS (Complex of Proteins Associated with Set1) which includes a number of auxiliary proteins required for transition between the three methylation states (Miller *et al.* 2001; Schneider *et al.* 2005). Genome-wide localization studies place H3K4me3 at the 5' ends of transcriptionally active genes, suggesting that this modification may be linked to transcription elongation (Schübeler *et al.* 2004; Bernstein *et al.* 2005; Pokholok *et al.* 2005; Barski *et al.* 2007). Indeed, COMPASS associates with elongating RNAPII when its CTD is phosphorylated at serine 5 (Ng *et al.* 2003). This interaction is dependent on the PAF (Polymerase Associated Factor) complex, which is thought to act as a bridge, linking the methyltransferase and the polymerase (Krogan *et al.* 2003a). Since phosphorylation of serine 5 by the TFIIF-associated kinase Kin28 occurs during promoter escape, and dephosphorylation of this residue by Rtr1 occurs during early elongation, the pattern of H3K4me3 follows suit peaking at the 5' end of genes (Rodriguez *et al.* 2000; Mosley *et al.* 2009). As discussed in the previous section, methylation of H3K4 and K36 can act as platforms for recruitment of chromatin regulatory complexes such as HATs, presumably to maintain a chromatin structure permissible to multiple rounds of transcription (MacDonald and Howe 2009). Although histone methylation was once thought of as a stable mark, the dynamic nature of this

modification became apparent upon discovery of the existence of histone demethylases (HDM). In *S. cerevisiae*, Jhd2 is the HDM responsible for demethylation of H3K4 (Liang *et al.* 2007; Seward *et al.* 2007). Its activity is negatively regulated by the presence of H3K14ac, ensuring that methylation is only removed following gene inactivation (Maltby *et al.* 2012b).

Unlike Set1, Set2 functions independently of other proteins to methylate H3K36. Genome-wide localization studies of H3K36me3 show that this modification is enriched further into gene bodies than H3K4me3 (Schübeler *et al.* 2004; Bernstein *et al.* 2005; Pokholok *et al.* 2005; Barski *et al.* 2007). Similar to methylation by COMPASS, this pattern of H3K36 methylation is a result of the passage of elongating RNAPII, as Set2 interacts directly with serine 2 phosphorylation on the CTD (Fuchs *et al.* 2012). As serine 2 is not phosphorylated by Ctk1 until elongation is underway, this explains the later enrichment in H3K36me3 compared to H3K4me3 (Cho *et al.* 2001). This pattern of deposition has important consequences for initiation of transcription from cryptic promoters within the gene body of actively transcribed genes. These promoters are normally inaccessible to the transcriptional machinery due to unfavorable nucleosome positioning, but become activated following RNAPII elongation if chromatin structure is not restored. As previously discussed, Eaf3, one of the members of the Rpd3S histone deacetylase complex, contains a chromodomain that recognizes H3K36me3, resulting in stimulation of its activity and removal of histone acetylation (Li *et al.* 2009a). This restores chromatin structure within gene bodies, and prevents these cryptic promoters from initiating transcription (Carrozza *et al.* 2005; Keogh *et al.* 2005; Joshi and Struhl 2005). H3K36 methylation can also act as a beacon to recruit chromatin-modifying factors, as previously discussed.

1.5 Chromatin-Targeting Domains

Histone modifications can be deposited or removed by various chromatin-modifying complexes. These “writers” and “erasers” of chromatin modifications include HATs, HMTs, HDACs, HDMs, and numerous other complexes. “Readers” of histone modifications also exist, which bind to chromatin through histone PTM recognition domains in order to facilitate chromatin targeting or stimulate complex activity. The complex interplay of these chromatin readers is critical in the regulation of chromatin structure and transcription. Although the existence of chromatin readers has long been hypothesized, the first example was not identified until 1999 when the bromodomain of the human PCAF HAT complex was discovered to recognize acetylated histones (Dhalluin *et al.* 1999). Since then a number of different readers of histone modifications have been identified, including those that recognize acetylation, methylation, phosphorylation, and several other PTMs. Chromatin regulatory complexes often contain multiple readers within one or many subunits that each show specificity for a particular histone PTM. One example of this which will be discussed in great detail within this thesis is the NuA3 histone acetyltransferase complex. This HAT contains three chromatin-targeting domains – a PHD finger, a PWWP domain, and a YEATS domain – which recognize H3K4me3, H3K36me3, and H3K9ac, respectively (Martin *et al.* 2006b; Taverna *et al.* 2006; Gilbert *et al.* 2014; Shanle *et al.* 2015). This type of combinatorial readout of histone modifications can have two functions. First, the interaction between PTMs and readers may be cumulative, increasing in strength with each additional interaction. For example, the mammalian chromatin remodeler BPTF contains a PHD finger and bromodomain which recognize H3K4me3 and H4K16ac, respectively, and which function together to increase binding by two-fold over either of the individual domains (Li *et al.* 2006). Secondly, the interactions between multiple readers and their respective PTMs may be required for complex recruitment in an “all or nothing” manner. Although this has been described for individual chromatin-targeting domains, such as the previously described chromodomain of the Arabidopsis CMT3 methyltransferase, this has yet to be observed for multiple

domains within the same complex (Lindroth *et al.* 2004). Nonetheless, many researchers believe that it's a combination of both these mechanisms that regulate the recruitment of chromatin-modifying complexes throughout eukaryotes.

Readers of histone methylation are the largest and most thoroughly characterized group of histone PTM readers. The most well studied members of this group include the chromodomain, MBT (Malignant Brain Tumor) domain, PHD (Plant HomeoDomain) finger, PWWP (Pro-Trp-Trp-Pro) domain, Tudor domain, and WD40 domain. To date, all known methyl-lysine binding domains consist of an aromatic cage, formed by two to four aromatic residues (Musselman *et al.* 2012). Specificity for a particular site is imparted by surrounding residues of both the aromatic cage and target histone residue, although not all methyl-readers display the same degree of specificity. Unlike the large family of methyl-histone readers, the bromodomain spent most of the last two decades known as the only histone acetyl-targeting domain. More recently a handful of additional acetyl readers have been identified, including the double PHD finger (DPF) domain of human Dpf3b, the double pleckstrin homology (PH) domain of yeast Rtt106, and (as will be discussed in Chapter 4) the YEATS domain of human AF9 (Zeng *et al.* 2010; Su *et al.* 2012; Li *et al.* 2014). These domains contain no common structural recognition motif, and similar to histone methyl-readers, vary in the degree of their specificity and promiscuity (Musselman *et al.* 2012).

1.6 The NuA3 Histone Acetyltransferase Complex

SAS3 was first identified as a homolog of SAS2 in a screen aimed at determining regulators of silencing in yeast (Reifsnnyder *et al.* 1996). It was soon after revealed to encode a HAT belonging to the MYST family of histone acetyltransferases along with human Tip60, MOZ, MORF, HBO1 and MOF, and yeast Sas2 and Esa1 (Takechi and Nakayama 1999). Similar to many HATs, Sas3 functions as part of a larger complex known as NuA3 (Nucleosome Acetyltransferase of H3) along with five additional subunits (Eaf6, Nto1,

Pdp3, Taf14, and Yng1) that are thought to be involved in chromatin targeting and complex stability (John *et al.* 2000; Howe *et al.* 2002; Taverna *et al.* 2006; Gilbert *et al.* 2014). The complex acetylates the N-terminal tail of histone H3 at lysines 14 and 23, and is thought to be closely related to mammalian MOZ and MORF (Howe *et al.* 2001; Taverna *et al.* 2006; Avvakumov and Côté 2007b). Until recently, the only characterized mechanism of NuA3 recruitment was through interaction of the PHD finger of Yng1 with H3K4me3 (Martin *et al.* 2006b; Taverna *et al.* 2006). Interestingly, recruitment of the HAT to chromatin is also dependent on H3K36me3, suggesting the presence of at least one additional chromatin-targeting domain within the complex (Martin *et al.* 2006a).

In addition to the PHD finger of Yng1, the NuA3 complex contains four other potential chromatin-targeting domains: two PHD fingers in Nto1, a PWWP domain in Pdp3, and a YEATS domain in Taf14 (Taverna *et al.* 2006). The PWWP domain is a known methyl histone binding domain that generally has strong specificity for H3K36me3, making it a strong candidate for the additional chromatin-targeting domain within the HAT complex (Vezzoli *et al.* 2010; Dhayalan *et al.* 2010; Wu *et al.* 2011; Maltby *et al.* 2012a; van Nuland *et al.* 2013; Li *et al.* 2013b). Furthermore, the YEATS domain has long been thought to be involved in recruitment to chromatin, and more recently has been shown to be a reader of histone acetylation in higher eukaryotes (Li *et al.* 2014). The mechanisms regulating recruitment of chromatin regulatory complexes is often complex, suggesting that either or both of these reader domains may be involved in targeting NuA3 to specific regions of the genome.

1.7 Histone Variants

In addition to the core histones that make up a canonical nucleosome, non-allelic forms - known as histone variants - also exist. These non-conventional histones in most cases differ from their canonical counterparts by only a few residues, but play an important role in regulating chromatin structure,

transcription, DNA repair, and chromosome dynamics. In *S. cerevisiae*, only two variants exist outside of the canonical histones H2A, H2B, H3, and H4. This includes H2A.Z, an H2A variant, and Cse4, an H3 variant that exclusively replaces H3 at centromeric nucleosomes. In metazoans, including humans, four major histone variants have universally been identified: CENP-A (the centromeric H3), H3.3, H2A.Z, and H2A.X. Humans also differ from yeast in that they contain two canonical versions of H3, H3.1 and H3.2, that differ by only a single amino acid. Canonical histones are almost exclusively expressed during S-phase, and deposited onto chromatin in a replication-dependent manner, while variants are expressed throughout the cycle and deposited independently of DNA replication.

Histone variants are typically thought to regulate chromatin dynamics by two main mechanisms. First, post-translational modifications that are unique to variants have been shown to produce specific outcomes. An example of this is phosphorylation of S139 in H2A.X upon DNA damage, which facilitates the recruitment of chromatin remodelers and proteins involved in the DNA damage response (Morrison *et al.* 2004; van Attikum *et al.* 2004; Biterge and Schneider 2014). Several PTM sites within CENP-A have also been identified that are suggested to influence the confirmation of centromeric chromatin. Phosphorylation of several sites within its N-terminal tail, for example, have been shown to be required for mitotic progression (Goutte-Gattat *et al.* 2013). Histone variants are also thought to affect chromatin dynamics through the introduction of structural changes to the nucleosome that alter nucleosome stability and chromatin compaction. One example, albeit controversial, is the effect of the introduction of H2A.Z into a nucleosome. While some studies suggest that this results in subtle destabilization of the interface between the H2A.Z-H2B dimer and the H3₂-H4₂ tetramer, others have shown that incorporation of the variant actually increases the salt-dependent stability of the nucleosome (Suto *et al.* 2000; Park *et al.* 2004; Zhang *et al.* 2005). Whatever the outcome, H2A.Z appears to have some effect on the stability of the nucleosome, with potential implications on chromatin structure. Together, these mechanisms of

histone variant function provide a better understanding of how histone variants regulate chromatin structure and processes.

Work in Chapter 4 of this thesis focuses on the histone variants H3.1, H3.2, and H3.3. Although the canonical histones H3.1 and H3.2 only vary by a single amino acid, H3.3 differs from H3.1 and H3.2 by five or four residues, respectively. This difference may seem little, but H3.3 displays differential characteristics from its canonical counterparts, including localization to transcriptionally active regions of the genome (Schwartz and Ahmad 2005; Mito *et al.* 2005). This suggests a role for this variant in transcriptional activity. In agreement with this, H3.3 is enriched in modifications associated with transcription such as H3K4me3 compared to H3.1 or H3.2, and has been shown to impair higher order chromatin structure (Hake *et al.* 2005; Chen *et al.* 2013). Furthermore, H3.3 co-localizes at promoters with H2A.Z – a histone variant that has also been linked to transcription (Jin *et al.* 2009). Indeed, nucleosomes containing H3.3 and H2A.Z are less stable than canonical nucleosomes or those containing H2A.Z and canonical H3 (Jin and Felsenfeld 2007). Since S31, I89, and G90 are conserved in yeast H3 and human H3.3, but not H3.1 or H3.2, yeast H3 is considered to be most closely related to the H3.3 variant. Indeed, the yeast genome is generally considered more transcriptionally active than the human genome, supporting the idea that the more transcriptionally active H3.3 variant may be more yeast-like. Nonetheless, yeast H3 and human H3.3 still differ by 13 residues, suggesting a diverged function.

Histone variants are deposited onto chromatin with the help of histone chaperones, which can be general or specific in terms of variant. As the canonical histones H3.1 and H3.2 are expressed only in S phase, they are deposited through replication-coupled (RC) histone deposition by the histone chaperone Chromatin Assembly Factor 1 (CAF-1) (Smith and Stillman 1989). On the other hand, since H3.3 is expressed throughout the cell cycle, its deposition is carried out primarily through replication-independent (RI) histone deposition, involving two different histone chaperones for distinct regions of the genome. HIRA (Histone Cell Cycle Regulator) is responsible for deposition of H3.3 at active regions of the

genome, while DAXX/ATRX promotes deposition at pericentric heterochromatin and telomeres (Goldberg *et al.* 2010; Lewis *et al.* 2010). In *S. cerevisiae*, histone H3 can be deposited by both RC and RI histone deposition pathways. Similar to in higher eukaryotes, the RC pathway involves deposition and chromatin assembly by the histone chaperone CAF-1, while the RI pathway promotes deposition by the HIR complex (ATRX has no homolog in yeast).

```

yH3  MARTKQTARKSTGGKAPRKQLASKAARKSAPSTGGVKKPHRYRPGTVALREIRRQKSTELLIRKLPFQR 70
H3.3 MARTKQTARKSTGGKAPRKQLATKAARKSAPSTGGVKKPHRYRPGTVALREIRRYQKSTELLIRKLPFQR 70
H3.1  MARTKQTARKSTGGKAPRKQLATKAARKSAPATGGVKKPHRYRPGTVALREIRRQKSTELLIRKLPFQR 70
H3.2  MARTKQTARKSTGGKAPRKQLATKAARKSAPATGGVKKPHRYRPGTVALREIRRYQKSTELLIRKLPFQR 70

yH3  LVREIAQDFKTDLRFQSSAIGALQESVEAYLVSLFEDTNLCAIHAKRVTIQKKDIQLARRRGERSS 136
H3.3 LVREIAQDFKTDLRFQSSAIGALQEASEAYLVGLFEDTNLCAIHAKRVTIMPKDIQLARRRGERA 136
H3.1  LVREIAQDFKTDLRFQSSAVMALQEACEAYLVGLFEDTNLCAIHAKRVTIMPKDIQLARRRGERA 136
H3.2  LVREIAQDFKTDLRFQSSAVMALQEASEAYLVGLFEDTNLCAIHAKRVTIMPKDIQLARRRGERA 136

```

Figure 1.2: Yeast histone H3 is more closely related to the human histone H3 variant H3.3 than to H3.1 or H3.2.

Amino acid sequences of histone H3 in *S. cerevisiae* and H3.1, H3.2, and H3.3 in humans. Divergent amino acids are highlighted in blue.

1.8 Chapter Summaries

Previous work by our lab, and others, has shown that the NuA3 histone acetyltransferase complex is recruited to chromatin through interaction with H3K4me3 via the PHD finger of one of its subunits, Yng1 (Martin *et al.* 2006b; Taverna *et al.* 2006). Nonetheless, evidence exists suggesting the presence of at least one additional chromatin-targeting domain. Candidates for this domain include the two PHD fingers of Nto1, the PWWP domain of Pdp3, and the YEATS domain of Taf14. PHD fingers are found in more than one hundred proteins across eukaryotes, and largely associate with tri-methylated lysines on histone tails

(Sanchez and Zhou 2011). The PWWP domain is a poorly conserved domain that binds predominantly to H3K36me3 histones (Vezzoli *et al.* 2010; Dhayalan *et al.* 2010; Wu *et al.* 2011; Maltby *et al.* 2012a; van Nuland *et al.* 2013; Li *et al.* 2013b). Conversely, the YEATS domain is a conserved eukaryotic domain that was recently shown to bind acetylated histones (Li *et al.* 2014). We therefore hypothesized that one of these domains is acting to recruit NuA3 to chromatin along with the PHD finger of Yng1.

In Chapter 2 of this thesis we demonstrated that Sas3, the catalytic subunit of the NuA3 complex, steadily increased in occupancy across gene bodies, peaking at +5 to +6 nucleosomes. Localization of the complex correlated positively with H3K36me3, and interaction of Sas3 with chromatin was dependent on both lysine 36 methylation and Set2 – the methyltransferase responsible for this modification. Using a genetic approach, we showed that Pdp3 is the probable subunit of NuA3 responsible for this interaction, and identify the PWWP domain as the likely chromatin-targeting domain. Taken together we suggest a mechanism by which the PWWP domain of Pdp3 recruits NuA3 to the H3K36me3, providing wider coverage of the complex across gene bodies.

In Chapter 3 of this thesis we demonstrated that residues within the YEATS domain of Taf14 were critical for association of the complex with chromatin. Using a modified histone peptide array, we identified H3K9 and 18 acetylation, and to a lesser degree H3K27 acetylation, as binding partners of Taf14, and showed that these modifications correlated weakly, but positively, with Sas3 occupancy across nucleosomes. Furthermore, as these modifications are catalyzed by the Gcn5 histone acetyltransferase complex, we went on to show that recruitment of NuA3 to chromatin was dependent on this HAT.

Histones are among the most conserved proteins known, but organismal differences do exist. In Chapter 4, we examine the contribution that divergent amino acids within histone H3 make to cell growth and chromatin structure in *S. cerevisiae*. We showed that, while amino acids that define histone H3.3 are dispensable for yeast growth, substitution of residues within the histone H3 α 3 helix with their human

counterparts resulted in a severe growth defect. Mutations within this domain also resulted in altered nucleosome positioning, both *in vivo* and *in vitro*, which was accompanied by increased preference for nucleosome favoring sequences. These results suggest that divergent amino acids within the histone H3 $\alpha 3$ helix play organismal roles in defining chromatin structure.

CHAPTER 2:

RECRUITMENT OF NUA3 TO CHROMATIN IS DEPENDENT ON H3K36ME3 AND THE PWWP DOMAIN PROTEIN PDP3

2.1 INTRODUCTION

The MYST (*MOZ-YBF2/SAS3-SAS2-TIP60*) family of HATs – named after its four founding members – play an important role in histone acetylation, and thus chromatin regulation, across eukaryotes. The defining feature of this family is a conserved MYST domain composed of an acetyl-CoA-binding domain and a zinc finger, although some members contain additional domains including chromodomains, PHD fingers, and others (Utley and Côté 2003). These HATs function as part of multi-subunit complexes, with the associated proteins playing roles in chromatin-targeting, specificity, and complex stability. In addition to a MYST family member, most complexes include an Inhibitor of Growth (ING) family member, Eaf6, and at least one additional subunit. In humans, five MYST HATs have been identified – Tip60, MOZ, MORF, HBO1, and MOF – while yeast possess three – Sas2, Sas3, and Esa1. These HATs are associated with diverse nuclear processes, and as such, it is not surprising that mutations within members of this family have been linked to a number of human diseases, including cancer (Avvakumov and Côté 2007a; b; Lafon *et al.* 2007).

In yeast, the NuA3 histone acetyltransferase complex (containing the MYST family member Sas3) is the closest homolog to human MOZ and MORF (Lafon *et al.* 2007). It is a histone H3-specific HAT, with activity towards K14 and K23 (Howe *et al.* 2001; Taverna *et al.* 2006). CHIP-chip studies examining the genome-wide localization of Sas3 or the NuA3 subunit Yng1 have placed the complex throughout the transcribed region of active genes, with a peak at the 5' end (Taverna *et al.* 2006; Vicente-Muñoz *et al.* 2014). Unlike many other histone acetyl marks, H3K14 and 23 acetylation are found in high levels not only

at the promoters of genes, but also throughout the transcribed region with a similar enrichment at 5' ends. Nonetheless, little is known about how NuA3 is targeted to specific regions of the genome.

One mechanism by which NuA3 is recruited to chromatin is through association with H3K4me3. This modification is deposited by the histone methyltransferase Set1, which associates with the tail of elongating RNAPII upon phosphorylation of serine 5 by Kin28 (Ng *et al.* 2003). This interaction is dependent on the PAF complex, which is thought to bridge the interaction between methyltransferase and polymerase (Krogan *et al.* 2003b). Because phosphorylation of serine 5 occurs during promoter escape, and dephosphorylation occurs during early elongation, H3K4me3 is localized to the 5' ends of transcribed genes, but absent from the 3' ends (Mosley *et al.* 2009; Rodriguez *et al.* 2000 Barski *et al.* 2007; Bernstein *et al.* 2005; Pokholok *et al.* 2005; Schübeler *et al.* 2004). Within NuA3, the PHD finger of Yng1 is able to interact with H3K4me3, providing a mechanism for recruitment to the 5' end of genes (Martin *et al.* 2006b; Taverna *et al.* 2006). Despite this, deletion of *SET1*, or the PHD finger of Yng1, does not abolish the interaction between NuA3 and chromatin. Furthermore, genome-wide localization studies of Sas3 and Yng1 place the complex across the entire gene body – not restricted to the 5' end. Taken together, this suggests the existence of at least one additional chromatin-targeting domain within the NuA3 complex.

Previous studies determined that NuA3 recruitment is dependent not only on H3K4me3, but also on H3K36me3 (Martin *et al.* 2006a). This modification is deposited by Set2, which is recruited through interaction with phosphorylated serine 2 on the CTD of elongating RNAPII (Fuchs *et al.* 2012). Since phosphorylation of serine 2 isn't catalyzed until elongation is underway, this modification, and subsequently H3K36me3, is enriched further into gene bodies than H3K4me3 (Cho *et al.* 2001; Schübeler *et al.* 2004; Bernstein *et al.* 2005; Pokholok *et al.* 2005; Barski *et al.* 2007). Considering that a mechanism exists to explain the recruitment of NuA3 to the 5' ends of genes, but not the remainder of gene bodies,

this strongly suggests that H3K36me3 may function together with H3K4me3 to recruit the complex across the entire transcribed region.

In addition to Sas3, NuA3 is composed of at least four additional subunits: Yng1, Nto1, Taf14, and Eaf6. Evidence also exists that Pdp3 – a previously uncharacterized protein of unknown function – may be a transient member of the complex (Krogan *et al.* 2006; Taverna *et al.* 2006; Vicente-Muñoz *et al.* 2014). With the exception of Eaf6, each of these members contains at least one potential chromatin-targeting domain. Nto1 contains tandem PHD fingers, one of which has been shown to interact with H3K36me3 *in vitro* (Shi *et al.* 2006b). Taf14 contains a YEATS domain, which was recently shown to bind H3K9 acetylated histones (Shanle *et al.* 2015). Finally Pdp3 contains a PWWP domain – a known methyl-lysine binding domain that interacts almost exclusively with H3K36me3 in the other proteins in which it is found (Vezzoli *et al.* 2010; Dhayalan *et al.* 2010; Wu *et al.* 2011; Maltby *et al.* 2012a; van Nuland *et al.* 2013; Li *et al.* 2013b).

In this study, we use ChIP-seq technology to confirm that Sas3 is localized across transcribed regions, and further show that it is enriched at +5 and +6 nucleosomes. While Sas3 occupancy correlates positively with H3K4me3, a meta-analysis comparing Sas3 occupancy with that of over 126 different ChIP-seq and ChIP-ChIP datasets revealed H3K36me3 to correlate more strongly than any other modification or factor. Indeed, we demonstrate that *SET1* and *SET2* are both required for efficient recruitment of NuA3 to chromatin. Finally we show that Pdp3 is a bona fide member of the NuA3 complex, and implicate its PWWP domain in recruitment of NuA3 to H3K36 methylated regions of the genome. This suggests a novel mechanism by which NuA3 is recruited to transcriptionally active regions of the genome.

2.2 MATERIALS AND METHODS

2.2.1 Yeast Strains and Plasmids

All strains in this study are isogenic to S288C, and are listed in Table 2.1. Yeast culture and genetic manipulations were performed using standard protocols (Ausubel FM, Brent R, Kingston RE, Moore DD, Seidman JG, Smith JA 1987). Genomic deletions were verified by PCR analysis and whole cell extracts were generated as previously described (Ausubel FM, Brent R, Kingston RE, Moore DD, Seidman JG, Smith JA 1987; Kushnirov 2000).

Table 2.1: Yeast strains used in this study

Yeast Strain	Mating Type	Genotype
YLH101	Mat a	<i>his3Δ200 leu2Δ1 lys2-128δ ura3-52 trp1Δ63</i>
YLH126	Mat a	<i>his3Δ200 leu2Δ1 lys2-128δ ura3-52 trp1Δ63 SAS3TAP::TRP</i>
YLH367	Mat a	<i>his3Δ200 leu2Δ1 lys2-128δ ura3-52 trp1Δ63 gcn5::HIS3 sas3::KAN</i>
YLH452	Mat a	<i>his3Δ200 leu2Δ1 lys2-128δ ura3-52 trp1Δ63 set1::HISMx6 SAS3TAP::TRP</i>
YLH517	Mat a	<i>his3Δ200 leu2Δ1 lys2-128δ ura3-52 trp1Δ63 (hht1-hhf1)::LEU2 (hht2-hhf2)::KAN</i>
YLH550	Mat a	<i>his3Δ200 leu2Δ1 lys2-128δ ura3-52 trp1Δ63 set2::KAN SAS3TAP::TRP</i>
YLH551	Mat a	<i>his3Δ200 leu2Δ1 lys2-128δ ura3-52 trp1Δ63 set1::HISMx6 set2::KAN SAS3TAP::TRP</i>
YLH665	Mat a	<i>his3Δ200 leu2Δ1 lys2-128δ ura3-52 trp1Δ63 SAS3TAP::TRP PDP3-6HA::HIS yng1::KAN</i>
YLH682	Mat a	<i>his3Δ200 leu2Δ1 lys2-128δ ura3-52 trp1Δ63 SAS36HA::TRP pdp3::HIS</i>
YLH670	Mat a	<i>his3Δ200 leu2Δ1 lys2-128δ ura3-52 trp1Δ63 SAS3TAP::TRP pdp3::HIS</i>

Yeast Strain	Mating Type	Genotype
YLH690	Mat a	<i>his3Δ200 leu2Δ1 lys2-128δ ura3-52 trp1Δ63 (hht1-hhf1)::LEU2 (hht2-hhf2)::KAN SAS3-6HA::HIS pHHT2-HHF2.416</i>
YLH691	Mat a	<i>his3Δ200 leu2Δ1 lys2-128δ ura3-52 trp1Δ63 (hht1-hhf1)::LEU2 (hht2-hhf2)::KAN SAS3-6HA::HIS pHHF2.HHT2K4R</i>
YLH692	Mat a	<i>his3Δ200 leu2Δ1 lys2-128δ ura3-52 trp1Δ63 trp1D63 (hht1-hhf1)::LEU2 (hht2-hhf2)::KAN SAS3-6HA::HIS pHHF2.HHT2K36R</i>
YLH693	Mat a	<i>his3Δ200 leu2Δ1 lys2-128δ ura3-52 trp1Δ63 (hht1-hhf1)::LEU2 (hht2-hhf2)::KAN SAS3-6HA::HIS pHHF2.HHT2K4RK36R</i>
YLH843	Mat a	<i>his3Δ200 leu2Δ1 lys2-128δ ura3-52 trp1Δ63 gcn5::TRP yng1DPHD::HISMx6 pdp3::KANMX4</i>
YVM103	Mat a	<i>his3Δ200 leu2Δ1 lys2-128δ ura3-52 trp1Δ63 gcn5::TRP pdp3::HIS</i>
YVM107	Mat a	<i>his3Δ200 leu2Δ1 lys2-128δ ura3-52 trp1Δ63 gcn5::TRP yng1DPHD::HISMx6</i>
YVM110	Mat a	<i>his3Δ200 leu2Δ1 lys2-128δ ura3-52 trp1Δ63 gcn5::TRP</i>
YVM142	Mat a	<i>his3Δ200 leu2Δ1 lys2-128δ ura3-52 trp1Δ63 SAS3-6HA::HIS set1D::KANMX6 set2D::TRP</i>
YVM146	Mat a	<i>his3Δ200 leu2Δ1 lys2-128δ ura3-52 trp1Δ63 SAS3-6HA::TRP</i>
YVM157	Mat a	<i>his3Δ200 leu2Δ1 lys2-128δ ura3-52 trp1Δ63 SAS3-6HA::TRP set1D::HISMx6</i>
YVM158	Mat a	<i>his3Δ200 leu2Δ1 lys2-128δ ura3-52 trp1Δ63 SAS3-6HA::TRP set2D::HISMx6</i>
YVM214	Mat a	<i>his3Δ200 leu2Δ1 lys2-128δ ura3-52 trp1Δ63 SAS3TAP::TRP eaf6D::KAN PDP3-6HA::HIS</i>
YVM241	Mat a	<i>his3Δ200 leu2Δ1 lys2-128δ ura3-52 trp1Δ63 SAS3TAP::TRP PDP3-6HA::HIS</i>

All plasmids used in this study are listed in Table 2.2. Genetic manipulations were performed using standard protocols (Gillam and Smith 1979) on readily available yeast vectors (Sikorski and Hieter 1989; Mumberg *et al.* 1994). All genes are under the expression of their own promoters.

Table 2.2: Plasmids used in this study

Plasmid	Description
p184	pGCN5-FLAG.416
P258	pHHF2.HHT2.414
P306	pHHF2.HHT2K4R.414
P309	pHHF2.HHT2K36R.414
P310	pHHF2.HHT2K4RK36R.414

2.2.2 Chromatin Immunoprecipitation (ChIP) for Sequencing

The chromatin immunoprecipitation protocol used was modified from that outlined in Maltby *et al.* 2012. Yeast strains YLH146 and YLH101 were grown in 1L YPD to an OD₆₀₀ of 0.8 at which point they were cross-linked with 1% formaldehyde for 30 minutes at room temperature. Cross-linking was stopped by the addition of 125 mM glycine followed by a further 15 minute incubation at room temperature. Cells were harvested at 7000 rpm for 10 minutes, washed twice in cold PBS, and split into ten tubes before each being re-suspended in 600 μ L lysis buffer (50 mM HEPES-KOH pH 7.5, 140 mM NaCl, 1 mM EDTA, 1 % Triton X-100, 0.1% sodium deoxycholate). Cells were lysed mechanically by the addition of 1 mL glass beads followed by vortexing (Scientific Industries Disruptor Genie) for 25 minutes at 4 °C. Chromatin from the resulting lysates was pelleted at 15 000 g for 30 minutes, and washed with NP-S Buffer (0.5 mM spermidine, 1 mM β -ME, 0.075% NP-40, 50 mM NaCl, 10 mM Tris pH 7.4, 5 mM MgCl₂, 1 mM CaCl₂).

To prepare for MNase digestion, the chromatin pellets were re-suspended in 900 μ L NP-S buffer. Reactions were initiated by the addition of 400 U MNase to each sample followed immediately by incubation at 37°C for 10 minutes to obtain predominantly mono-nucleosomal DNA. The reaction was stopped by the addition of 10 mM EDTA and placement on ice. Digested lysates were clarified by centrifugation at 9000 g for 5 minutes and pooled. To extract insoluble Sas3-6HA that may be present in the chromatin pellet, these pellets were re-suspended in 300 μ L lysis buffer with 0.02% SDS, and sonicated (Diagenode Bioruptor) at high output for 30 seconds on/30 seconds for a total of 4 minutes. They were then re-clarified by centrifugation at 9000 g for 5 minutes, and the supernatant added to the pre-existing pool. The buffer composition of the lysate was adjusted to that of the original lysate buffer, and 10% was set aside as input.

Prior to immunoprecipitation, the supernatant was pre-cleared by addition of 100 μ L Magnetic Protein-G Dynabeads (Life Technologies) and incubation at 4°C for 1 hour. Once the beads were removed, 5 μ g of α -HA antibody (Table 2.3) was added to the lysate and incubated at 4°C overnight. The following day, 100 μ L Magnetic Protein-G Dynabeads were added to complete the immunoprecipitation, and incubation at 4°C was continued for a further hour. Beads were washed and sample eluted, followed by reversal of cross-links and DNA purification as per Maltby et al. 2012.

Table 2.3: Antibodies used in this study

Antibody	Animal	Dilution	Company	Catalogue Number
α H3	Rabbit	1:5000	GenScript	Custom antibody raised to yeast specific antigen: CKDIKLARRLRGERS
α HA	Rat	1:500	Roche	11867431001
α HA-HRP	Rat	1:5000	Roche	12013819001

Antibody	Animal	Dilution	Company	Catalogue Number
α IgG	Rabbit	1:5000	Chemicon	PP64
α Rabbit-HRP	Rabbit	1:5000	GE HealthCare	NA934V
α PAP	Rabbit	1:5000	Sigma-Aldrich	P1291
α Rat (800CW)	Goat	1:25000	Licor	926 32219
α Rabbit (680CW)	Goat	1:25000	Licor	926 32210

2.2.3 Library Preparation, Illumina Sequencing, and Data Analysis

Library construction and paired-end sequencing on an Illumina HiSeq 2000 platform was performed as described in Maltby et al. 2012. Reads were aligned to the *S. cerevisiae* genome (Saccer3 genome assembly) using BWA (Li and Durbin 2009). Inputs were subtracted from ChIP samples, and the resultant files converted to a Z-score using the java genomics toolkit (<http://palpant.us/java-genomics-toolkit/>). Average gene profiles were generated by aligning reads relative to the +1 dyad using the sitepro tool in the CEAS genome package (<http://liulab.dfci.harvard.edu/CEAS/>), and the average profiles by quartile were constructed in R. Values past the polyadenylation sequence (Park et al. 2014) were excluded from the average calculation, and the fraction of genes included in the average calculation at any given distance from the +1 nucleosome determined. Midpoints were generated using bedtools (v2.21.1: <http://bedtools.readthedocs.org/en/latest/>), and scatter plots performed using ggplot2 (<http://ggplot2.org/>) with the following ChIP-seq data sets: H3K14ac, H3K23ac, H3K4me3, H3K36me3 (Weiner et al. 2015), and RNAPII (Wong et al. 2014).

2.2.4 Immunoblot Analysis

Immunoprecipitations and lysates were analyzed by SDS-PAGE and immunoblotting with the antibodies and dilutions listed in Table 2.3. Signal was visualized either by infrared detection and quantification using the Licor Odyssey System, or by enhanced chemoilluminescence using a Konica Minolta SRX-101A processor.

2.2.5 Modified Chromatin Immunoprecipitation (mChIP)

The modified chromatin immunoprecipitation protocol was performed as described in Lambert et al. 2009, with the exception that after extract preparation, extracts were clarified by centrifugation at 12,000 rpm (Eppendorf microfuge, model 5415D) for 5 minutes at 4°C. Following incubation for 6 hours at 4°C, beads were washed and incubated at 65°C for 10 minutes with SDS loading buffer lacking β -mercaptoethanol (which was added back following elution from beads).

2.2.6 Chromatin Immunoprecipitation and Quantitative PCR (ChIP-qPCR)

The chromatin immunoprecipitation protocol used in this study was adapted from that performed by Nelson, Denisenko, and Bomsztyk 2006. Cells were grown in 50 mL YPD to an OD₆₀₀ of 0.8 and cross-linked with 1% formaldehyde for 30 minutes at room temperature. The reaction was stopped by the addition of 125 mM glycine, and incubation at room temperature for a further 15 minutes. Pellets were washed twice with cold PBS.

Following resuspension in 300 μ L lysis buffer (50 mM HEPES pH 7.5, 140 mM NaCl, 0.5 mM EDTA, 1% triton X-100, 0.1% sodium deoxycholate), cells were lysed mechanically by the addition of 500 μ L glass beads followed by vortexing (Scientific Industries Disruptor Genie) for 20 minutes at 4°C. Lysates were sonicated at high output for 30 seconds on/30 seconds off for 10 minutes to obtain an average

fragment length of approximately 500 bp. A further 400 μ L lysis buffer was added to each sample, and the lysates were clarified by centrifugation at 10 000 rpm for 10 minutes. Ten percent of the lysate was reserved for input.

Lysates were incubated with 0.25 μ g anti-HA antibody (Table 2.3) and rotated at 4°C overnight, followed by pull out with 100 μ L Protein G Dynabeads (Life Technologies) at 4°C for 1 hour. Beads were washed twice each with lysis buffer (50 mM HEPES pH 7.5, 140 mM NaCl, 0.5 mM EDTA, 1% Triton-X-100, and 0.1% sodium deoxycholate), lysis buffer + 500 mM NaCl, and lithium chloride buffer (10 mM Tris-Cl pH 8.0, 250 mM LiCl, 0.6% NP-40, 0.5% sodium, deoxycholate, and 1 mM EDTA), followed by a single wash with TE. The beads were then resuspended in 100 μ L of a 10% chelex 100 slurry and boiled for 10 minutes to inactivate DNases. Cross-links were reversed and DNA isolated by the addition of 20 μ g proteinase K and incubation at 55°C for 30 minutes, followed by boiling for 10 minutes to inactivate the proteinase. Samples were centrifuged for 1 minute at 13,000 rpm (Eppendorf microfuge, model 5415D), and supernatant transferred to a fresh tube. The beads were then washed in 120 μ L dH₂O, and the supernatant pooled with that from the previous step.

Immunoprecipitated and input DNA were amplified using an Applied Biosystems Step One Plus Real-Time PCR System using the primer pairs listed in Table 2.4. Each PCR reaction consisted of 2 mM Tris-Cl, 1 mM KCl, 1 mM (NH₄)₂SO₄, 0.2 mM MgSO₄, 0.01% Triton-X-100, 0.2 mM dNTPs, 1.6 mM of each primer, 1x SYBR green, and 0.5 μ L homemade Taq polymerase to a volume of 25 μ L. PCRs went through a program of 94°C for 2 minutes followed by 40 cycles of the following: 94°C for 30 seconds, 58°C for 1 minute, and 72°C for 30 seconds. Percent IP values were calculated and shown relative to wild type.

Table 2.4: Primers used in this study

Primer Name	Sequence
COX10-s	CGG AAT CAT GGC GGG AAA C
COX10-a	GGA AGT TGT GTG CTT GCA TCG

2.3 RESULTS

2.3.1 NuA3 preferentially binds di-nucleosomes

Previous ChIP-chip studies have placed NuA3 across the entirety of transcribed genes, with a slight enrichment at 5' ends similar to that observed for H3K4me3 (Pokholok *et al.* 2005; Taverna *et al.* 2006; Vicente-Muñoz *et al.* 2014). Since we were interested in deciphering the various mechanisms by which NuA3 is recruited to chromatin, we wished to re-examine the genome-wide localization of NuA3 using ChIP-seq, as it offers a better signal-to-noise ratio and greater resolution than ChIP-chip (Ho *et al.* 2011). We therefore performed ChIP-seq from micrococcal nuclease (MNase) treated extracts of a Sas3-6HA and an untagged strain using an α HA antibody (Table 2.3). MNase digestion was used to fragment DNA rather than sonication, as previous data from our lab suggested that both H3K4 and H3K36 methylation function in targeting the NuA3 complex to chromatin, and Sas3 was able to co-precipitate DNA and histone H3 from MNase-treated lysates (data not shown) (Martin *et al.* 2006a). DNA was successfully isolated from the Sas3-6HA ChIP at a concentration of 0.07 ng/uL, whereas any DNA present in the untagged control was below the limits of detection (Figure 2.1A). Since paired-end sequencing was performed, the distribution of read lengths was determined. A maximum equivalent number of reads between the Sas3 ChIP and Sas3 input (8 691 422 reads) were randomly sampled (Figure 2.1B). As expected, DNA was digested primarily to mono-nucleosomes and to a lesser degree di-nucleosomes, as observed by the bimodal distribution of reads with peak midpoints at approximately 150 bp and 300 bp, respectively.

Interestingly, the di-nucleosomal peak was enriched in the ChIP relative to the input, suggesting that NuA3 preferentially interacts with di-nucleosomes. To ensure that this enrichment was specific to Sas3-associated DNA, and not an artifact of the ChIP, the maximum equivalent number of reads between all ChIPs and inputs (83 588 reads) were randomly sampled and the distribution of read lengths determined (Figure 2.1C). As is shown in Figure 2.1C, despite little DNA being recovered from the ChIP of the untagged strain, amplification and sequencing produced a small number of background reads likely caused by non-specific binding to the beads. As a much smaller sample size was therefore used in this analysis (83 588 reads versus the 8 691 422 reads used in the analysis of Figure 2.1B) kernel density estimation was applied to allow for smoothing. Although an enrichment in di-nucleosomal DNA was still found for the Sas3 ChIP, this enrichment was not observed in the control ChIP, suggesting that the preference for di-nucleosomes seen for NuA3 is real.

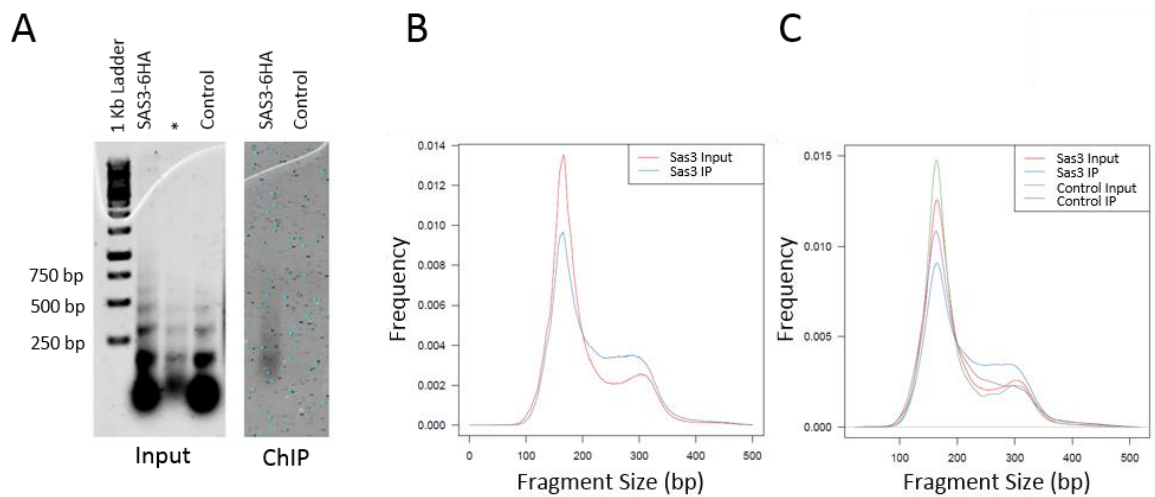


Figure 2.1: Sas3 preferentially binds di-nucleosomes.

(A) Syto60-stained agarose gel image of un-crosslinked input and ChIP DNA prior to library preparation. The lane denoted by * is misloaded. (B) Histogram of Sas3-6HA ChIP and input paired-end read lengths. (C) Kernel density plot of Sas3-6HA and control ChIP and input paired-end read lengths.

2.3.2 Sas3 occupancy peaks at +5 and +6 nucleosomes

It was previously observed that the occupancy of two subunits within NuA3 - Sas3 and Yng1 - peak at the 5' end of genes and taper off towards the 3' end of genes similar to the profile observed for H3K14 acetylation (Pokholok *et al.* 2005; Taverna *et al.* 2006; Vicente-Muñoz *et al.* 2014). We mapped all sequencing reads to the genome, and plotted the normalized cumulative read count relative to the +1 nucleosome of all yeast genes (Figure 2.2A). As genes vary in length, the fraction of genes included in the analysis at any distance from the +1 nucleosome is also shown. Unlike the occupancy profile for Yng1 observed by Taverna *et al.* 2006 and Vicente-Muñoz *et al.* 2014, we found that Sas3 steadily increases in occupancy throughout gene bodies, peaking over +5 and +6 nucleosomes. This holds true for genes of any length greater than approximately 500bp, as genes shorter than this contain too few nucleosomes (data not shown). As these groups plotted their data as a function of gene percent, we re-plotted our data in a

similar manner in order to more directly compare datasets. To do this, each gene's coding sequence was split into 100 windows, and the mean Sas3 enrichment for each window calculated. The 500 bp upstream and downstream of each gene was appended to this, and the average Sas3 enrichment of each region plotted. Remarkably, plotting Sas3 occupancy by gene percent rather than by cumulative read count produced a similar profile to that observed by Taverna *et al.* 2006 and Vicente-Muñoz *et al.* 2014 in which the peak is shifted closer to the 5' end of genes (Figure 2.2B). This is likely due to the pattern of Sas3 enrichment over long genes, as the peak at +5 and +6 nucleosomes is pushed closer to the 5' end when the genes are plotted by percent. Indeed, a progressive 5' shift in Sas3 enrichment was observed when genes were binned by increasing gene length (data not shown). This suggests that our genome-wide localization data for Sas3 is in agreement with those of other studies.

Since +1 nucleosomes are more sensitive to MNase digestion, and thus more likely to fully digest to mono-nucleosomes, it's possible that the observed enrichment in Sas3 at +5 and +6 nucleosomes is due to its preference to bind di-nucleosomes (Chereji *et al.* 2015). To test this, we plotted the midpoint of each read for both input and ChIP relative to the +1 nucleosome of all yeast genes (Figure 2.2C). MNase-seq data from an untagged strain was also used as a control. Although Sas3 read midpoints were enriched in inter-nucleosomal regions (consistent with binding to di-nucleosomes), the enrichment at +5 and +6 nucleosomes was still observed. This enrichment was also observed when reads over 250 bp were removed (data not shown). This suggests that the increase in Sas3 occupancy at +5 and +6 nucleosomes is not due to a preference in di-nucleosome binding.

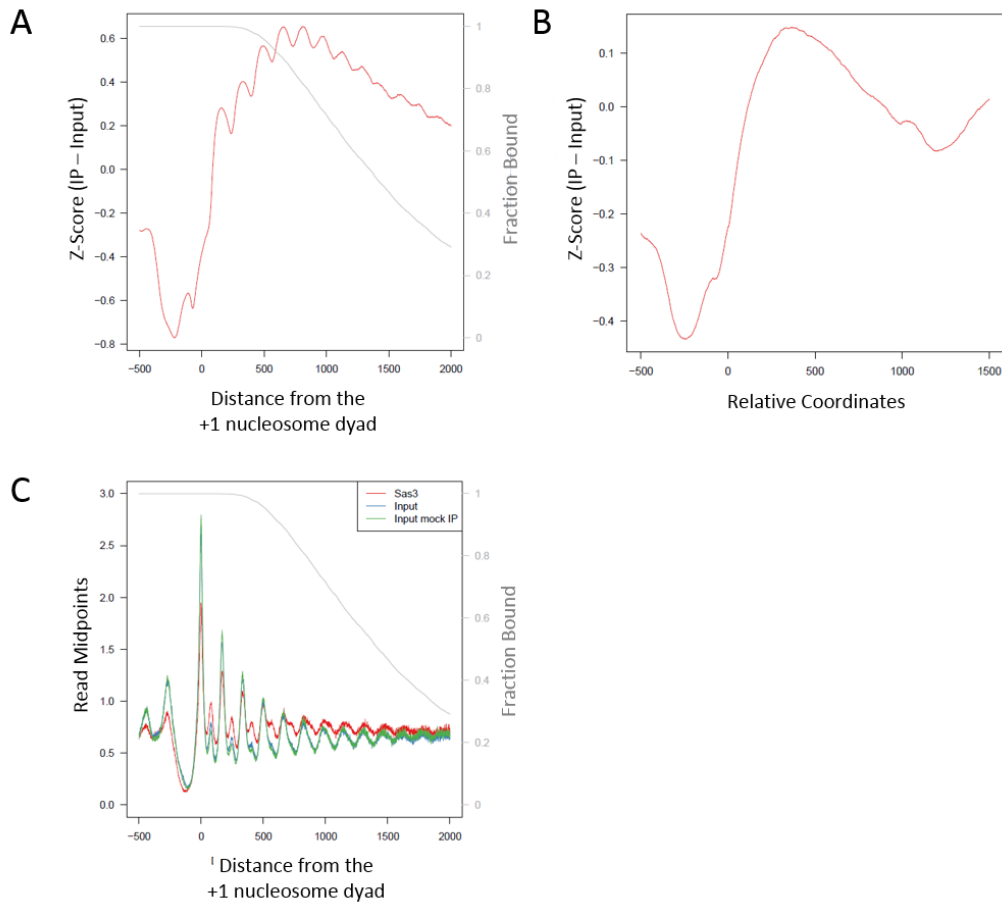


Figure 2.2: Sas3 occupancy peaks at +5 and +6 nucleosomes.

(A) Normalized cumulative read count plot of Sas3-6HA relative to the +1 nucleosome dyad of all yeast genes. (B) Normalized cumulative read count plot of Sas3-6HA as a function of gene percent relative to the +1 nucleosome dyad of all yeast genes. (C) Normalized cumulative read count plot of read midpoints in the indicated samples relative to the +1 nucleosome of all yeast genes. The input mock IP sample is from unpublished data in our lab. For both (A) and (C) genes were plotted from 500 bp upstream of the +1 nucleosome to their poly(A) termination site. The grey line represents the fraction of genes included in the analysis at any given distance from the +1 nucleosome.

2.3.3 Sas3 occupancy correlates with transcription and H3K4me3, but not H3K14ac or H3K23ac

As NuA3 catalyzes the acetylation of H3K14 and H3K23, we were interested in examining the relationship between the complex and each modification (Howe *et al.* 2001; Martin *et al.* 2006a; Taverna *et al.* 2006). Interestingly, no significant correlations were observed between Sas3 occupancy and H3K14ac (Spearman correlation of -0.09) or H3K23ac (Spearman correlation of 0.01) (Figures 2.3A and C). We have previously shown that deletion of *SAS3* on its own does not result in loss of H3K14ac in bulk histones (Maltby *et al.* 2012b). As Gcn5 also targets H3K14 and H3K23 for acetylation, the lack of correlation between Sas3 and these modifications is likely due to redundancy between the two HATs (Kuo and Andrews 2013). To look more closely at the relationship between these modifications and Sas3 localization, we binned Sas3 occupancy by quartiles of H3K14ac and H3K23ac enrichment, and plotted the normalized cumulative read count for each quartile relative to the +1 nucleosome of all yeast genes (Figure 2.3B and D). Although no differences in Sas3 occupancy were observed for quartiles of H3K14ac or H3K23ac enrichment at the 5' ends of genes, a strong negative correlation was observed between the modifications and Sas3 at the 3' ends of genes. This apparent contradiction in HAT complex and HAT target localization is likely at least in part due to the post-transcriptional removal of acetylation at the 3' ends of genes by the HDAC Rpd3S (Carrozza *et al.* 2005). Indeed, treatment of cells with the HDAC inhibitor trichostatin A (TSA) extends H3K23ac further into transcribed genes (unpublished data from our lab).

Next we decided to look at co-localization of Sas3 with H3K4me3, as we previously demonstrated that the PHD finger of Yng1 binds this modification, recruiting NuA3 to chromatin (Martin *et al.* 2006b). If this was the sole determinant for complex recruitment, we would expect to see a correlation between Sas3 occupancy and H3K4me3 across the genome. Pokholok *et al.* 2005 showed that H3K4me3 peaks at the 5' end of genes, dropping towards the 3' end. It is therefore unsurprising that only a moderate correlation was observed between the modification and Sas3 occupancy (Spearman correlation of 0.29) (Figure 2.4A). To help further tease apart this relationship, we binned Sas3 occupancy by quartiles of

H3K4me3 enrichment, and plotted the normalized cumulative read count for each quartile relative to the +1 nucleosome of all yeast genes (Figure 2.4B). While increased levels of occupancy were observed in the top three quartiles of H3K4me3-enriched genes, there was a significant drop in Sas3 occupancy in the bottom quartile, in agreement with the modification playing a role in NuA3 recruitment. However, the peak in occupancy at +5 and +6 nucleosomes was maintained even in genes with reduced or depleted H3K4me3, suggesting that another factor must be involved in recruiting the complex to this region.

Acetylation is closely linked to transcription, and consequently we also probed the relationship between NuA3 and RNAPII occupancy. A moderate Spearman correlation of 0.17 was observed between the two complexes (Figure 2.4C), and upon binning and plotting Sas3 occupancy by RNAPII enrichment as described above, we saw that Sas3 maintained the trend of peaking further into genes regardless of transcription rate (Figure 2.4D). Thus, although NuA3 recruitment is tied to transcription, its general profile across a gene is independent of the rate at which that transcription occurs.

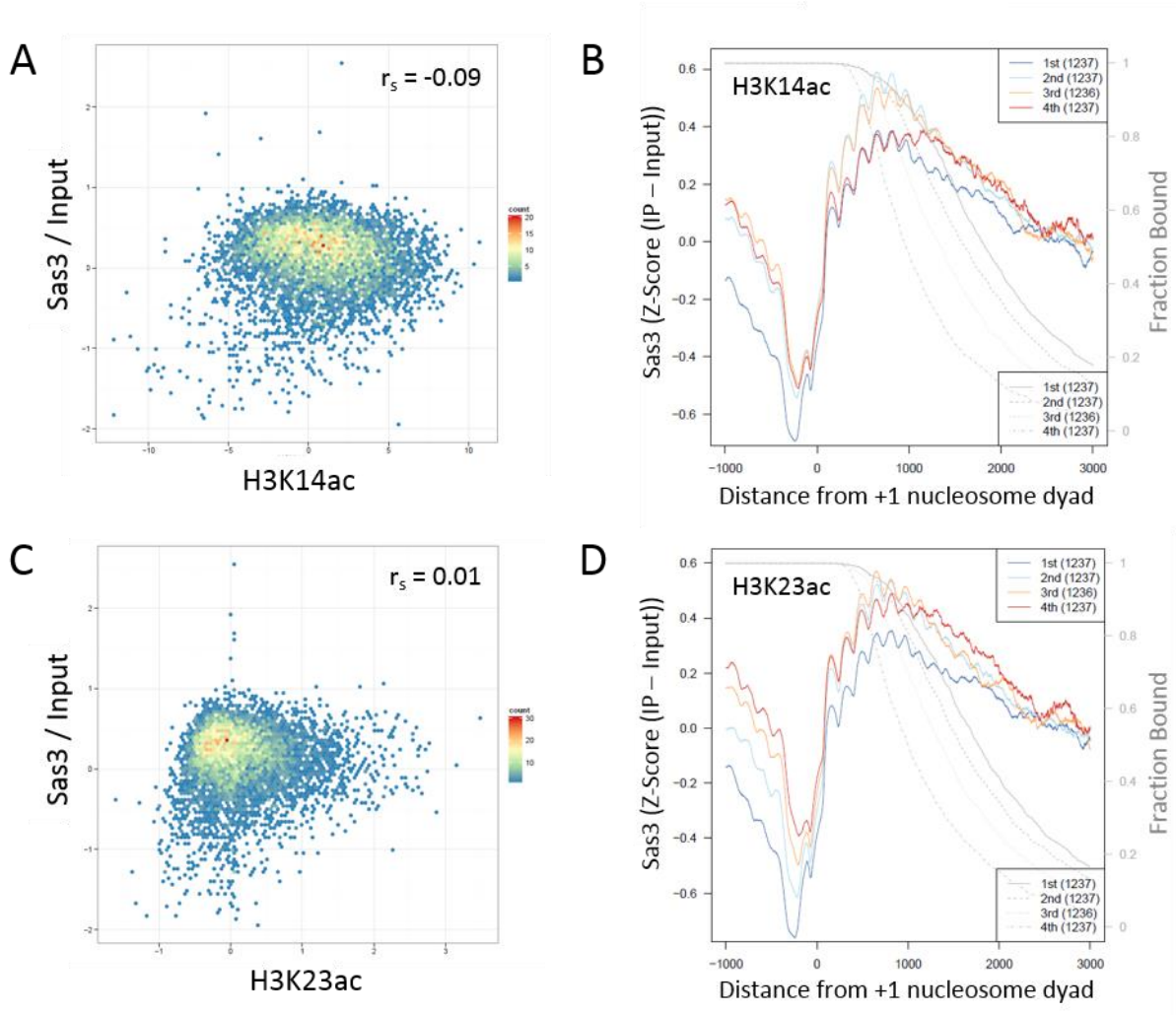


Figure 2.3: Sas3 Occupancy does not correlate with H3K14 or K23 acetylation. (A)(C) Scatter plots of Sas3 occupancy (normalized to input) versus (A) H3K14ac (Spearman correlation: -0.09) and (C) H3K23ac (Spearman correlation: 0.01) across all genes (Weiner *et al.* 2015). (B)(D) Cumulative read count plots of Sas3 (normalized to input) per quartile of (B) H3K14ac and (D) H3K23ac enrichment across genes. Sas3 occupancy is plotted relative to the +1 nucleosome dyad of all yeast genes. Genes were plotted from 1000 bp upstream of the +1 nucleosome to their poly(A) termination site. Grey lines represent the fraction of genes included in the analysis at any given distance from the +1 nucleosome.

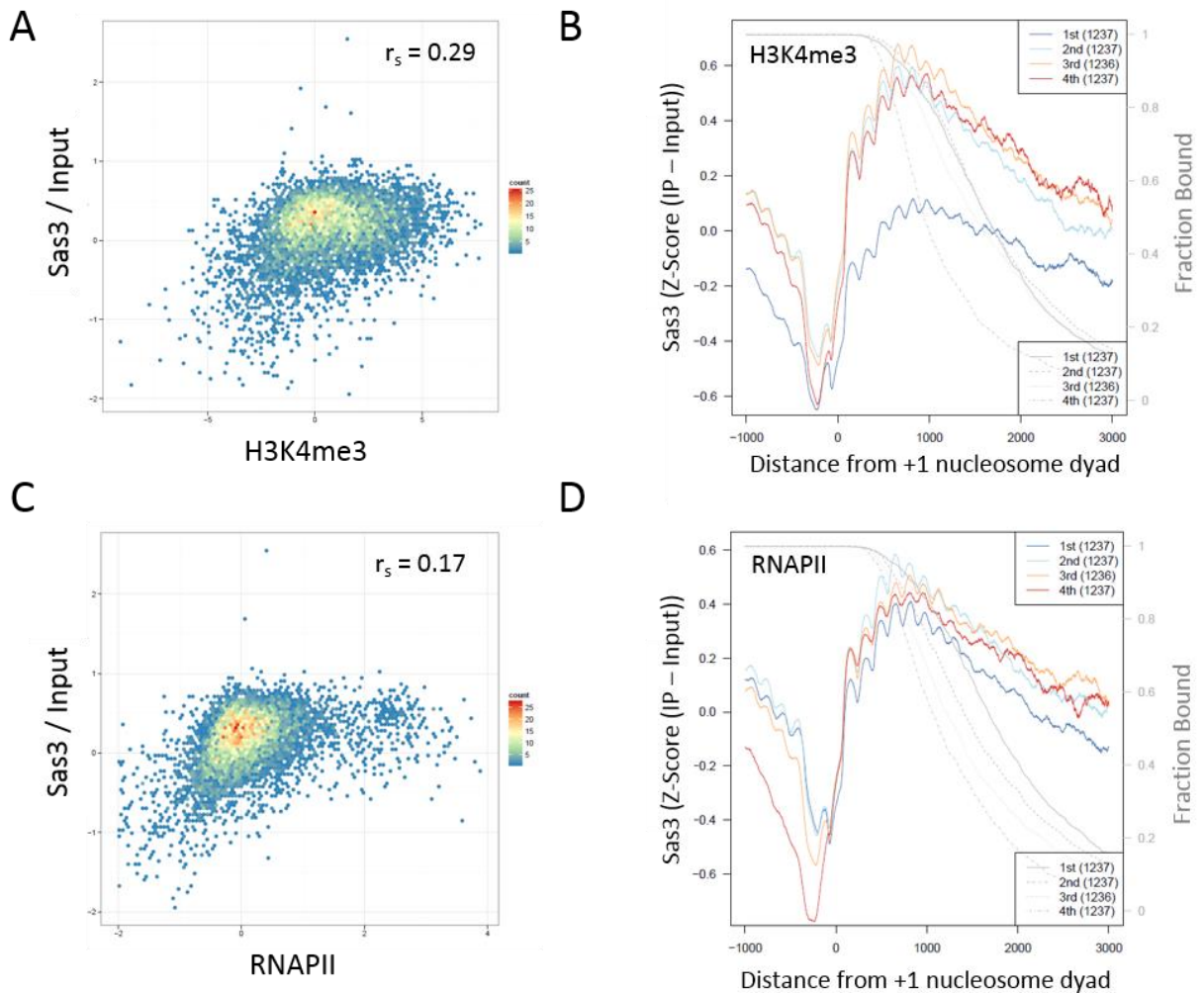


Figure 2.4: Sas3 Occupancy positively correlates with H3K4me3 and RNAPII occupancy. (A)(C) Scatter plots of Sas3 occupancy (normalized to input) versus (A) H3K4me3 (Spearman correlation 0.29) (Weiner *et al.* 2015) and (C) RNAPII occupancy (Spearman correlation: 0.17) (Wong *et al.* 2014) across all genes. (B)(D) Cumulative read count plots of Sas3 (normalized to input) per quartile of (B) H3K4me3 and (D) RNAPII enrichment across genes. Sas3 occupancy is plotted relative to the +1 nucleosome dyad of all yeast genes. Genes were plotted from 1000 bp upstream of the +1 nucleosome to their poly(A) termination site. Grey lines represent the fraction of genes included in the analysis at any given distance from the +1 nucleosome.

2.3.4 Meta-Analysis of Sas3 occupancy reveals strong correlation with H3K36me3

In order to explore the relationship between NuA3 and other histone modifications as well as chromatin-related complexes, we performed a meta-analysis comparing our Sas3 ChIP-seq data with that from over 126 different ChIP-seq and ChIP-ChIP experiments (Figure 2.5). Interestingly, one of the highest observed correlations was between Sas3 occupancy and H3K36me3 (Spearman correlation of 0.6) (Figure 2.6 and 2.7A). This is particularly interesting, as H3K36me3 is enriched at +5 and +6 nucleosomes in much the same manner as our observed profile for Sas3 occupancy (Weiner *et al.* 2010). Furthermore, factors involved in the H3K36 methylation pathway, such as Ctk1 and Rpb1 CTD phosphorylation at serine 2, were also found to positively correlate with Sas3 occupancy (Figure 2.6). In order to further elucidate the relationship between this HAT and H3K36me3, we binned Sas3 occupancy by quartiles of H3K36me3 enrichment, and plotted the normalized cumulative read count for each quartile relative to the +1 nucleosome of all yeast genes (Figure 2.7B). While high levels of occupancy were observed in the top two quartiles of H3K36me3-enrichment, Sas3 occupancy dropped in the third and fourth quartiles, respectively, suggesting that this modification plays a crucial role in NuA3 recruitment. Furthermore, the peak in occupancy at +5 and +6 nucleosomes was almost entirely abolished in the bottom quartile of H3K36me3 enrichment, suggesting the tantalizing possibility that this modification may in fact be responsible for the presence of Sas3 at these regions.

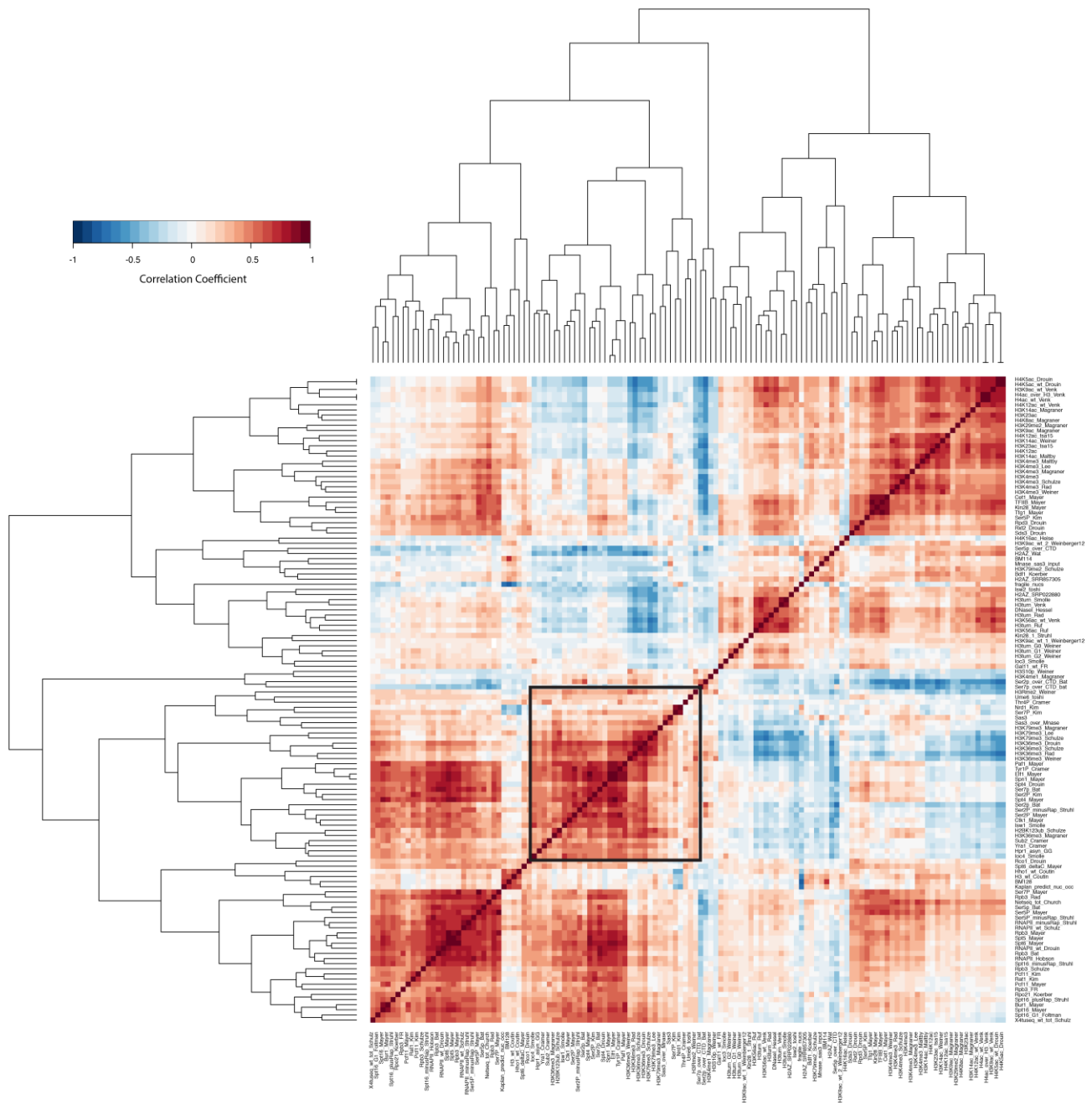


Figure 2.5: Meta-analysis of Sas3 occupancy reveals strong positive correlation with H3K36me3.

Heatmap and hierarchal clustering of meta-analysis data from 126 different ChIP-seq and ChIP-Chip experiments including data from the current study. Spearman correlations for all pairwise factors were determined based on average enrichment per nucleosome. The black box represents those factors showing the highest positive correlation with Sas3 occupancy, and is magnified in Figure 2.6.

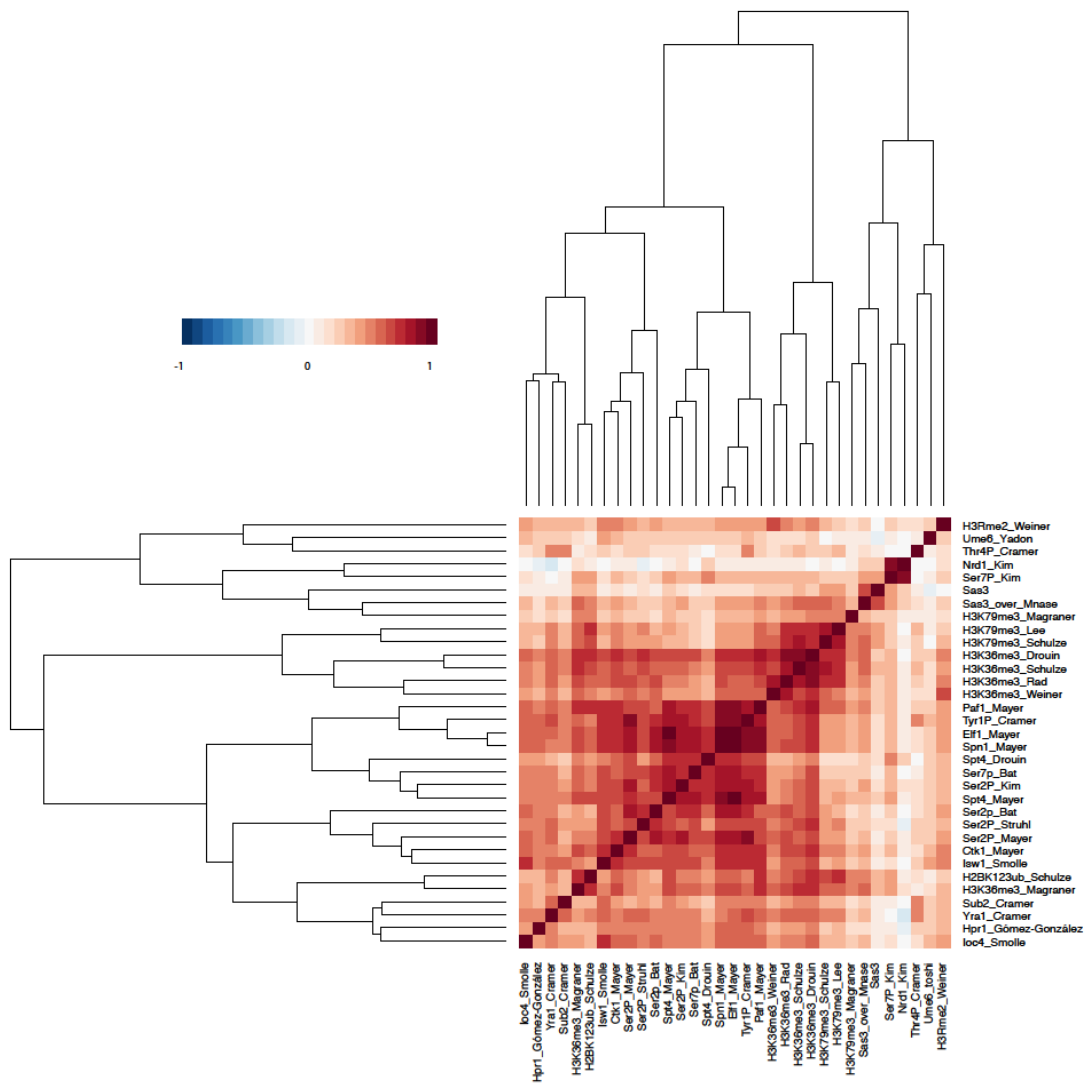


Figure 2.6: Meta-analysis of Sas3 occupancy reveals strong positive correlation with H3K36me3.

Heatmap and hierarchal clustering of meta-analysis data for 32 of the factors that show the highest positive correlation with Sas3 from Figure 2.5. Spearman correlations for all pairwise factors were determined based on average enrichment per nucleosome.

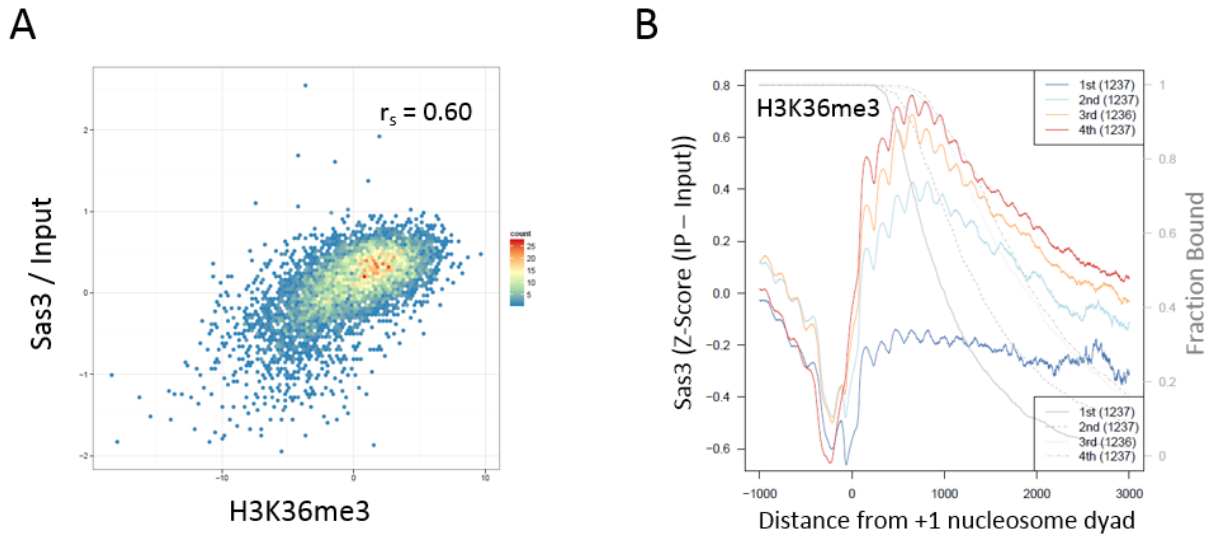


Figure 2.7: Sas3 Occupancy is highly positively correlated with H3K36me3. (A) Scatter plot of Sas3 (normalized to input) versus H3K36me3 for all the genes in the genome (Spearman correlation: 0.60) (Weiner *et al.* 2015). (B) Cumulative read count plots of Sas3 (normalized to input) per quartile of H3K36me3 enrichment across genes. Sas3 occupancy is plotted relative to the +1 nucleosome dyad of all yeast genes. Genes were plotted from 1000 bp upstream of the +1 nucleosome to their poly(A) termination site. Grey lines represent the fraction of genes included in the analysis at any given distance from the +1 nucleosome.

2.3.5 H3K4me3 and H3K36me are both required for efficient recruitment of NuA3.

In *S. cerevisiae*, the histone methyltransferases Set1 and Set2 are responsible for mono, di, and tri-methylation of H3K4 and H3K36, respectively (Briggs *et al.* 2001; Roguev 2001; Strahl *et al.* 2002; Krogan *et al.* 2002). In order to determine whether H3K36me3 plays a role in NuA3 recruitment, modified ChIP (mChIP) was used to test the ability of Sas3 to bind histones in a *set1Δ*, *set2Δ*, and double mutant deletion strain. Unlike traditional ChIP, mChIP allows for the efficient purification of protein-DNA macromolecules from mildly sonicated and gently clarified cellular extracts (Lambert *et al.* 2009). Interestingly, although histones co-purified with Sas3 in a wild type strain, deletion of *SET1* resulted in a complete loss of this interaction, while deletion of *SET2* resulted in only a partial loss (Figure 2.8A). This

suggests that methylation of H3K4, rather than H3K36, is more important for NuA3 recruitment, which is surprising considering the strong correlation that exists between H3K36me3 enrichment and Sas3 occupancy. Since co-precipitation experiments look at bulk effects rather than effects at specific genes, we performed a Sas3-6HA CHIP using an α HA antibody at a region within the *COX10* gene where H3K4me3 and H3K36me3 overlap (Figure 2.8B) (Weiner *et al.* 2015). This gene was selected as it was previously shown to be strongly targeted by NuA3 (Rosaleny *et al.* 2007). Unlike the mChIP data, deletion of *SET1* or *SET2* resulted in an equal loss of Sas3 occupancy at *COX10*, and this loss was not enhanced in the double mutant (Figure 2.8C). A similar trend was seen when the experiment was repeated in strains in which H3K4 and H3K36 were mutated to arginine (Figure 2.8D). Since H3K4me3 peaks at the 5' ends of genes while H3K36me3 peaks further into gene bodies, this may suggest that these two modifications function together to help recruit NuA3 across the entire length of a gene.

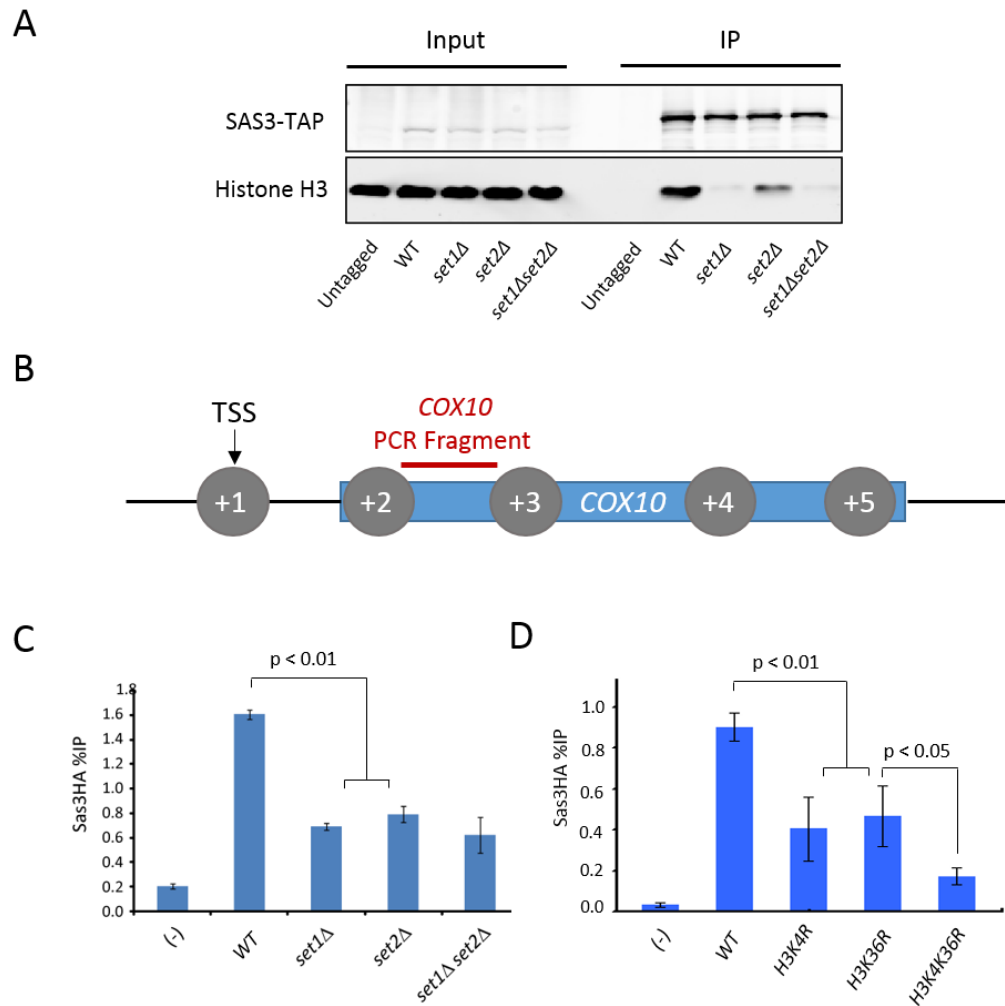


Figure 2.8: H3K4 and H3K36 methylation are both required for recruitment of Sas3 to chromatin.

(A) Sas3 was TAP-tagged in a wild type, *set1Δ*, *set2Δ*, and *set1Δset2Δ* strain and purified using IgG beads. Co-purifying histone H3 was detected by immunoblot with an α H3 antibody. An IgG antibody was used to show equal purification of Sas3-TAP. (B) Schematic representation of the *COX10* gene used for ChIP-qPCR analysis in (C) and (D). The positioning of nucleosomes, the transcription start site (Park *et al.* 2014), and the region amplified by qPCR using the primers in Table 2.4 are indicated. (C) (D) Levels of Sas3 at the 5' end of the *COX10* gene were measured by ChIP-qPCR in the indicated strains. The amount of Sas3 was measured as a percentage of input (%IP). Error bars indicate the standard error from the mean from three biological replicates, and p-values determined using a t-test are listed.

2.3.6 Identification of Pdp3 as a novel subunit of the NuA3 complex

Previous unpublished work in our lab has excluded both Nto1 and Eaf6 as additional chromatin-targeting candidates within NuA3, and although Taf14 is involved in chromatin targeting (as will be discussed in Chapter 3), its function is not dependent on H3K36me3. Interestingly, Pdp3, a protein of unknown function, is known to purify with members of the NuA3 complex (Krogan *et al.* 2006; Taverna *et al.* 2006; Vicente-Muñoz *et al.* 2014). In order to confirm the interaction between NuA3 and Pdp3, a Sas3-TAP mChIP was performed in a strain in which Pdp3 was HA-tagged. Indeed the two proteins co-purified, suggesting that this is a bona fide interaction (Figure 2.9A). We also performed the co-precipitation in a strain lacking *EAF6* and *YNG1*, as previous data in our lab suggested that the interaction between Pdp3 and NuA3 may be mediated through these subunits. Indeed deletion of *EAF6* resulted in a significant loss of Pdp3 from NuA3, while deletion of *YNG1* resulted in an even more dramatic loss, suggesting that Pdp3 interacts with the complex through Eaf6 and Yng1.

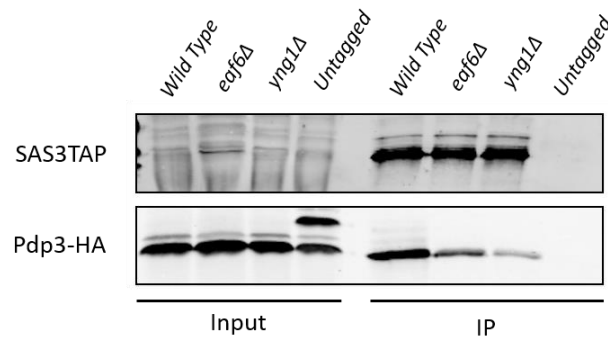


Figure 2.9: The association of Pdp3 with Sas3 is dependent on Eaf6 and Yng1. Sas3 was TAP-tagged in a wild type, *eaf6Δ*, and *yng1Δ* strain, and affinity purified using IgG beads. Co-purifying Pdp3-HA was detected by immunoblot using an α HA antibody.

2.3.7 Pdp3 and Yng1 function together to recruit NuA3 to chromatin

Pdp3 is an attractive candidate for targeting NuA3 to H3K36me3, as it possesses a conserved histone methyl binding domain: the PWWP domain. Furthermore, the majority of characterized PWWP domains have been shown to interact specifically with H3K36me3 (Vezzoli *et al.* 2010; Dhayalan *et al.* 2010; Wu *et al.* 2011; Maltby *et al.* 2012a; van Nuland *et al.* 2013; Li *et al.* 2013b). In order to determine whether Pdp3 is involved in NuA3 recruitment (possibly through interaction with H3K36me3), we took advantage of a known genetic interaction between *SAS3* and the gene encoding the other primary histone H3-specific HAT, *GCN5*. Deletion of *SAS3* alone does not have an effect on cell viability; however, deletion of the loci coding for *GCN5* and *SAS3* results in a synthetic lethal phenotype due to Gcn5's inability to acetylate Rsc4 in combination with loss of H3 acetylation (Howe *et al.* 2001; Choi *et al.* 2008). Interestingly, the same strain harboring a deletion of the PHD finger of Yng1 in place of *SAS3* deletion is viable, providing further evidence that NuA3's ability to interact with nucleosomes isn't entirely dependent on recruitment through the PHD finger of Yng1 (Martin *et al.* 2006b). This suggests that there is another subunit within NuA3 that is able to target the complex to chromatin, and taken together with our previous data it suggests that this recruitment likely occurs through H3K36me3. As such, we reasoned that deletion of both chromatin-targeting domains may be required to produce a synthetic lethal phenotype with deletion of *GCN5*.

To test whether Pdp3 functions in NuA3 recruitment, we asked whether deletion of *PDP3* is able to reproduce the *sas3Δ* phenotype in a *yng1ΔPHD* background. We created a strain lacking *GCN5* and the PHD finger of Yng1, and then either deleted *PDP3* or left it intact. *GCN5* was added back on a *URA3*-based vector, which can be selected against using media containing 5-fluoroorotic acid (5-FOA). The uracil biosynthetic pathway analog 5-FOA is converted to a toxic product in the presence of the Ura3 enzyme, so that cells which have lost the wild type *GCN5* plasmid can grow on media containing 5-FOA (Boeke *et*

al. 1984). Although deletion of *PDP3* or the PHD finger of Yng1 resulted in no additional phenotype in combination with deletion of *GCN5*, deletion of all three domains/subunits resulted in a synthetic sick phenotype similar to that seen in a *gcn5Δ sas3Δ* strain (Figure 2.10A). This phenotype is likely not due to complex instability caused by deletion of *PDP3*, as *pdp3Δ* had no effect on the levels of Sas3 in the cell (Figure 2.10B). Taken together this strongly suggests that Pdp3 and the PHD finger of Yng1 function together to recruit NuA3 to chromatin.

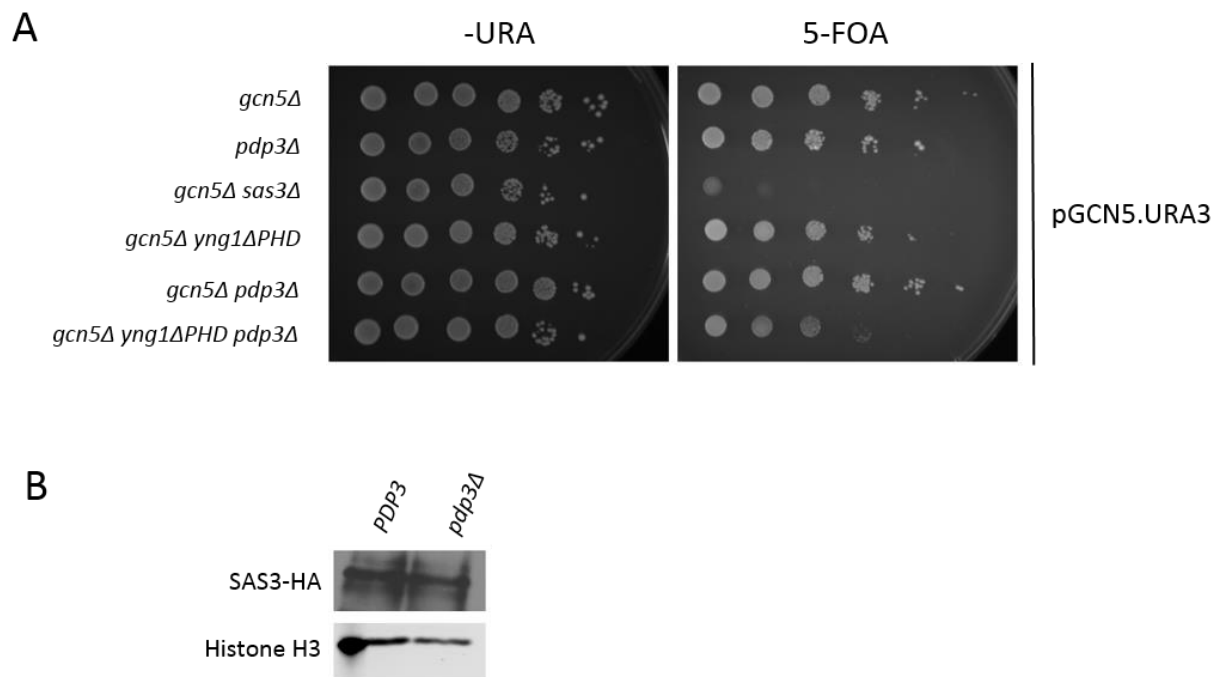


Figure 2.10: Deletion of *PDP3* results in a synthetic growth defect in combination with deletion of *GCN5* and loss of the PHD finger of *YNG1*. (A) Ten-fold serial dilutions of the indicated strains were plated on synthetic drop-out (-URA) media or synthetic complete media containing 5-FOA for three days at 30° C. (B) Immunoblot of Sas3-HA from WCEs of a *PDP3* and *pdp3Δ* strain using an αHA antibody. An αH3 antibody was used as a loading control.

Next, we sought to determine whether the PWWP domain of Pdp3 is involved in the chromatin-targeting of NuA3 by asking whether point mutations in the conserved residues of the domain also show a synthetic lethal phenotype in combination with *gcn5Δ yng1ΔPHD*. To this end we cloned three PWWP domain mutants of Pdp3 under the expression of their endogenous promoter into a *LEU2* based CEN vector. Residues F19, W20, and F47 were selected to be mutated to alanine, as the analogous residues in other PWWP domains make up the conserved methyl-binding pocket that is necessary for interaction with histones (Figure 2.11A and B)) (Vezzoli *et al.* 2010; Wu *et al.* 2011; Maltby *et al.* 2012a). As expected, a vector carrying a wild type copy of *PDP3* rescued growth in a *gcn5Δ yng1ΔPHD pdp3Δ* strain, confirming that the synthetic lethal phenotype was in fact due to loss of this gene (Figure 2.12). Surprisingly, the three Pdp3 PWWP domain mutants also rescued this synthetic growth defect. This is unexpected considering that the PWWP domain is the only annotated domain within the protein (Zdobnov and Apweiler 2001); however, since the exact cause of the *gcn5Δ sas3Δ* synthetic lethality is not fully understood, this does not exclude the possibility that the PWWP domain of Pdp3 is acting as a chromatin-targeting domain within NuA3.

A

HeHDGF	10-102	YKCGDLVFAKMKGPHNPARIDEMPEAA-----VKSTAN-KYQVF	FGTHETAFLGPKDLFPYEESEKFKGKP--NKRKGFSEGLWEIENNPVKAAGYQS
HePSIP1	5-97	FKPGDLIFAKMKGPHNPARVDEVPDGA-----VKPPTN-KLPIF	FGTHETAFLGPKDIFPYSENKEKYGKP--NKRKGFNEGLWEIDNNPKVKFSSQQA
HeDNMT3b	230-325	FGIGDLVWGIKGFENWPAWVSVKATS-----KRQAMSGMRWVQ	FGDGKFSVSDKLVALGLFSQHFNLATFNKLVSYRKAMYHALEKARVRAGKTFP
HeDNMT3A	340-435	FGIGELVWGLRGEENWPRIVSWMTG-----RSRAAEGTRWVM	FGDGKFSVVCVEKLMPLSSFCSAFHQATYNKQPMYRKAIEVQLVASSRAGKLF
ScYLR455w	5-103	IRIGDLVLCVGSFPNPAVVFQRLLRNDV---YRKRKSNCAVCF	FNDFTYYWEQPSRLKELDQDSIHNFILHNSKNANQRELVNAYKEAKNFDDFNVL
SpPDP1	50-148	LNFGRILVKAPGFPWNPALLRRKETKDSLNTNSSFNVLKVL	FPDFNFAMVKRNSVKPLDSEIAKFLG--SSKRKSKELIAYEASKTPPDLKEES
SpPDP2	123-272	YKPGMRVLTKMSGFPWNPMSVVTESKMTSVARKSKPKRAGTFYPVI	FPNKEYLWTGSDSLIPLTSEAISQFLE--KPKPKTASLIKAYKMAQSTPDLDSLS
ScIOC4	6-170	FQPTDIVLAKVKGFSANPAMIIINELIP-----KNDTLKSTYCVK	FCDDSYIWKPMMDMKILTSEDCKRWLGGKQRKNKKLIPAYEMMRGKNGIDIWEF

B

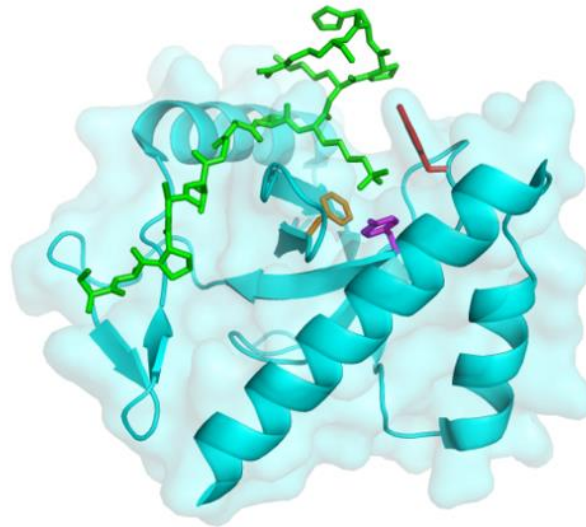


Figure 2.11: The PWWP domain of Pdp3 possesses the conserved residues that make up the H3K36me3-binding pocket of other PWWP domain proteins. (A) Protein sequence alignment of the PWWP domains of *S. cerevisiae* Pdp3 and loc4, *S. pombe* Pdp1 and Pdp2, and *H. sapien* HDGF, PSIP1, Dnmt3a and Dnmt3b. Residues predicted to make up the aromatic methyl-binding cage are highlighted as in (B). Note that in this alignment, *S. cerevisiae* Pdp3 is listed under its systematic name: YLR455w (B) Pymol structure of the PWWP domain of Brpf1 (Protein Database ID: 2X4X (Vezzoli, et al. 2010)). Residues Y1096 (red), Y1099 (purple), and F1147 (orange) form an aromatic pocket which interacts with the three K36 methyl groups of an H3 peptide (green).

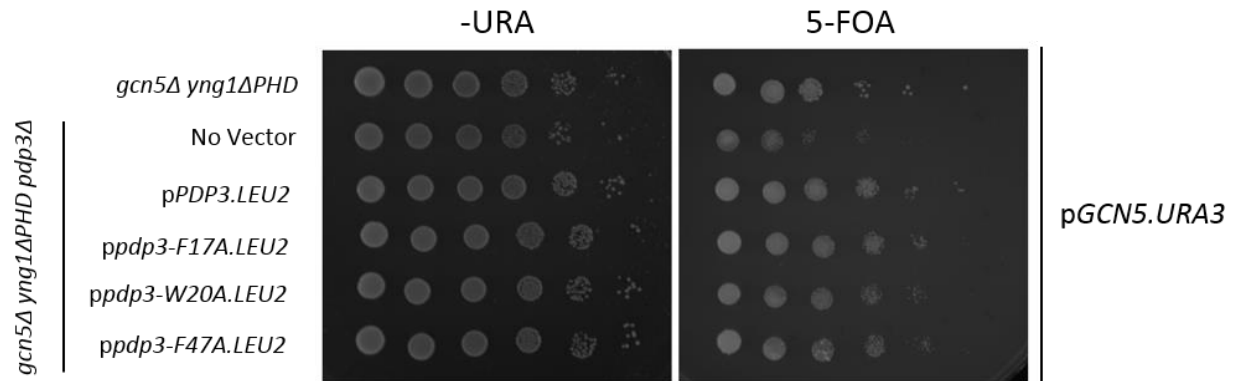


Figure 2.12: Pdp3 mutants with mutations in the residues making up the methyl-binding pocket do not result in a growth defect in a *gcn5Δ yng1ΔPHD* strain. Ten-fold serial dilutions of the indicated strains were plated on synthetic drop-out (-URA) media or synthetic complete media with containing 5-FOA for three days at 30° C.

2.4 DISCUSSION AND CONCLUSIONS

In this study we show that recruitment of the NuA3 HAT complex to specific regions of the genome is dependent on H3K36me3, and implicate the PWWP domain of Pdp3 in mediating this interaction. Previous studies suggested that recruitment of NuA3 to chromatin was dependent on both H3K4 and H3K36 methylation, leading to the hypothesis that multiple chromatin-targeting domains exist within the complex (Martin *et al.* 2006a). The PHD finger of Yng1 was the first chromatin-targeting domain of NuA3 to be identified, linking HAT activity to H3K4me3 (Martin *et al.* 2006b; Taverna *et al.* 2006). We introduce a novel subunit of the NuA3 complex, Pdp3, and implicate its PWWP domain in interaction with H3K36me3. We also present evidence that Sas3 - the catalytic subunit of the NuA3 complex - is found across gene bodies, and enriched at +5 and +6 nucleosomes similar to H3K36me3. Taken together we suggest a mechanism by which the PWWP domain of Pdp3 and the PHD finger of Yng1 function in combination to recruit NuA3 across the length of actively transcribed genes.

Our genome-wide localization data for Sas3, and by extension the NuA3 histone acetyltransferase complex, demonstrated that the complex localizes across gene bodies with a peak in enrichment at +5 and +6 nucleosomes. Despite an initial discrepancy between our data and that of Taverna *et al.* 2006 and Vicente-Muñoz *et al.* 2014, we showed that our data is in fact in agreement with theirs, and that this incongruity was due to differences in the method of statistical analysis employed. This highlights the importance of being cautious when interpreting sequencing data, as different methods of analysis can bias data in different ways. Nonetheless, we argue that we provide higher resolution data and more accurate mapping of NuA3 across the genome than these earlier datasets. In order to determine genome-wide localization of NuA3, Taverna *et al.* 2006 and Vicente-Muñoz *et al.* 2014 combined the use of DNA sonication and tiling microarrays (ChIP-chip). As sonication is limited to a minimal fragment length of approximately 200 bp even after extensive sonication, this limits the resolution of data acquired by this method (Fan *et al.* 2008). In the current study we chose to digest the DNA with micrococcal nuclease, as previous data from our lab suggested that both H3K4 and H3K36 methylation function in targeting of the NuA3 complex to chromatin, and Sas3 was able to co-precipitate DNA and histone H3 from MNase-treated lysates (data not shown) (Martin *et al.* 2006a). This increased the resolution of our data, as we were able to digest DNA to an average mono-nucleosome length of approximately 150 bp. Furthermore, we used paired-end Illumina sequencing (ChIP-seq) as our final method of detection which offers better resolution, higher signal-to-noise ratio, and greater dynamic range than hybridization to a microarray (Ho *et al.* 2011).

In this work we show evidence that the interaction of NuA3 with chromatin is dependent on H3K4me3 and H3K36me3. Previously published chromatin pulldown assays from our lab have shown that although both these modifications mediate the interaction of NuA3 with chromatin, loss of H3K36 methylation had a greater effect than loss of H3K4 methylation (Martin *et al.* 2006a). This contradicts work from this chapter, in which we showed that co-immunoprecipitation of Sas3 and histone H3 is only reduced by half upon deletion of *SET2*, but abolished entirely upon deletion of *SET1*. As both these assays

rely on immunoblotting as their read out, this discrepancy may be due to the semi-quantitative nature of this technique. To further complicate matters, ChIP-qPCR of Sas3 at the *COX10* gene suggests that these two modifications contribute equally to targeting of NuA3; however as only a single gene was tested, this may be a gene-specific event. Furthermore, H3K4me3 and H3K36me3 show different profiles of enrichment along gene bodies, suggesting that different results may be observed using primers specific for the 5' versus the 3' end of the gene (Pokholok *et al.* 2005). The results from these three different experiments allow us to conclude that methylation of both H3K4 and H3K36 is involved in targeting NuA3 to chromatin, but more work will need to be completed in order to determine the extent to which each of these modifications functions in this process.

Considering that in this chapter we show that the interaction between NuA3 and chromatin is dependent on H3K36 methylation, and that Sas3 occupancy correlates strongly with H3K36me3 in particular, it is tempting to speculate that recruitment through this modification may account for the enrichment in Sas3 observed at +5 and +6 nucleosomes; however the targets of other chromatin-targeting domains within the complex must also be considered. Although the PHD finger of Yng1 shows the strongest affinity for tri-methylated H3K4 which peaks at the 5' ends of genes, it also binds with slightly lower affinity to di-methylated H3K4 which shows a broader distribution, peaking at the 3' ends of actively transcribed genes (Pokholok *et al.* 2005; Martin *et al.* 2006b; Taverna *et al.* 2006). If NuA3 is capable of binding H3K4me2 and H3K4me3 through Yng1, and H3K36me3 through another chromatin-targeting domain, then this could account for the presence of Sas3 across the entirety of gene bodies, as well as its peak at +5 and +6 nucleosomes.

Data from our lab and others has demonstrated that the Yng1 PHD finger interacts with H3K4me3 but not H3K36me3, suggesting that some other subunit within the complex may be responsible for the latter interaction. (Martin *et al.* 2006b; Taverna *et al.* 2006). We use a genetic approach to identify Pdp3

as the likely candidate for this interaction. Pdp3 has a conserved PWWP domain that has been shown to be capable of specific interaction with H3K36me3 in a number of other eukaryotic proteins (Vezzoli *et al.* 2010; Dhayalan *et al.* 2010; Wu *et al.* 2011; Maltby *et al.* 2012a; van Nuland *et al.* 2013; Li *et al.* 2013b). Furthermore the PWWP domain of Pdp3 contains all the residues required for the formation of the H3K36me3-binding pocket (Vezzoli *et al.* 2010; Wu *et al.* 2011; Maltby *et al.* 2012a). Despite this, mutants of Pdp3 in which the residues making up this binding pocket have been replaced with alanine are not synthetically lethal in combination with deletion of *gcn5* and the PHD finger of *YNG1*. Although this is surprising, it can perhaps be explained by the sensitivity of the *gcn5Δsas3Δ* phenotype, which can be rescued by very minimal amounts of either HAT. Returning *SAS3* to the strain under the control of the *GAL1* promoter (which should only be activated in the presence of galactose) rescues growth even when plated on dextrose (data not shown). This suggests that “leaky” expression of *SAS3* from the *GAL1* promoter is enough to restore histone acetylation to a level that allows for growth in this strain. Although individual mutations of the three residues making up the H3K36me3-binding pocket of another yeast PWWP protein, *loc4*, reduces binding to chromatin, it does not abolish it completely (Maltby *et al.* 2012a). If this were also the case with the Pdp3 PWWP mutants, then it is possible that the residual binding to chromatin in a *yng1ΔPHD* strain is enough to rescue the synthetic lethality. It is also worth noting that although this phenotype is thought to be a result of Gcn5’s inability to acetylate Rsc4 in combination with loss of H3 acetylation, the mechanism underlying this synthetic lethality is poorly understood (Howe *et al.* 2001; Choi *et al.* 2008).

Further studies on the PWWP domain of Pdp3 and its role in targeting NuA3 to chromatin through interaction with H3K36me3 were precluded, as our hypothesis was shown to be correct in work published by Dr. Sean Taverna (Gilbert *et al.* 2014). Like us, his lab also identified Pdp3 as a member of the NuA3 histone acetyltransferase complex, and went on to show that it binds with specificity to H3K36 trimethylated peptides. This interaction is dependent on the aromatic residues making up the conserved

methyl-binding pocket. The interaction was also demonstrated *in vivo*, as deletion of *SET2* results in loss of Pdp3 from bulk chromatin. Furthermore, loss of *PDP3* results in decreased transcription at NuA3-regulated loci, demonstrating the importance of its chromatin-targeting activity. This data supports our hypothesis that the PWWP domain of Pdp3 interacts with H3K36me3, and in doing so plays a role in NuA3 recruitment.

Interestingly, Gilbert et al. 2014 found that deletion of *SET2* results in complete loss of Pdp3, but not Yng1, from bulk chromatin, suggesting that H3K36 methylation is required for the association of Pdp3 with NuA3. They also go on to show that *PDP3* is not synthetically lethal with *GCN5*, as the combined loss of these two genes does not result in the synthetic lethality observed in a *gcn5Δsas3Δ* strain. In contrast they find that deletion of *GCN5* and *YNG1* do produce this phenotype, and they use both these pieces of data as evidence that NuA3 exists in two functionally distinct forms: NuA3a and NuA3b. They argue that NuA3a, which is composed of all members of the complex except Pdp3, associates with promoter and 5' regions of genes through the H3K4me3-Yng1PHD finger interaction. As such, they posit that this subcomplex of NuA3 is involved in transcription initiation through acetylation of H3K14 and 23. In contrast they argue that NuA3b, which contains all members of the complex including Pdp3, interacts with H3K36me3 through the PWWP domain of this subunit, and is involved in transcription elongation within gene bodies. However, data from this chapter has shown that the interaction between Pdp3 and NuA3 is mediated by Yng1. It is therefore reasonable to assume that the synthetic lethality that is observed upon the combined loss of *GCN5* and *YNG1* is due not only to loss of chromatin targeting by the PHD finger of this subunit, but also to loss of the PWWP domain of Pdp3. Yng1, on the other hand, remains associated with NuA3 in the absence of Pdp3, allowing for chromatin-targeting through its PHD finger, and maintaining viability in the absence of *GCN5*. As such, we argue that although NuA3 may exist in two forms, the hypothesis that these forms are functionally distinct is not supported by the genetic data presented by Gilbert et al. 2014.

By now it is well accepted in the field of chromatin research that transcription and acetylation are inextricably linked. Numerous studies have confirmed that histone acetylation at promoters enhances binding of TATA box-binding protein (TBP) and the RNAPII holoenzyme, presumably by altering chromatin structure in such a way as to make the promoter more accessible to these factors (Bhaumik and Green 2002; Qiu *et al.* 2004). In agreement with a role in transcription initiation, genome-wide localization studies show that histone acetylation generally peaks in promoter regions (Schübeler *et al.* 2004; Kurdistani *et al.* 2004; Pokholok *et al.* 2005; Barski *et al.* 2007; Wang *et al.* 2008). Nonetheless, some acetylation marks such as H3K14ac, H3K23ac, H4K12ac, and H4K16ac are also found throughout transcribed genes suggesting a role in transcription elongation. Indeed, several HATS – including Gcn5 – have been shown to be recruited to transcribed genes through association with the phosphorylated CTD of elongating RNAPII (Govind *et al.* 2007). Furthermore, loss of two H3 HATs, Gcn5 and Elp3, results in a decrease in transcription at multiple genes without affecting TBP binding, suggesting that loss of histone acetylation is disrupting a step downstream of initiation (Kristjuhan *et al.* 2002). In this study, we provide evidence of the recruitment of another H3 HAT, NuA3, to actively transcribed gene bodies through association with both H3K4me3 and H3K36me3. This suggests a role for H3K14 and 23 acetylation in transcription elongation, most likely of which is the disruption of DNA-histone or histone-histone contacts following the passage of RNAPII in order to create a chromatin structure more permissive to multiple rounds of transcription. This has been demonstrated for both Gcn5 and NuA4, which are recruited to coding regions to increase nucleosome eviction and stimulate RNAPII processivity (Govind *et al.* 2007; Ginsburg *et al.* 2009). More work will need to be done in order to determine whether recruitment of NuA3 to coding regions has a similar effect on transcription elongation.

Overall, our study combined with that of Gilbert *et al.* 2014 details a targeting mechanism for the NuA3 complex, which in turn provides a targeting mechanism for global acetylation. The PHD finger of Yng1 is able to interact with methylated H3K4, and the PWWP domain of Pdp3 is able to interact with

methyated H3K36. Together these two chromatin-targeting domains recruit NuA3 across the entirety of gene bodies, where Sas3 is able to catalyze the acetylation of H3K14 and H3K23.

CHAPTER 3:

THE YEATS DOMAIN OF TAF14 RECRUITS NUA3 TO CHROMATIN THROUGH INTERACTION WITH GCN5-TARGETED ACETYLATION

3.1 INTRODUCTION

In eukaryotes, DNA is packaged into a nucleoprotein structure consisting of DNA, histones, and non-histone proteins. Regulation of this structure plays an important role in controlling gene expression by preventing or enabling the accessibility of DNA to the transcriptional machinery. In *S. cerevisiae*, there are currently three known mechanisms by which chromatin structure is regulated: the post-translational modification of histones, the ATP-dependent remodeling of chromatin, and the deposition of histone variants. All of these activities are catalyzed by multi-protein complexes that are targeted to specific regions of the genome. One way in which this specific chromatin targeting can occur is through readers of histone post-translational modifications. An increasing number of these conserved protein domains have been identified and characterized over the past few decades; however the protein domains responsible for recruitment of many chromatin-modifying complexes remain unknown.

The YEATS domain is a conserved eukaryotic domain that is present exclusively in transcription-related complexes. It is found in more than 100 proteins from over 70 organisms, and receives its name from the first five proteins in which it was found to occur (Yaf9, ENL, AF-9, Taf14 and Sas5) (Schulze *et al.* 2009). In *S. cerevisiae*, three YEATS domain proteins exist: Taf14, Yaf9 and Sas5. In humans, ENL, AF9 and GAS41 are the three best characterized YEATS domain proteins, and mutation of each has implications in cancer (Schulze *et al.* 2009). The structures of the YEATS domains of Taf14 and Yaf9 reveal that it adopts an immunoglobulin (IgG) fold - a common fold of varying functionality that is generally involved in protein-ligand interactions (Williams and Barclay 1988; Wang *et al.* 2009; Zhang *et al.* 2011). Indeed, the YEATS domains of two human proteins, ENL and AF9, target the Super Elongation Complex (SEC) to actively transcribed regions of the genome through direct association with the PAF complex (He *et al.* 2011).

Additional evidence suggests that the YEATS domain also binds histones. The YEATS domain of yeast Yaf9 has been demonstrated to bind histones H3 and H4, and that of human ENL to bind histones H3 and H1 *in vitro* (Zeisig *et al.* 2005; Wang *et al.* 2009). More recently, human AF9 was shown to bind H3K9 acetylation, and to a lesser degree H3K18 and 27 acetylation, and this interaction was demonstrated to be mediated through its YEATS domain (Li *et al.* 2014). This raises the question of whether the YEATS domain is a universal reader of histone acetylation, or whether its function is protein dependent.

In *S. cerevisiae*, Taf14 is the YEATS domain protein present in the greatest number of chromatin-modifying complexes (SWI/SNF, INO80, NuA3, TFIID, and TFIIF). Of these, the NuA3 histone acetyltransferase complex is the least well studied. The complex is composed of at least six subunits (Sas3, Taf14, Yng1, Nto1, Pdp3 and Eaf6) and catalyzes the acetylation of H3K14 and 23 (Howe *et al.* 2001; Taverna *et al.* 2006). Previous studies have shown that the PHD finger of Yng1 and the PWWP domain of Pdp3 are able to bind H3K4me3 and H3K36me3, respectively, functioning together to recruit NuA3 across the length of actively transcribed genes (Gilbert *et al.* 2014; D. G. E. Martin, Baetz, *et al.* 2006; Taverna *et al.* 2006 and Chapter 2). Although Sas3 occupancy correlates strongly with H3K36me3, supporting a role for Pdp3 in chromatin targeting, it correlates modestly with H3K4me3 (Chapter 2). This is surprising considering that the interaction between the PHD finger of Yng1 and H3K4me3 is the proposed mechanism for recruitment of NuA3 to the 5' end of genes where H3K14 and 23 acetylation are most enriched, and suggests the existence of another chromatin-targeting domain within the complex that aids in this function.

In addition to Sas3, Gcn5 is the other major histone H3 acetyltransferase in yeast. It is localized primarily to promoters through interaction with transcriptional activators, and to a lesser degree within the transcribed region of genes where it associates with the elongating polymerase (Kuo *et al.* 1998, 2000; Robert *et al.* 2004; Govind *et al.* 2007; Xue-Franzén *et al.* 2010). This is reflected in genome-wide patterns of histone acetylation, which show a similar enrichment in promoters that trails into gene bodies

(Schübeler *et al.* 2004; Kurdistani *et al.* 2004; Pokholok *et al.* 2005; Barski *et al.* 2007; Wang *et al.* 2008). Gcn5 functions as the catalytic subunit of three HAT complexes - SAGA, SLIK/SALSA and ADA - all of which contain the Gcn5/Ada2/Ada3 HAT module, but vary in auxiliary subunits (Grant *et al.* 1997; Eberharter *et al.* 1999; Sterner *et al.* 2002; Pray-Grant *et al.* 2002). Together, these complexes are thought to target the tail of histone H3 for acetylation at K4, K9, K14, K18, K23, K27, and K36 (Morris *et al.* 2007; Guillemette *et al.* 2011; Kuo and Andrews 2013). Interestingly, although both Gcn5 and Sas3 catalyze the acetylation of H3K14, deletion of *GCN5*, but not *SAS3*, results in loss of H3K14ac from bulk histones (Maltby *et al.* 2012b). Furthermore, a positive correlation exists between Gcn5 occupancy and loss of H3K14ac in a *gcn5Δ* strain, but not in a *sas3Δ* strain (Rosaleny *et al.* 2007).

In this study we present evidence that the YEATS domain of Taf14 is a histone acetyl-binding domain that functions in recruitment of NuA3 to actively transcribed genes. Using peptide-binding assays, we showed that Taf14 binds independently to H3K9, 18, and 27 acetylated peptides. This interaction was dependent on conserved residues within the YEATS domain, which were also required for association of NuA3 with chromatin. Furthermore recruitment of NuA3 to chromatin was dependent on Gcn5. Finally, we used a genetic approach to confirm that H3K14 and 23 are the targets of the histone acetyltransferase activity of NuA3. Overall, we have elucidated a novel mechanism by which Gcn5-deposited histone acetylation promotes further acetylation of H3K14 and 23 by recruitment of NuA3.

3.2 MATERIALS AND METHODS

3.2.1 Yeast Strains and Plasmids

All strains in this study are isogenic to S288C, and are listed in Table 3.1. Yeast culture and genetic manipulations were performed using standard protocols (Ausubel FM, Brent R, Kingston RE, Moore DD, Seidman JG, Smith JA 1987). Genomic deletions were verified by PCR analysis and whole cell extracts were

generated as previously described (Ausubel FM, Brent R, Kingston RE, Moore DD, Seidman JG, Smith JA 1987; Kushnirov 2000).

Table 3.1: Yeast strains used in this study

Yeast Strain	Mating Type	Genotype
YKM011	Mat a	<i>his3Δ1 leu2Δ0 met15Δ0 ura3Δ0 ies2::KAN</i>
YKM012	Mat a	<i>his3Δ1 leu2Δ0 met15Δ0 ura3Δ0 swi3::KAN</i>
YLH101	Mat a	<i>his3Δ200 leu2Δ1 lys2-128δ ura3-52 trp1Δ63</i>
YLH348	Mat a	<i>his3Δ200 leu2Δ1 lys2-128δ ura3-52 trp1Δ63 (hht1-hhf1)::LEU2 (hht2-hhf2)::HIS3 gcn5::KAN</i>
YLH367	Mat a	<i>his3Δ200 leu2Δ1 lys2-128δ ura3-52 trp1Δ63 trp1D63 gcn5::HIS3 sas3::KAN</i>
YLH370	Mat a	<i>his3Δ200 leu2Δ1 lys2-128δ ura3-52 trp1Δ63 taf14::KAN</i>
YLH427	Mat a	<i>his3Δ200 leu2Δ1 lys2-128δ ura3-52 trp1Δ63 gcn5::TRP taf14::KAN</i>
YLH428	Mat a	<i>his3Δ200 leu2Δ1 lys2-128δ ura3-52 trp1Δ63 gcn5::TRP taf14::KAN yng1DPHD::HIS</i>
YLH755	Mat a	<i>his3Δ200 leu2Δ1 lys2-128δ ura3-52 trp1Δ63 taf14::KAN SAS3-6HA::TRP</i>
YLH856	Mat a	<i>his3Δ200 leu2Δ1 lys2-128δ ura3-52 trp1Δ63 SAS3TAP::TRP taf14::KAN TAF14::LEU</i>
YLH857	Mat a	<i>his3Δ200 leu2Δ1 lys2-128δ ura3-52 trp1Δ63 SAS3TAP::TRP taf14::KAN TAF14-LH58AA::LEU</i>
YLH858	Mat a	<i>his3Δ200 leu2Δ1 lys2-128δ ura3-52 trp1Δ63 SAS3TAP::TRP taf14::KAN TAF14-PPF72AAA::LEU</i>
YLH859	Mat a	<i>his3Δ200 leu2Δ1 lys2-128δ ura3-52 trp1Δ63 SAS3TAP::TRP taf14::KAN TAF14-GWG80AAA::LEU</i>
YLH889	Mat a	<i>his3Δ200 leu2Δ1 lys2-128δ ura3-52 trp1Δ63 gcn5::TRP Sas3-6HA::HIS</i>
YVM110	Mat a	<i>his3Δ200 leu2Δ1 lys2-128δ ura3-52 trp1Δ63 gcn5::TRP</i>
YVM107	Mat a	<i>his3Δ200 leu2Δ1 lys2-128δ ura3-52 trp1Δ63 gcn5::TRP yng1DPHD::HISMX6</i>
YVM146	Mat a	<i>his3Δ200 leu2Δ1 lys2-128δ ura3-52 trp1Δ63 SAS3-6HA::TRP</i>

All plasmids used in this study are listed in Table 3.2. Genetic manipulations were performed using standard protocols (Gillam and Smith 1979) on readily available yeast vectors (Sikorski and Hieter 1989; Mumberg *et al.* 1994). A *TRP1* plasmid expressing wild-type *HHT2* and *HHF2* was constructed by ligation of the *SpeI* restricted fragment from pDM18 into the *SpeI* site of pRS414 (Duina and Winston 2004). Plasmids expressing mutant versions of H3 were constructed by replacing the *BamHI/XhoI* fragment from this plasmid with synthesized DNA fragments. All genes are under the expression of their endogenous promoters.

Table 3.2: Plasmids used in this study

Plasmid	Description
p170	pTAF14FLG.416
p184	pGcn5FLG.416
p417	pTAF14.405
p418	pTAF14-L58AH59A.405
p477	pTAF14-PPF72AAA.405
p481	pTAF14-GWG80AAA.405
p499	pHHF2.hht2K9,14,18,23Q.414
p500	pHHF2.hht2K9Q.414
p501	pHHF2.hht2K14Q.414
p502	pHHF2.hht2K18Q.414
p503	pHHF2.hht2K23Q.414
p529	pHHF2.hht2K9,14Q.414
p530	pHHF2.hht2K9,18Q.414
p531	pHHF2.hht2K14,18Q.414

Plasmid	Description
p532	pHHF2.hht2K14,23Q.414
p533	pHHF2.hht2K9,14,18Q.414
p542	pGST-Taf14
p543	pGST-Taf14-GWG80AAA

3.2.2 Immunoblot Analysis

Immunoprecipitations and lysates were analyzed by SDS-PAGE and immunoblotting with the antibodies and dilutions listed in Table 3.3. Signal was visualized either by infrared detection and quantification using the Licor Odyssey System, or by enhanced chemoilluminescence using a Konica Minolta SRX-101A processor.

Table 3.3: Antibodies used in this study

Antibody	Animal	Dilution	Company	Catalogue Number
α GST	Rabbit	1:5000	Santa Cruz Biotechnology	sc-459
α H3	Rabbit	1:5000	GenScript	Custom antibody raised to yeast specific antigen: CKDIKLARRLRGERS
α HA	Rat	1:500	Roche	11867431001
α HA-HRP	Rat	1:5000	Roche	12013819001
α IgG-HRP	Rabbit	1:5000	GE HealthCare	NA934V
α PAP	Rabbit	1:5000	Sigma-Aldrich	P1291
α Taf14	Rabbit	1:5000	From Dr. Joseph Reese	N/A

3.2.3 Peptide Pulldowns

Biotinylated histone peptides were synthesized by Anaspec. For pull-down assays, approximately 1 µg of GST-tagged recombinant protein was incubated with 1 µg of biotinylated histone peptides in binding buffer (50 mM Tris-HCl, pH 7.5, 150 mM NaCl, 0.05% NP-40) overnight at 4°C with rotation. After a 1 hour incubation with streptavidin M-280 Dynabeads (Life Technologies) and extensive washing, bound proteins were analyzed by SDS-PAGE and immunoblotting using an anti-GST antibody (Table 3.3).

3.2.4 MODified Histone Peptide Array

A MODified Histone Peptide Array (Active Motif) was blocked in 5 mL TTBS buffer (10 mM Tris-Cl pH 7.4, 0.05% Tween-20, 150 mM NaCl) with 5% skim milk for 4 hours at room temperature with gentle shaking. After performing three 5 minute washes in TTBS buffer, the array was incubated with 50 µg recombinant GST-Taf14 diluted in 5 mL binding buffer (50 mM Tris-HCl pH 7.5, 150 mM NaCl, 0.05% NP-40) at 4°C overnight with gentle shaking. Following incubation with αGST and αRabbit-IgG-HRP antibodies, signal was visualized by enhanced chemoilluminescence. Quantification and analysis of interactions was performed using Active Motif Array Analyze Software (<http://www.activemotif.com/catalog/668/modified-histone-peptide-array>).

3.2.5 Chromatin Immunoprecipitation and Quantitative PCR (ChIP-qPCR)

The chromatin immunoprecipitation protocol used in this study was adapted from that performed by Nelson, Denisenko, and Bomsztyk 2006. Cells were grown in 50 mL YPD to an OD₆₀₀ of 0.8 and cross-linked with 1% formaldehyde for 30 minutes at room temperature. The reaction was stopped by the

addition of 125 mM glycine, and incubation at room temperature for a further 15 minutes. Pellets were washed twice with cold PBS.

Following resuspension in 300 μ L lysis buffer (50 mM HEPES pH 7.5, 140 mM NaCl, 0.5 mM EDTA, 1% triton X-100, 0.1% sodium deoxycholate), cells were lysed mechanically by the addition of 500 μ L glass beads followed by vortexing (Scientific Industries Disruptor Genie) for 20 minutes at 4°C. Lysates were sonicated at high output for 30 seconds on/30 seconds off for 10 minutes using a Diagenode Bioruptor to obtain an average fragment length of approximately 500 bp. A further 400 μ L lysis buffer was added to each sample, and the lysates were clarified by centrifugation at 10 000 rpm for 10 minutes. Ten percent of the lysate was reserved for input.

Lysates were incubated with 0.25 μ g anti-HA antibody (Table 2.3) and rotated at 4°C overnight, followed by pull out with 100 μ L Protein G Dynabeads (Life Technologies) at 4°C for 1 hour. Beads were washed twice each with lysis buffer (50 mM HEPES pH 7.5, 140 mM NaCl, 0.5 mM EDTA, 1% Triton-X-100, and 0.1% sodium deoxycholate), lysis buffer + 500 mM NaCl, and lithium buffer (10 mM Tris-Cl pH 8.0, 250 mM LiCl, 0.6% NP-40, 0.5% sodium, deoxycholate, and 1 mM EDTA), followed by a single wash with TE. The beads were then resuspended in 100 μ L of a 10% chelex 100 slurry and boiled for 10 minutes to inactivate DNases. Cross-links were reversed and DNA isolated by the addition of 20 μ g proteinase K and incubation at 55°C for 30 minutes, followed by boiling for 10 minutes to inactivate the proteinase. Samples were centrifuged for 1 minute at 13,000 rpm (Eppendorf microfuge, model 5415D), and supernatant transferred to a fresh tube. The beads were then washed in 120 μ L dH₂O, and the supernatant pooled with that from the previous step.

Immunoprecipitated and input DNA were amplified using an Applied Biosystems Step One Plus Real-Time PCR System using the primer pairs listed in Table 3.4. Each PCR reaction consisted of 2 mM Tris-Cl, 1 mM KCl, 1 mM (NH₄)₂SO₄, 0.2 mM MgSO₄, 0.01% Triton-X-100, 0.2 mM dNTPs, 1.6 mM of each primer,

1x SYBR green, and 0.5 μ L Taq polymerase to a volume of 25 μ L. PCRs went through a program of 94°C for 2 minutes followed by 40 cycles of the following: 94°C for 30 seconds, 58°C for 1 minute, and 72°C for 30 seconds. Percent IP values were calculated and shown relative to wild type.

Table 3.4: Primers used in this study

Primer Name	Sequence
COX10-s	CGG AAT CAT GGC GGG AAA C
COX10-a	GGA AGT TGT GTG CTT GCA TCG

3.3 RESULTS

3.3.1 The YEATS domain of Taf14 mediates the interaction between NuA3 and histone H3

It has long been suggested that the YEATS domain is involved in chromatin targeting. In order to test this function in the NuA3 histone acetyltransferase complex, we once again took advantage of the *sas3 Δ gcn5 Δ* synthetic lethal phenotype discussed in Chapter 2, and asked whether deletion of *TAF14* is able to reproduce a *sas3 Δ* phenotype in a *yng1 Δ PHD* background. We created a strain lacking *GCN5* and the PHD finger of Yng1, and then added back *GCN5* on a *URA3*-based vector which can be selected against using media containing 5-FOA. We then either deleted *TAF14* or left it intact. Interestingly, deletion of *TAF14* alone resulted in a slight growth defect in combination with deletion of *GCN5*, and deletion of all three domains/subunits resulted in a synthetic lethal phenotype similar to that seen in a *gcn5 Δ sas3 Δ* strain (Figure 3.1A). Although this at first suggested to us that Taf14 and Yng1 function together to target NuA3 to chromatin, Sas3 levels were significantly reduced in the whole cell extracts of *taf14 Δ* mutants indicating that the phenotype may be the result of complex instability (Figure 3.1B). In order to further

probe the role of Taf14 in NuA3, its function in complex recruitment must be separated from its function in complex stability.

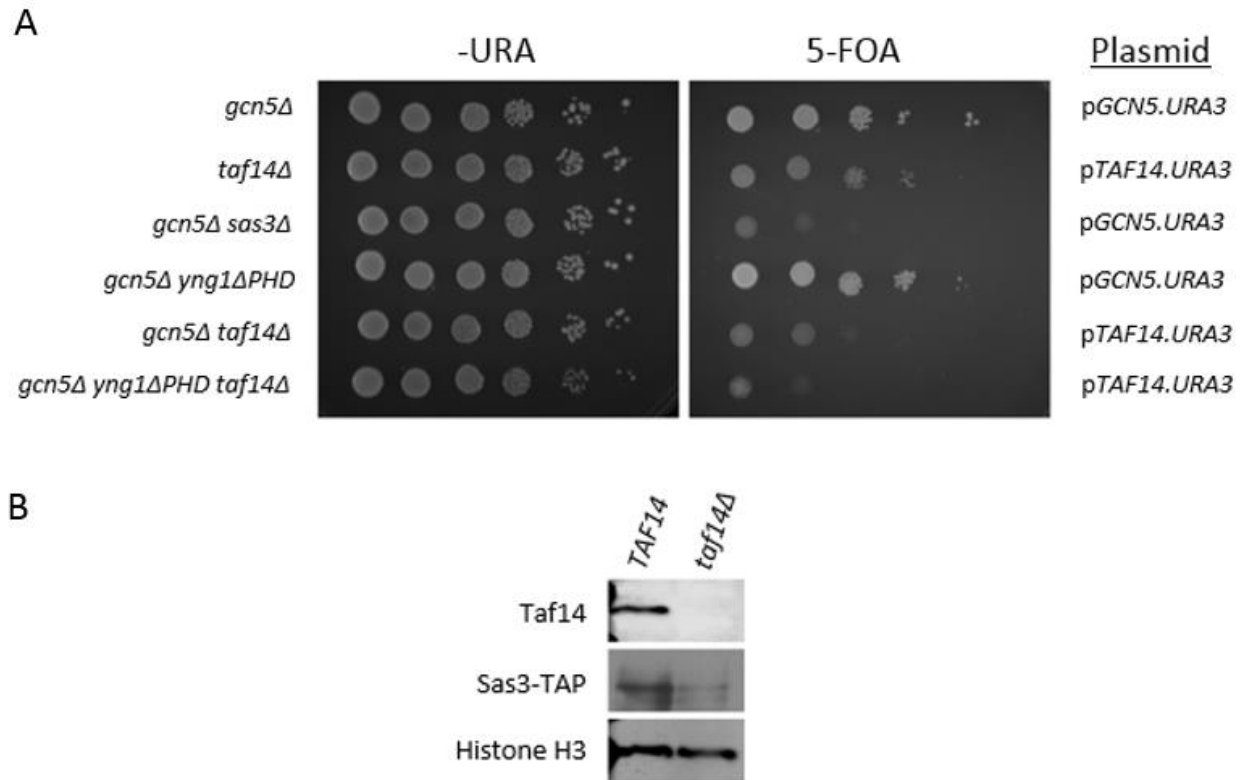
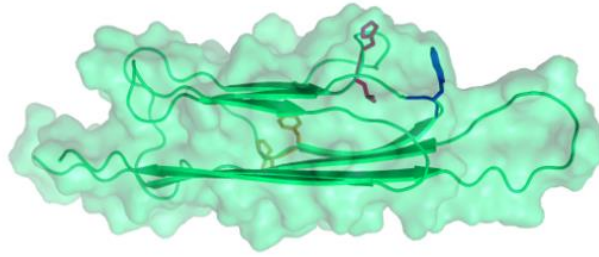


Figure 3.1: Deletion of *TAF14* results in a synthetic lethal phenotype in combination with deletion of *GCN5* and the PHD finger of *YNG1*. (A) Ten-fold serial dilutions of the indicated strains were plated on synthetic drop-out (-URA) media or synthetic complete media containing 5-FOA for three days at 30°C. (B) Immunoblot of Sas3-HA from WCEs of a *TAF14* and *taf14Δ* strain using an αHA and αTaf14 antibody. An αH3 antibody was used as a loading control.

Taf14 contains a YEATS domain – a conserved eukaryotic domain of unknown function found exclusively in general transcription factors and chromatin-remodeling and modifying complexes (Schulze *et al.* 2009). In order to try to separate the effect of Taf14 on complex recruitment and stability, mutations

were made within conserved residues of the YEATS domain in the hopes of disabling the chromatin-targeting function while maintaining the structural integrity of NuA3 (Figure 3.2A and B). Two sets of consecutively conserved residues within the YEATS domain of Taf14 were mutated to alanine (L58/H59 and G80/W81/G82). Three additional conserved residues were also selected for mutation (P72/P73/F74), as they were shown to confer sensitivity to MMS, HU, and temperature when mutated in Taf14 and Yaf9 (Zhang *et al.* 2004). Unlike complete loss of *TAF14*, neither mutation of L58/H59 nor mutation of G80/W81/G82 resulted in a growth defect, suggesting that these residues are not involved in protein or complex stability (Figure 3.3A). In contrast, the PPF72AAA mutant exhibited a similar growth defect to that of a *taf14Δ* strain, indicating that these residues play a role in some essential function. Considering that these residues are buried within the YEATS domain and form a sharp β -turn connecting β -sheets 4 and 5, it is likely that mutation of these residues would result in an unstable protein (Figure 3.2A). Nonetheless, in order to gain insight into the potential role of L58/H59, P72/P73/F74, and G80/W81/G82 in chromatin-targeting, the YEATS domain mutants were tested for their ability to recapitulate a *sas3Δ* phenotype in a *gcn5Δ yng1ΔPHD* strain. Although the PPF72AAA mutant recapitulated the synthetic lethality of a *sas3Δ gcn5Δ* strain, both the LH58AA and GWG80AAA mutants exhibited no growth defect (Figure 3.3B); however, this does not exclude the possibility that these mutants, or other mutants within the YEATS domain of Taf14, function in chromatin-targeting of the NuA3 complex, since the exact cause of the *gcn5Δ sas3Δ* synthetic lethality is not fully understood.

A



B

ScYAF9	64-129	FKLHDTYPNFVRSIEA PP ELIET GW GEFDINIKVYFVEEANEKVLNFYHRLRLHPYANP-----VPNSDNGNEQNTIDHNS
HsGAS41	68-129	FKLHESYGNPLRVVTK PP VEITET GW GEFEI ¹ IKIFFIDPN-ERFVTLYHLLKLF-----QSDINAML
HsAF9	50-162	FHLHESFPRPKRVCKD PP YKVEESGYAGFILPIEVYFKNKEEPRKVRFDYDLFLHLEGHPVNHLCRCEKLTFN ² NPTEDFRKLLKAGGDPNRSIH ³ SSSSSSSSSSSSSS
HsENL	50-160	FWLHDSFFPKPRVCKE PP YKVEESGYAGFIMPIEVHFKNKEEPRKVCFTYDLFLNLEGNPPVNHLCRCEKLTFN ² NPTTEFRYKLLRAGG--VMVMPEGADIVSRSPDYPM
ScTAF14	56-110	YHLHPTFANFNRTFTD PP FRIEEQ GW GFPLDISVFLLEKAGERKIPHDNLFLQES-----YEVEHV ⁴ IQIPLNKPLL
ScSAS5	57-111	YHLHSSFKQPKRRLNS LP FIKET GW GFNLKIECFFIGNAGKFSIEHDLTFEDDA-----YAVDYIVDVPHEFSHL

Figure 3.2: Conserved residues within the YEATS domain of Taf14. (A) Crystal structure of the YEATS domain of Taf14 with residues L58 and H59 highlighted in red, residues G80, W81, and G82 highlighted in blue, and residues P72, P73, and F74 highlighted in yellow. (B) Sequence alignments of YEATS domains in Taf14, Sas5, and Yaf9, as well as in higher eukaryotes. The residues selected for mutation to alanine are highlighted in the same colours as in (A).

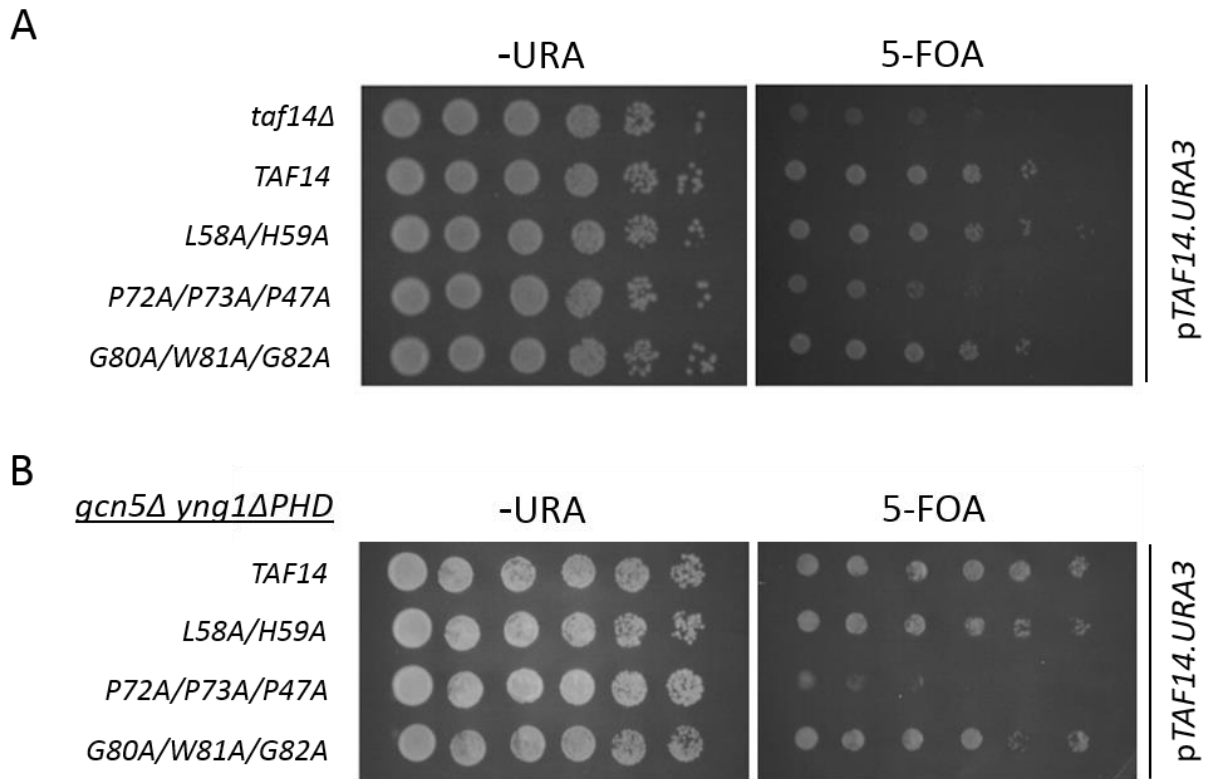


Figure 3.3: Taf14 YEATS domain mutants have no growth defects on their own or in a *gcn5Δ yng1ΔPHD* strain under regular growth conditions (A)(B) Ten-fold serial dilutions of the indicated strains were plated on synthetic drop-out (-URA) media or synthetic complete media containing 5-FOA and grown for three days at 30°C.

If the YEATS domain of Taf14 is responsible for recruitment of NuA3 to chromatin, then disruption of this function should disrupt the interaction between the complex and histone H3. To test this, we TAP-tagged Sas3 and performed a modified chromatin immunoprecipitation (mChIP) in strains expressing either wild type *TAF14* or the YEATS domain mutants. Unlike traditional ChIP, mChIP allows for the efficient purification of protein-DNA macromolecules from mildly sonicated and gently clarified cellular

extracts (Lambert *et al.* 2009). As expected, histone H3 co-purified with Sas3 in a wild type strain. Not surprisingly, mutation of P72, P73, and F74 to alanine resulted in lower than average levels of both Taf14 and Sas3, as well as complete disruption of the interaction between NuA3 and histone H3 (Figure 3.4A). Taken with the earlier growth rate data, this suggests that mutation of these residues destabilizes Taf14, and consequently Sas3, leading to their degradation. More interestingly, mutation of L58 and H59, or G80, W81, and G82 to alanine had no visible effect on Taf14 or Sas3 stability, but disrupted the interaction between Sas3 and histone H3 (Figure 3.4A and B). This strongly suggests that the YEATS domain of Taf14 is involved in mediating the interaction between NuA3 and chromatin.

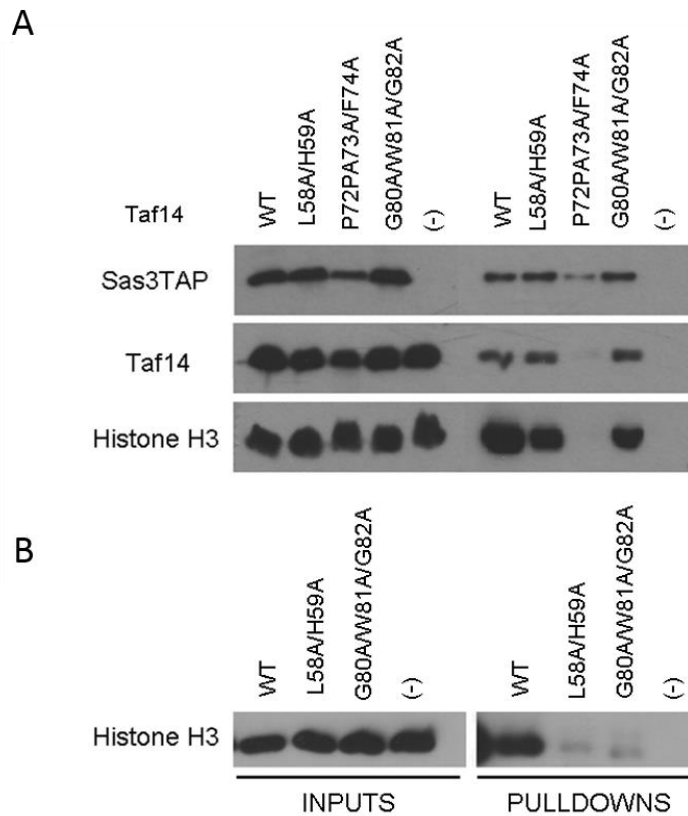


Figure 3.4: Taf14 YEATS domain mutants impair the interaction between Sas3 and histone H3. (A) Sas3 was TAP-tagged in wild type, *taf14-LH58AA*, *taf14-PPF72AAA*, and *taf14-GWG80AAA* strains, and purified by mChIP using IgG beads. Co-purifying Taf14 and histone H3 was detected by immunoblot using α Taf14 and α H3 antibodies. (B) Repetition of the immunoblot in (A) at a lower exposure. Input and pulldown lanes in (A) are as labeled in (B).

3.3.2 The YEATS domain of Taf14 interacts with acetylated H3K9, 18, and 27 *in vitro*

YEATS domains exist not only in *S. cerevisiae*, but in higher eukaryotes as well. It was recently shown that the YEATS domain of a human protein, AF9, interacts with H3K9 acetylation and to a lesser extent H3K18 and H3K27 acetylation (Li *et al.* 2014). Structural analysis of this protein reveals an aromatic cage within the YEATS domain that binds specifically to the acetylated lysine over the unmodified form.

Point mutation of any of the six residues making up this binding pocket (F28, H56, S58, F59, Y78, and F81) results in complete disruption between AF9 and H3K9 acetylated peptides. Interestingly, sequence alignment of the YEATS domains of AF9 and Taf14 revealed that H59 and W81 of the Taf14 LH58AA and GWG80AAA mutants were analogous to H56 and Y78 of the AF9 aromatic cage (Figure 3.2B). As these mutants disrupt the interaction between NuA3 and chromatin, it is highly likely that H59 and W81 also form a similar binding pocket in Taf14, and suggests that histone acetylation may be a target of its YEATS domain.

To determine whether the YEATS domain of Taf14 interacts with acetylated histones, we bacterially expressed and purified wild type Taf14 and the GWG80AAA mutant with amino-terminal GST tags. The recombinant proteins were incubated with biotinylated peptides corresponding to the H3 tail (residues 1-23) that were either unmodified, tri-acetylated (K9, 14, and 18), or tri-acetylated (K9, 14, and 18) and tri-methylated at H3K4. The effect of H3K4me3 on the binding of Taf14 to acetylated peptides was tested, as this modification is involved in the recruitment of NuA3 to chromatin through the PHD finger of Yng1 (Martin *et al.* 2006b; Taverna *et al.* 2006). The peptides were immobilized on streptavidin dynabeads and the bound protein detected by immunoblot using an α GST antibody. Indeed, wild type Taf14 was unable to bind unmodified H3 peptides, but showed a strong interaction when the peptides were acetylated (Figure 3.5A). Furthermore, this interaction was not affected by methylation of H3K4, suggesting that the ability of Taf14 to bind acetylated histones is independent of this modification. In contrast, mutation of the YEATS domain (GWG80AAA) completely abolished the interaction with both acetylated peptides. Taken together, this strongly supports the hypothesis that the YEATS domain of Taf14 binds acetylated histones.

In order to determine the specific acetylated lysine or lysines that interact with the YEATS domain of Taf14, we employed a modified histone peptide array that contained 384 unique histone modification

combinations, including up to four separate modifications on the same 19 residue peptide. Recombinant GST-tagged Taf14 was used to probe this array, and bound protein was detected using an α GST antibody (Figure 3.5B). Interestingly, the strongest interactions between Taf14 and individually modified histone peptides were with H3K9ac, H3K18ac, and H3K27ac, similar to what is observed with the YEATS domain of AF9 (Figure 3.5C). However, unlike the YEATS domain of AF9 which shows preference for H3K9ac and compromised binding to H3K18ac and H3K27ac, Taf14 bound with equal strength to H3K9ac and H3K18ac, while H3K27ac exhibited a 50% reduction in affinity. This suggests that the YEATS domain of Taf14 may function in chromatin-targeting predominantly through interaction with H3K9ac and H3K18ac, and to a lesser degree H3K27ac. None of the other 59 individually modified peptides produced signal above the background threshold (Figure 3.5C).

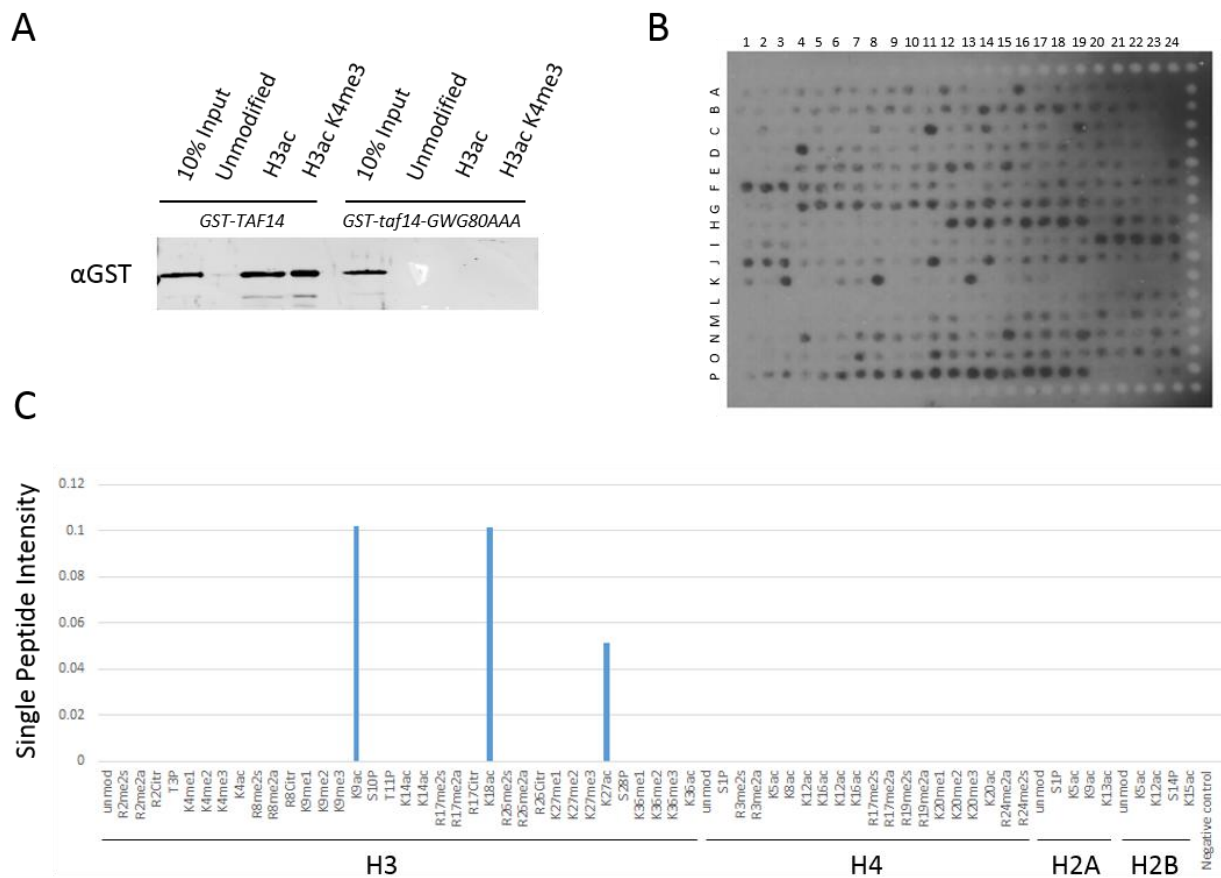


Figure 3.5: The YEATS domain of Taf14 interacts with H3K9, 18, and 27 acetylated peptides. (A) Recombinant GST-Taf14 and GST-Taf14-GWG80AAA were incubated with unmodified, H3K9, 14, 18 acetylated, or H3K9, 14, 18 acetylated/K4 methylated biotinylated peptides, and immunoprecipitated using streptavidin beads. Co-immunoprecipitating Taf14 was detected by immunoblot using an αGST antibody. (B) Wild type GST-Taf14 was used to probe a MODified Histone Peptide Array (Active Motif). Bound protein was detected by immunoblot using an αGST antibody. The reference excel file with the corresponding histone peptide content can be downloaded from www.activemotif.com/modified. (C) Background controlled peptide intensities for all singly modified histone peptides from the peptide array.

Examination of the sequences surrounding H3K9ac (K₄-Q₅-T₆-A₇-R₈-Kac₉-S₁₀), H3K18ac (G₁₃-K₁₄-A₁₅-P₁₆-R₁₇-Kac₁₈-Q₁₉), and H3K27ac (T₂₂-K₂₃-A₂₄-A₂₅-R₂₆-Kac₂₇-S₂₈) revealed a common R-Kac motif unique to these lysines, suggesting that an N-terminal arginine may play a role in recognition of the acetylated lysine. Indeed, H3R8 forms charge-stabilized hydrogen bonds with the YEATS domain of AF9, and substitution of this arginine for alanine reduces binding by approximately 200 fold (Li *et al.* 2014). To gain insight into whether modification of neighbouring residues has an effect on the interaction of Taf14 with its targets, the binding of all peptides with histone modification combinations including H3K9ac, H2K18ac, or H3K27ac were analyzed. Surprisingly, despite the common R-Kac motif observed in all three lysine acetylation targets, modification of neighbouring arginines did not have a consistent effect on Taf14-Kac interactions (Figures 3.6A, B, and C). Although di-methylation or citrullination of H3R8 on an H3K9ac peptide resulted in loss of Taf14, this trend did not reliably continue when additional modifications were added to the peptide (Figure 3.6). Instead, we observed that phosphorylation of S10 or T11 completely abolished the interaction between H3K9ac and the protein, suggesting that these residues play a critical role in target recognition. Similar results were obtained for H3K27ac peptides. Modification of R26 resulted in inconsistent effects on the Taf14-H3K27ac interaction, but phosphorylation of S28 resulted in complete disruption of this interaction for all peptides tested (Figure 3.6C). Contrary to the results obtained for H3K9 and H3K27 acetylated peptides, all H3K18ac peptides in which R17 had been modified (di-methylation or citrullination) exhibited significantly reduced, if not abolished, binding to Taf14 (Figure 3.6B). H3K18 does not possess a C-terminal serine or threonine, and thus recognition of acetylation at this residue by the YEATS domain of Taf14 may be more dependent on an unmodified N-terminal arginine than recognition of acetylation at H3K9 or K27. This suggests that residues directly C-terminal to acetylated K9 and K27 function in target recognition, while the arginine directly N-terminal to K18 functions in recognition of acetylated H3K18.

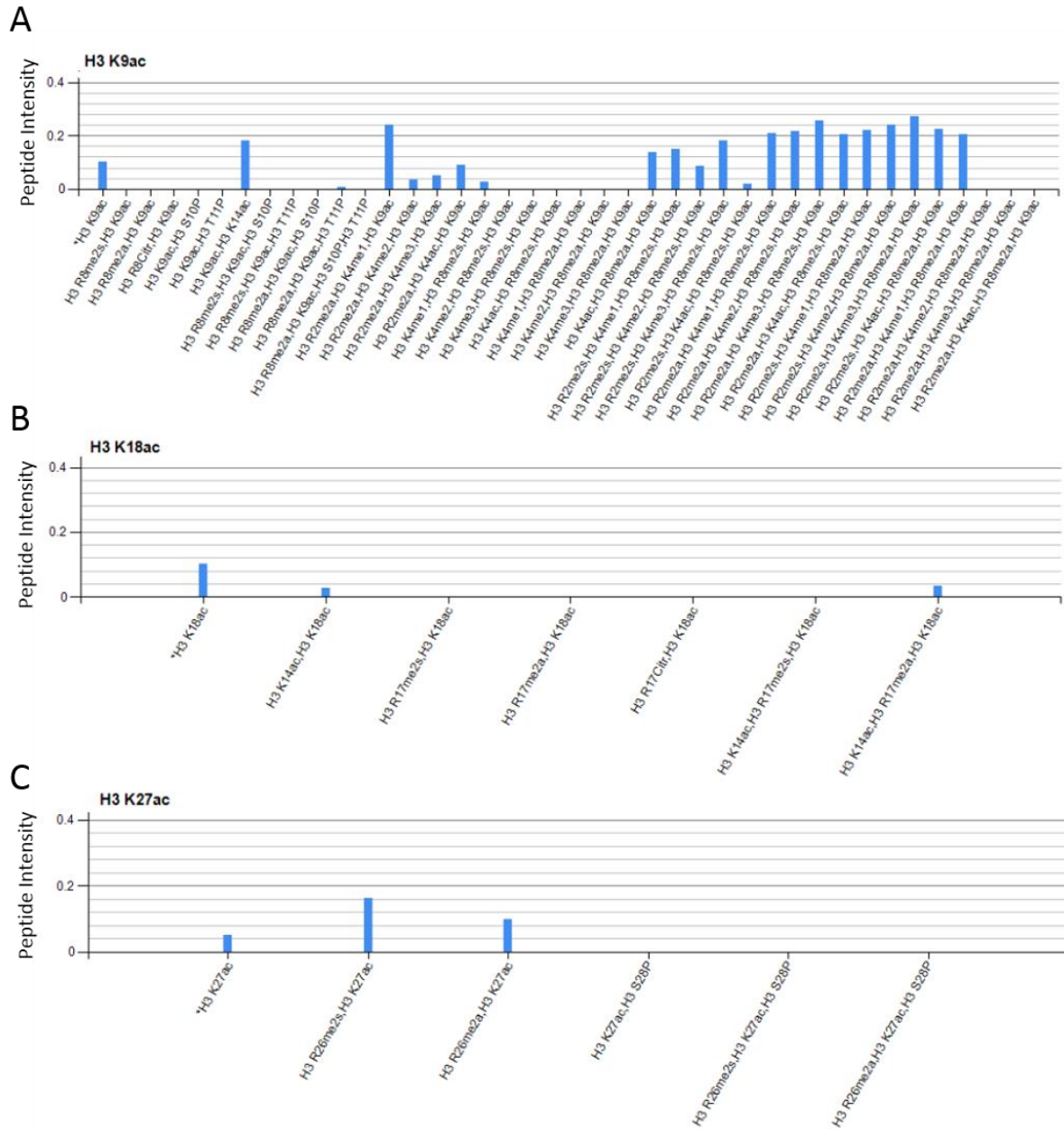


Figure 3.6: The YEATS domain of Taf14 interacts with a common R-Kac motif unique to H3K9, 18, and 27 acetylation. Wild type GST-Taf14 was used to probe a Modified Histone Peptide Array (Active Motif). Bound protein was detected by immunoblot using an α GST antibody. The background controlled peptide intensities of GST-Taf14 for all peptides acetylated at (A) H3K9, (B) H3K18, and (C) H3K27 are shown.

3.3.3 Sas3 occupancy shows weak but positive correlations with H3K9ac, H3K18ac, and H3K27ac

Previously published work, as well as work completed in Chapter 2 of this thesis, has established that NuA3 is recruited to chromatin through interaction of the PHD finger of Yng1 with H3K4me3 and interaction of the PWWP domain of Pdp3 with H3K36me3 (Martin *et al.* 2006b; Taverna *et al.* 2006; Gilbert *et al.* 2014). As such, both H3K4me3 and H3K36me3 positively correlate with Sas3 occupancy (Chapter 2). If the YEATS domain of Taf14 also functions to recruit NuA3 to chromatin through interaction with H3K9, 18, and 27 acetylation, then we would also expect to see a correlation between NuA3 occupancy and these modifications across the genome. In order to determine whether this is the case, we took advantage of our Sas3 ChIP-seq data from Chapter 2, as well as published H3K9ac, H3K18ac, and H3K27ac ChIP-seq datasets (Weiner *et al.* 2015). Indeed, weak but positive correlations exist between each modification and Sas3 occupancy, with the strongest correlation occurring with H3K18ac (r_s H3K9ac = 0.13; r_s H3K18ac = 0.21; r_s H3K27ac = 0.11) (Figure 3.7A, C, and E). To gain further insight into this relationship, we binned Sas3 occupancy by quartiles of H3K9ac, H3K18ac, or H3K27ac enrichment, and plotted the normalized cumulative read count for each quartile relative to the +1 nucleosome of all yeast genes (Figure 3.7B, D, and F). As genes vary in size, the fraction of genes included in the analysis at any distance from the +1 nucleosome is also shown. Remarkably, Sas3 is enriched throughout genes in the top three quartiles of H3K9 and H3K18 acetylated genes, but drops substantially in genes in the bottom quartile. This is in contrast to H3K27 acetylated genes, where changes in Sas3 occupancy between the top and bottom quartile of enriched genes is minimal. This supports the earlier peptide array data suggesting that Taf14 has highest affinity for H3K9 and K18 acetylated peptides, and reduced affinity for H3K27 acetylated peptides. Furthermore, it supports the hypothesis that H3K9ac and H3K18ac (and to a lesser degree perhaps H3K27ac) function in recruiting NuA3 to chromatin through the YEATS domain of Taf14.

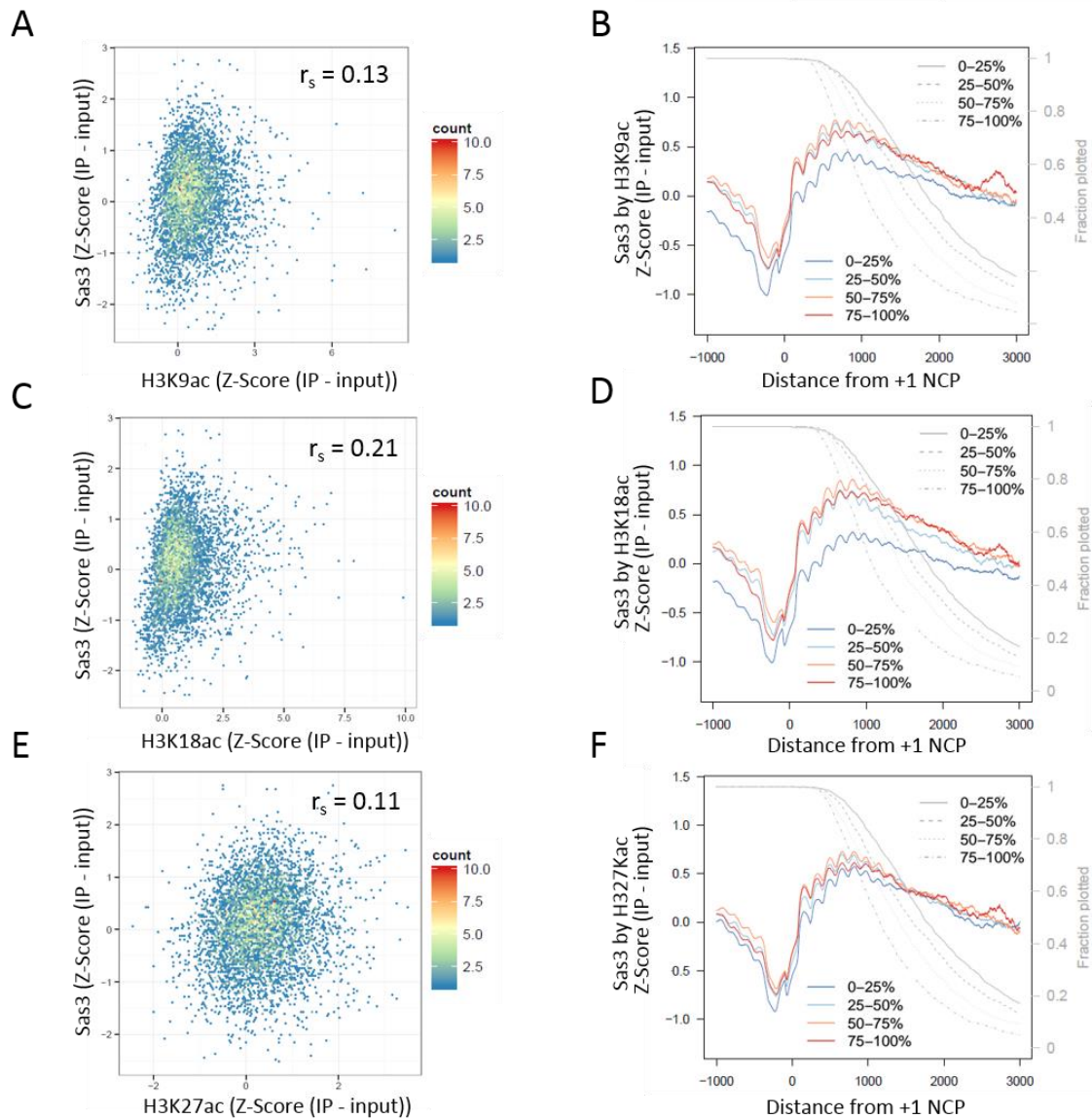


Figure 3.7: Sas3 occupancy shows weak, but positive, correlations with H3K9, 18, and 27 acetylation. (A)(C)(E) Scatter plots of Sas3 occupancy (normalized to input) versus (A) H3K9ac (Spearman correlation: 0.13), (C) H3K18ac (Spearman correlation: 0.21), and (E) H3K27ac (Spearman correlation: 0.11) across nucleosomes (Weiner *et al.* 2015). (B)(D)(F) Cumulative read count plots of Sas3 (normalized to input) per quartile of (B) H3K9ac, (D) H3K18ac, and (F) H3K27ac enrichment across genes. Sas3 occupancy is plotted relative to the +1 nucleosome of all yeast genes. Genes were plotted from 1000 bp upstream of the +1 nucleosome to their poly(A) termination site. Grey lines represent the fraction of genes included in the analysis at any given distance from the +1 nucleosome.

3.3.4 The YEATS domain of Taf14 recruits NuA3 to chromatin through Gcn5-deposited acetylation

Strikingly, H3K9, 18, and 27 are all targets of Gcn5 histone acetyltransferase complexes (Kuo and Andrews 2013). This suggested to us a mechanism by which Gcn5-deposited acetylation of H3K9, 18, and 27 results in further acetylation of histone H3 through recruitment of NuA3. Alternately, the weak but positive correlation between Sas3 occupancy and H3K9, 18, and 27 acetylation could also be the downstream effects of a shared pathway. To determine whether recruitment of NuA3 is in fact dependent on Gcn5, we performed a Sas3-6HA ChIP to examine interaction at the 5' end of the *COX10* gene using an α HA antibody. This gene was selected as it was previously shown to be strongly targeted by NuA3, and to contain moderate levels of H3K9, 18, and 27 acetylation within the 5' region (Rosaleny *et al.* 2007; Weiner *et al.* 2015). As expected, loss of *GCN5* resulted in an approximately fifty percent drop in NuA3 recruitment at this gene compared to a wild type strain (Figure 3.8). This supports our hypothesis that Gcn5-deposited histone acetylation functions to recruit NuA3 to chromatin to allow for acetylation of H3K14 and 23. It should be noted, however, that loss of *GCN5* does result in a slight transcriptional defect at *COX10* (\log_2 gcn5/WT = -0.26), which may also contribute to loss in NuA3 recruitment at this gene (Kemmeren *et al.* 2014).

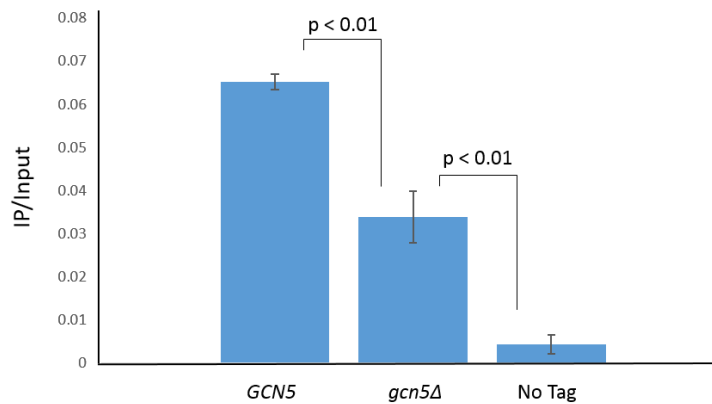


Figure 3.8: Gcn5 is required for efficient recruitment of NuA3 at COX10. Levels of Sas3 at the 5' end of the *COX10* gene were measured by CHIP-qPCR in the indicated strains. The amount of Sas3 (normalized to input) was measured. Error bars indicate the standard error from the mean from three biological replicates, and p-values determined using a t-test are listed.

Interestingly, both Sas3 and Gcn5 have been implicated in the acetylation of H3K14 and K23, suggesting that some redundancy may exist between the two HATs (Howe *et al.* 2001; Taverna *et al.* 2006; Kuo and Andrews 2013). Indeed, no loss in H3K14 acetylation is observed upon deletion of *SAS3* by either immunoblot of CHIP-chip, suggesting that Gcn5 is able to acetylate K14 in the absence of Sas3 (Rosaleny *et al.* 2007; Maltby *et al.* 2012b). More surprisingly, the same is not true for deletion of *GCN5*, which results in a noticeable loss of acetylation at this lysine (Rosaleny *et al.* 2007; Maltby *et al.* 2012b). That said, if Gcn5-deposited acetylation is responsible for recruitment of NuA3, then one would expect to observe a greater loss in H3K14 and K23 acetylation upon deletion of *GCN5* due to the combined loss of both HATs. Since this hypothesis relies on the assumption that H3K14 and K23 are the *in vivo* targets of NuA3 HAT activity, and because all studies that have directly examined NuA3 targets have been performed *in vitro*, we wished to confirm the targets of NuA3 activity *in vivo* (Howe *et al.* 2001; Martin *et al.* 2006a; Taverna *et al.* 2006).

To confirm that Sas3 is responsible for acetylation of H3K14 and 23, we took a genetic approach in which we once again exploited the genetic interaction that exists between *SAS3* and *GCN5*. We asked whether deletion of *GCN5* is able to reproduce a *sas3Δ* phenotype when H3K9, 14, 18, or 23 were mutated to glutamine individually or in combination. Since Sas3 is still present and able to acetylate its substrates, a lethal phenotype should only be observed upon loss of its histone targets. We created a strain lacking the *GCN5*, *HHT1-HHF1*, and *HHT2-HHF2* genes, but carrying *HHT2-HHF2* on a *URA3* plasmid that could be selected against using 5-FOA. Plasmids expressing the *HHT2-HHF2* point mutants were introduced into yeast via plasmid shuffle. As expected, mutation of H3K14 resulted in a severe growth defect (Figure 3.9). Although mutation of H3K23 didn't have any observable defect in cell growth on its own, combined mutation of both K14 and 23 in a *GCN5* mutant was lethal. This supports previously published *in vitro* data suggesting that H3K14 and H3K23 are targets of the NuA3 histone acetyltransferase complex.

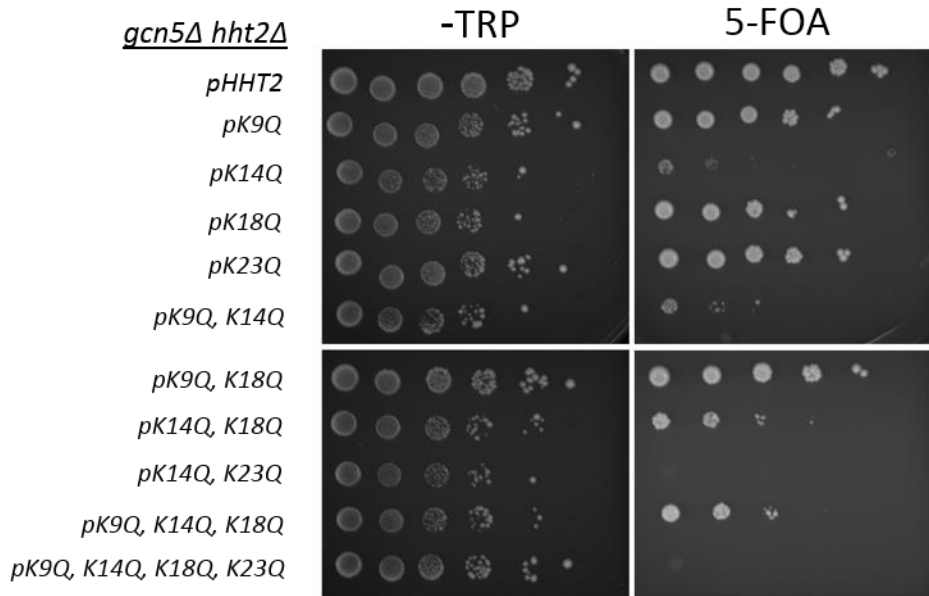


Figure 3.9: H3K14 and K23 are targets of Sas3 HAT activity. Ten-fold serial dilutions of the indicated strains were plated on synthetic drop-out (-TRP) media or synthetic complete media containing 5-FOA for three days at 30°C.

3.3.5 Taf14 YEATS domain mutants do not exhibit phenotypes indicative of loss of INO80 or SWI/SNF function

Besides NuA3, Taf14 is a member of four additional chromatin-related complexes: INO80, SWI/SNF, TFIID, and TFIIF (Schulze *et al.* 2009). Although TFIID and TFIIF are essential complexes, INO80 and SWI/SNF are non-essential, and mutants exhibit a variety of growth phenotypes when grown on various media (Brown *et al.* 2006; Villa-García *et al.* 2011; Qian *et al.* 2012). As the YEATS domain of Taf14 likely also functions as a reader of H3K9, 18, and 27 acetylation in these complexes, we were curious as to whether our Taf14 YEATS domain mutants would produce INO80 and SWI/SNF specific phenotypes. To determine whether this is the case, we tested yeast strains expressing the Taf14 LH58AA and GWG80AAA YEATS domain mutants for *snf2Δ* phenotypes on minimal media and media supplemented with ethanol

and benomyl, and for an *ino80Δ* phenotype on media lacking inositol. Strains lacking *TAF14*, *SWI3*, and *IES2* were used as controls. Although loss of *TAF14* produced the expected *snf2Δ* and *ino80Δ* phenotypes, strains expressing the YEATS domain mutants grew normally on all media tested (Figure 3.10). This suggests that the ability of the YEATS domain to bind acetylated K9, 18, and 27 is not essential to the function of SWI/SNF or INO80, or that its function is redundant with other modules within the complexes.

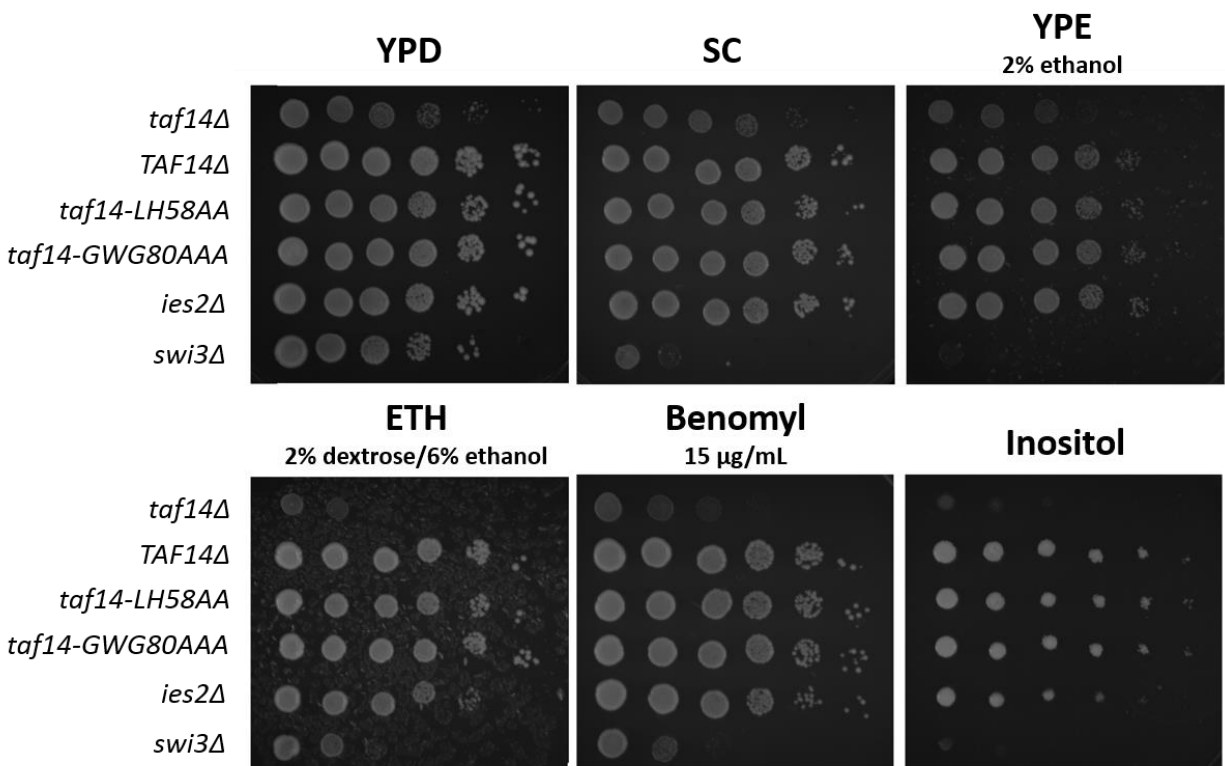


Figure 3.10: The YEATS domain of Taf14 is not essential for SWI/SNF or INO80 function. Ten-fold serial dilutions of the indicated strains were plated on YPD, synthetic complete media, YPE (2% ethanol as carbon source), ETH (YPD supplemented with 6% ethanol), media supplemented with 15 μg/mL benomyl, or media lacking inositol for three days at 30°C.

3.4 DISCUSSION AND CONCLUSIONS

In this study we show that the YEATS domain of Taf14 is a histone acetyl-binding domain that functions in recruitment of NuA3 to actively transcribed genes. We have provided evidence that Taf14 binds independently to H3K9ac, K18ac, and K27ac, and that recruitment of NuA3 to chromatin was dependent on acetylation by the Gcn5 HAT complex. Finally, we used a genetic approach to confirm that H3K14 and 23 were the targets of the histone acetyltransferase activity of NuA3. Overall, we have elucidated a novel mechanism by which Gcn5-deposited histone acetylation results in the recruitment of NuA3 to help “fill in the blanks” with acetylation of H3K14 and 23.

Shortly before the completion of this study, Shanle *et al.* 2015 published a paper confirming that the YEATS domain of Taf14 functions as a reader of histone acetylation. Using NMR chemical shift perturbation experiments on Taf14 in the presence of histone H3 peptides, they determined that Taf14 binds most strongly to an H3K9ac₁₋₁₂ peptide, while it binds to an H3K27ac₂₁₋₂₁ peptide with lower affinity. This agrees with results from our modified histone peptide array analysis suggesting that Taf14 has higher affinity for H3K9ac than H3K27ac. This is likely due to sequence discrepancy at positions surrounding the acetylated lysines. For example, whereas H3KQ5 contributes to the H3K9ac-YEATS domain interaction through hydrogen bonding to residues within Taf14 and AF9, the analogous interaction does not occur for H3K27ac, as this position is replaced with K23 (Li *et al.* 2014; Shanle *et al.* 2015). It is therefore unsurprising that H3K9ac has higher affinity for the domain than H3K27ac. Somewhat more surprising is our data suggesting that acetylated H3K18 binds the YEATS domain of Taf14 just as strongly as acetylated K9. Similar to H3K27, K18 contains a lysine in the position analogous to the Q5 of K9, suggesting that it should not form as strong of an interaction. However, the affinity of an H3K9ac peptide for the YEATS domain increases with length, suggesting that residues a distance away from the acetylated lysine may also function in substrate recognition (Shanle *et al.* 2015). If these distant residues are present for H3K9ac and

H3K18ac, but not H3K27ac, this could explain the discrepancy between their differing affinities for the YEATS domain of Taf14. This could also explain the weaker affinity of Taf14 for H3K18ac peptides compared to K9ac peptides observed by Shanle et al. 2015, as their peptides consisted of only the first 20 amino acids of the H3 N-terminal tail, while ours consisted of the first 23 amino acids. Nonetheless, they observed that combined acetylation of H3K9, 14, and 18 increases the binding affinity of Taf14 for the peptide three-fold over that of the single H3K9ac peptide. As both our modified peptide array data and that of Shanle et al. 2015 show little to no binding to H3K14ac peptides, this supports the idea that the YEATS domain of Taf14 has affinity for both acetylated H3K9 and 18.

In addition to our *in vitro* data, we also demonstrated that Sas3 occupancy is weakly, but positively, correlated with H3K9, 18, and 27 acetylation across nucleosomes. The weakness of these correlations is not surprising considering that the YEATS domain of Taf14 is one of three known chromatin-targeting domains within the NuA3 complex. The PHD finger of Yng1 and the PWWP domain of Pdp3 interact with H3K4me3 and H3K36me3, respectively, recruiting the HAT to regions of the genome enriched in these marks (Martin *et al.* 2006b; Taverna *et al.* 2006; Gilbert *et al.* 2014). As H3K4me3 peaks at the 5' ends of genes, while H3K36me3 peaks further into gene bodies, this results in recruitment of the complex across the entirety of actively transcribed regions (Pokholok et al. 2005; Chapter 2 of this thesis). It is therefore unsurprising that histone acetylation would correlate with Sas3 occupancy as weakly as it does, since acetylation is enriched at the promoters and 5' ends of actively transcribed genes, but depleted at the 3' ends.

Following identification of the YEATS domain as a reader of histone acetylation, we demonstrated that recruitment of NuA3 to chromatin is dependent on Gcn5. This is unsurprising, considering that Gcn5 is the major HAT responsible for acetylation of H3K9, 18, and 27 within cells (Kuo and Andrews 2013). Indeed, genome-wide localization studies have placed Gcn5 and Sas3 at a similar set of actively transcribed genes, consistent with the dependence of NuA3 targeting on Gcn5-deposited histone

acetylation (Rosaleny *et al.* 2007). This co-localization of Sas3 and Gcn5 is particularly interesting considering that both HATs target H3K14 and 23 for acetylation, and suggests that each HAT may be able to compensate for loss of the other. Indeed, little to no loss in H3K14 acetylation is observed upon deletion of *SAS3*, suggesting that Gcn5 is able to acetylate K14 in the absence of Sas3 (Rosaleny *et al.* 2007; Maltby *et al.* 2012b). In contrast, deletion of *GCN5* results in a significant loss in H3K14ac, which was long thought to suggest that unlike Gcn5, Sas3 was unable to compensate for loss of the other HAT (Rosaleny *et al.* 2007; Maltby *et al.* 2012b). The dependence of NuA3 recruitment on Gcn5 acetylation, however, presents an alternative explanation for the results of these studies. While Gcn5 is present to acetylate H3K14 in the absence of Sas3, loss of Gcn5 impairs recruitment of NuA3 to the 5' ends of genes, resulting in reduced levels of H3K14 acetylation in certain regions. The remaining acetylation is likely due to recruitment of NuA3 through its other chromatin-targeting domains, or through the activity of the putative Elp3 histone acetyltransferase, which has been shown to acetylate H3K14 *in vitro* (Winkler *et al.* 2002). In order to separate the activity of Gcn5 on H3K14 and 23 from its role in recruitment of NuA3 through H3K9, 18, and 27 acetylation, it would be interesting to see how mutation of the latter residues affects levels of H3K14ac genome-wide.

The dependence of NuA3 recruitment on Gcn5 could also explain the inability of Taf14 YEATS domain mutants to recapitulate a *sas3Δ* phenotype in a *gcn5Δ yng1ΔPHD* strain. In chapter 2 we demonstrated that this phenotype was dependent not only on loss of the PHD finger of Yng1, but also on the PWWP domain protein Pdp3. This is presumably due to a complete loss in NuA3 recruitment through H3K4 and K36 methylation, and therefore a parallel loss in activity. Interestingly, if chromatin-targeting of NuA3 is also dependent on Gcn5-deposited acetylation, then a *gcn5Δ* strain would already be expected to have impaired recruitment of NuA3 regardless of the presence or absence of the PHD finger of Yng1 or the PWWP domain of Pdp3. Thus, mutation of residues within the YEATS domain of Taf14 that are involved in its interaction with H3K9ac, K18ac, or K27ac would not be expected to have any additional phenotype,

precisely as observed. Remarkably, although combined loss of *GCN5*, *PDP3*, and the PHD finger of Yng1 resulted in a severe growth defect, it still did not recapitulate the synthetic lethality of a *sas3Δ gcn5Δ* strain (Chapter 2). This may suggest the existence of a fourth mechanism of chromatin-targeting, outside of the PHD finger of Yng1, the PWWP domain of Pdp3, and the YEATS domain of Taf14. Indeed, the YEATS domains of human ENL and AF9 have been shown to interact directly with the PAF complex, linking the Super Elongation Complex (SEC) with elongating RNAPII (He *et al.* 2011). Alternately, it's also possible that a HAT other than Gcn5 has residual activity at H3K9, 18, or 27, allowing for recruitment through the YEATS domain of Taf14 despite loss of *GCN5*. The histone acetyltransferase Rtt109, for example, has been shown to acetylate these residues *in vitro* (Abshiru *et al.* 2013).

In *S. cerevisiae*, Taf14 is present in four chromatin-related complexes in addition to the NuA3 complex. These include the chromatin remodelers INO80 and SWI/SNF, and the general transcription factors TFIID and TFIIF (Schulze *et al.* 2009). If the YEATS domain of Taf14 is a reader of Gcn5-deposited acetylation, then this suggests that acetylation of H3K9, 18, and 27 may also be a mechanism of recruitment for these complexes. Indeed, studies examining the genome-wide localization of INO80 and SWI/SNF have placed both these remodelers at the promoters and 5' ends of actively transcribed genes, similar to the pattern observed for acetylation of these residues (Schübeler *et al.* 2004; Kurdistani *et al.* 2004; Pokholok *et al.* 2005; Barski *et al.* 2007; Wang *et al.* 2008; Yen *et al.* 2012). TFIID and TFIIF are similarly recruited to active promoters during pre-initiation complex (PIC) formation, and TFIID has been shown to co-localize with Gcn5 at a subset of genes (Ohtsuki *et al.* 2009). Specific differences in localization of these Taf14-containing complexes can likely be attributed to additional chromatin-targeting domains within the complex. As an example, the SWI/SNF chromatin remodeling complex contains not only a YEATS domain, but a bromodomain, a SANT domain, and various other putative histone or DNA-binding domains. Additionally, three subunits within the complex - Snf2, Snf5, and Swi1 - interact directly with the activation domain of transcriptional activators (Neely *et al.* 2002). Nevertheless, a universal role for Gcn5-deposited

acetylation in the recruitment of Taf14-containing complexes underscores the importance of Gcn5 HAT function in both the direct and indirect regulation of chromatin structure.

In conclusion, we have demonstrated that the YEATS domain of Taf14 is a bona fide histone acetyl-binding domain, which recognizes acetylated K9, 18, and 27 on the tail of histone H3. This has implications not just for the NuA3 complex, but also for the four other chromatin remodeling complexes and general transcription factors of which Taf14 is a member. Taken together, our study details an additional targeting mechanism for the NuA3 histone acetyltransferase complex, in which Gcn5-deposited acetylation targets further acetylation by NuA3 to help “fill-in-the-blanks” at H3K14 and 23, ultimately leading to the changes in chromatin structure.

CHAPTER 4:

DIVERGENT RESIDUES WITHIN HISTONE H3 DEFINE A UNIQUE CHROMATIN STRUCTURE IN *S. CEREVISIAE*

4.1 INTRODUCTION

In eukaryotes, DNA is packaged into a nucleoprotein structure known as chromatin, which consists of DNA, histones, and non-histone proteins. The basic unit of chromatin is the nucleosome core particle, which is made up of an octamer of the four core histones, H2A, H2B, H3, and H4, wrapped with ~147 bp of DNA (Luger *et al.* 1997; Kornberg and Lorch 1999). Although nucleosomes will form on most sequences *in vitro*, they are not randomly positioned *in vivo*. Genome-wide mapping studies have shown that gene promoters and other regulatory regions tend to be nucleosome depleted due to two reasons (Hughes and Rando 2014). First, certain DNA sequences, such as AT-rich regions, are refractory to nucleosome formation. Second, trans-acting factors, such as transcriptional activators, RNA polymerases, and ATP-dependent chromatin remodelers can either evict or re-position nucleosomes. Nucleosomes immediately adjacent to nucleosome depleted regions (NDRs) are generally well-positioned, but nucleosome position shows more cell-to-cell variability with increasing distance from NDRs (Hughes and Rando 2014). This has led to the statistical positioning model in which strongly positioned nucleosomes create barriers against which other nucleosomes are packed into positioned and phased arrays (Kornberg and Stryer 1988).

Nucleosomes block access of proteins to DNA and thus chromatin structure can modulate DNA-dependent processes such as transcription, replication, recombination and DNA repair. Much of our insight into the role of chromatin in regulating the access of cellular machinery to DNA was driven by work with the budding yeast, *S. cerevisiae*. Both forward and reverse genetic analyses in this organism have revealed the roles played by histones and multi-protein complexes in regulating DNA-dependent processes (Rando and Winston 2012). However, although histones are amongst the most well conserved

proteins known, noted differences do exist between yeast and metazoan histones. First, although histone H4 is 92% conserved between *S. cerevisiae* and humans, H2A and H2B are less so (77% and 73% identity respectively), which is suggested to impact nucleosome stability (White *et al.* 2001). Second, while the majority of eukaryotes express distinct histone H3 variants for replication-coupled (RC; designated histone H3.1 and H3.2 in humans) and replication-independent (RI; designated histone H3.3 in humans) histone deposition, *S. cerevisiae* has retained a histone H3.3-like variant for both pathways.

The amino acid differences between RC and RI-specific H3 variants are proposed to restrict the histones to their requisite deposition pathways (Szenker *et al.* 2011), but studies have also shown that these variants can directly alter chromatin structure *in vitro* (Thakar *et al.* 2009; Chen *et al.* 2013). This together with the previously established link between H3.3 deposition and active transcription in metazoans has led to speculation that yeast have retained H3.3 due to its ability to promote an open chromatin conformation. In this study we sought to determine whether the divergent amino acids within histone H3 mediate chromatin structure in yeast. We found that, while H3.3-specific amino acids are dispensable for yeast growth, the $\alpha 3$ helix of histone H3 serves a yeast-specific function. Substitution of this region with the corresponding amino acids from human histone H3 resulted in a severe growth defect, increased nuclease sensitivity, loss of nucleosome positioning, and relocation of nucleosomes to predicated nucleosome-favoring sequences. Collectively these results suggest that the $\alpha 3$ helix of *S. cerevisiae* histone H3 promotes a unique chromatin structure in this organism

4.2 MATERIALS AND METHODS

4.2.1 Yeast Strains and Plasmids

The strain used in this study (YLH517) is isogenic to S288C, and is described further in Table 4.1. It was derived from FY2162, which has deletions of the *HHT1-HHF1* and *HHT2-HHF2* genes, and carries *HHT2-HHF2* on a *URA3* plasmid (Duina and Winston 2004).

Table 4.1: Yeast strain used in this study

Yeast Strain	Mating Type	Genotype
YLH517	Mat a	<i>his3Δ200 leu2Δ1 lys2-128δ ura3-52 trp1Δ63 (hht1-hhf1)::LEU2 (hht2-hhf2)::KAN</i>

All plasmids used in this study are listed in Table 4.2. A *TRP1* plasmid expressing wild-type *HHT2* and *HHF2* was constructed by ligation of the *SpeI* restricted fragment from pDM18 into the *SpeI* site of pRS414 (Duina and Winston 2004). Plasmids expressing mutant versions of H3 were constructed by replacing the *BamHI/XhoI* fragment from this plasmid with codon optimized, synthesized DNA fragments. Genetic manipulations were performed using standard protocols (Gillam and Smith 1979).

Table 4.2: Plasmids used in this study

Plasmid	Description
P634	pHHF2.HHT2.414 (pDM18)
P635	pHHF2.hht2.Q120M.K121P.K125Q.414
P636	pHHF2.hht2.Q120M.414
P637	pHHF2.hht2.K121P.414
P638	pHHF2.hht2.K125Q.414

Plasmid	Description
pJC093	pHHF2.hht2(61-134)-hH3.1(1-60).414
pJC094	pHHF2.hht2(61-134)-hH3.3(1-60).414
pJC095	pHHF2.hht2(61-119)-hH3.1(1-60,120-134).414
pJC096	pHHF2.hht2(61-119)-hH3.3(1-60,120-134).414
pJC098	pHHF2.hht2(1-119)-hH3.3(120-135).414
pJC120	pHHF2.hht2(120-134)-hH3.1(1-119).414
pJC121	pHHF2.hht2(120-134)-hH3.3(1-119).414

4.2.2 Chromatin Association Assay

Fifty milliliters of *S. cerevisiae* cultures were grown to an OD₆₀₀ of 1.0 in YPD, at which time sodium azide was added to 0.1%. After washing with 25 mL ddH₂O, cells were resuspended in 1.5 mL pre-spheroblast buffer (100 mM Tris-Cl pH 9.4, 10 mM DTT) and incubated at 30°C for 30 minutes. Samples were centrifuged for 2 minutes at 3000 rpm (Eppendorf microfuge, model 5415D), and resuspended in 1 mL spheroblast buffer (50 mM KPO₄ pH 7.5, 0.6 M sorbitol, 0.5 mM PMSF) with 40 µg zymolyase 20T (Amsbio). Samples were incubated at 30 °C, and the extent of spheroblast formation monitored by measuring the OD₆₀₀ of cells in 1% SDS. Once spheroblasting was complete, samples were centrifuged at 3000 rpm for 3 minutes, and resuspended in 250 µL cold lysis buffer (20 mM PIPES-KOH pH 6.8, 0.4 M sorbitol, 10 mM KOAc, 3 mM MgOAc, 0.5 mM PMSF, Roche protease inhibitor cocktail (PIC)). Spheroblasts were equally split between two tubes, and lysed by the addition of 1% triton X-100 and incubation on ice for 5 minutes. At this point one of the two lysates was saved for use as the whole cell extract sample. The other lysate was centrifuged at 12,000 rpm for 15 minutes at 4 °C, and 100 µL of supernatant saved for use as the supernatant fraction. The remaining pellet was washed in 50 µL

lysis-X buffer (lysis buffer with 1% triton X-100), and centrifuged at 10 000 rpm for 5 minutes at 4 °C. After removal of the supernatant, the pellet was resuspended in 200 µL lysis-X buffer, and used as the chromatin associated fraction.

4.2.3 Immunoblot Analysis

Samples analyzed by SDS-PAGE and immunoblotting with the antibodies and dilutions listed in Table 2.3. Signal was visualized either by infrared detection and quantification using the Licor Odyssey System.

Table 4.3: Antibodies used in this study

Antibody	Animal	Dilution	Company	Catalogue Number
αH3	Rabbit	1:5000	ActiveMotif	39163
αRabbit (680CW)	Goat	1:25000	Licor	926 32210

4.2.4 Micrococcal Nuclease Sequencing (MNase-Seq)

One hundred milliliters of *S. cerevisiae* cultures were grown to an OD₆₀₀ of 0.8 and cross-linked with 1% formaldehyde for 15 minutes before quenching the reaction with 125 mM glycine. Cells were washed three times with 1 mL wash buffer (10 mM Tris-Cl pH7.5 and 100 mM NaCl), and frozen at -80 °C. Thawed cell pellets were resuspended in 600 µL lysis buffer (50 mM Hepes pH 7.5, 140 mM NaCl, 1 mM EDTA, 1 Triton-X-100, 0.1% sodium deoxycholate, Roche protease inhibitor cocktail (PIC) and 0.2mM PMSF), and lysed by bead beating. The resulting lysate was centrifuged at 15 000g for 30 minutes and the chromatin pellet was washed and resuspended in 900 µL NP-S buffer (0.5 mM sperimidine, 1 mM β-

mercaptoethanol, 0.075% NP-40, 50 mM NaCl, 10 mM Tris-Cl pH 7.4, 5 mM MgCl₂, 1 mM CaCl₂, EDTA-free PIC, 2 mM PMSF). The resuspended pellet was added to 100 μL NP-S buffer containing 200 U micrococcal nuclease, and incubated at 37°C for 1 hour. The reaction was stopped by addition of EDTA to 10 mM. Cross-links were reversed by the addition of 1% SDS and 40 μg proteinase K followed by incubation at 65°C overnight. Following treatment with 20 μg RNase A, “spiked-in” synthetic DNA was added and construction of sequencing libraries was performed as described previously using 8 rounds of PCR amplification (Maltby *et al.* 2012b). Indexed samples were pooled and 100 bp paired-end sequencing performed by using an Illumina HiSeq.

4.2.5 Analysis of MNase-Seq Data

Fastq files were aligned to *saccer3*, the most recent build of the yeast genome (R64-1-1, released 03Feb2011; downloaded from <http://yeastgenome.org>), using the Burrows Wheeler Aligner (BWA) mem algorithm (Li and Durbin 2010). Samtools was used to filter for reads mapped to the genome and for a mapping quality score of at least 10 (Li *et al.* 2009b). Bedtools intersect was used to remove reads mapping to the rDNA locus on chrXII (Quinlan and Hall 2010). Reads longer than 200 bp were filtered out and the remaining data randomly sampled so as to have equivalent numbers of reads. The Java Genomics Toolkit (downloaded from <http://papant.us/java-genomics-toolkit/>) and Matrix2png (Pavlidis and Noble 2003) were used for all subsequent analysis.

Data deposition: The MNase-seq data reported in this chapter has been deposited in the Gene Expression Omnibus (GEO) database: www.ncbi.nlm.nih.gov/geo/were.

4.2.6 *In Vitro* Analysis of Nucleosome Positioning

Histones were expressed in *E. coli* BL21 (DE3) and purified to homogeneity through acid extraction, ion exchange (Maco-Prep Ion Exchange Media, BioRad) and reverse phase HPLC (C18-300, 20 mM x 4.6 mM, 5 μ M, ACE). Array DNA was prepared by digesting the pWM530 plasmid (Dorigo *et al.* 2003) with EcoRV to generate both the desired 25 repeat of the 197 bp 601 positioning sequence as well as plasmid backbone competitor DNA required for chromatin reconstitution. Individual lyophilized histones were combines in a 1:1:1:1 H2B:H2A:H3:H4 mole ratio, dissolved in unfolding buffer (7M GuHCl, 20 mM Tris pH 7., 1 mM DTT) and dialyzed against three changes of refolding buffer (2M NaCl, 10 mM Tris, pH 7.5, 1 mM EDTA). Reconstituted histone octamer was purified by size exclusion chromatography using refolding buffer (Superdex200 10/300 GL, GE Healthcare). Chromatinized arrays were assembled as previously described (Huynh *et al.* 2005) using a 1:1:1 (hH3) or 1:2:1 (yH3 and H3_{a3h}) octamer:DNA ratio. Each chromatin species was treated with Aval and HhaI, subjected to a PCR cleanup (EZ-10 spin column purification kit, Biobasic) and resolved on a 0.7% agarose gel in 0.2x tris-borate buffer.

4.3 RESULTS

4.3.1 Histone H3.3-defining amino acids are dispensable for growth of *S. cerevisiae*.

Histone H3 in *S. cerevisiae* shares 90% and 89% identity with human H3.3 and H3.1/2 respectively. We were interested in determining the contribution of divergent amino acids within histone H3 to chromatin structure. To this end, we identified three regions of histone H3 that exhibit sequence differences between yeast and human (Figures 1A and B) and generated codon-optimized constructs encoding yeast H3 that contained the human sequence for each region. Because human H3.1 and H3.3 differ in regions I and II, we generated two constructs with human versions of regions I and II to reflect differences between these variants. The resulting constructs were introduced into yeast via plasmid

shuffle and histone H3 expression was driven from a native H3 promoter. All constructs fully rescued growth on rich media (Figure 1C, bottom panel), with the exception of the one in which region III was substituted with the human counterpart. Histone H3 was expressed at wild type levels from this construct (Figure 1C middle panel), suggesting that the slow growth phenotype was due to a defect in H3 function rather than protein production.

The indistinguishable growth rates of cells expressing histone H3 with the human version of region I or II was intriguing as these regions include amino acids that differentiate histone H3.3 from H3.1 in metazoans. To further confirm that a histone H3.1-like variant can substitute for H3.3 in yeast, we created constructs expressing human histone H3 chimeras with human regions I, II, and yeast region III. These constructs rescued growth of yeast on various growth media (Figure 1D) and thus, despite the conservation of histone H3.3-specific amino acids from yeast to humans, these residues are not critical for cell growth in *S. cerevisiae*.

4.3.2 The $\alpha 3$ helix of yeast histone H3 mediates nucleosome positioning in vivo.

Region III of histone H3 encompasses the third alpha helix within the histone fold, plus four additional carboxyl terminal amino acids. Yeast and human histone H3 differ at five amino acids within this region (Figure 1A) but mutation of these amino acids individually did not result in a growth defect (Figure 2A and figure not shown). The viability of the Q120M and L130I individual substitutions was surprising as others have shown that substitution of these residues with glutamic acid and alanine respectively results in lethality (Dai *et al.* 2008), however the lack of phenotype in our study was most likely due to the more conservative nature of the substitutions. Three of the divergent residues within region III are located within the third alpha helix, which is close in proximity to the nucleosome dyad (Figure 2B). While yeast-to-human substitutions of these residues rescued growth of yeast on various growth media, mutation of all three residues in combination (designated yH3 $_{\alpha 3h}$) largely recapitulated the growth defect of the entire region III swap (Figure 2A). Moreover, cells expressing yH3 $_{\alpha 3h}$ also appeared to exhibit sensitivity to a range of drugs, including 6-azauracil, hydroxyurea, methyl methanesulfonate, caffeine, and formamide. These phenotypes should be interpreted with caution however as they may be a manifestation of the slow growth of the mutant. Histone protein levels were unchanged in the yH3 $_{\alpha 3h}$ mutant, indicating that the growth defect was not due to reduced histone content (Figures 2C and D). Collectively, these results suggest a yeast-specific function for the histone H3 $\alpha 3$ helix.

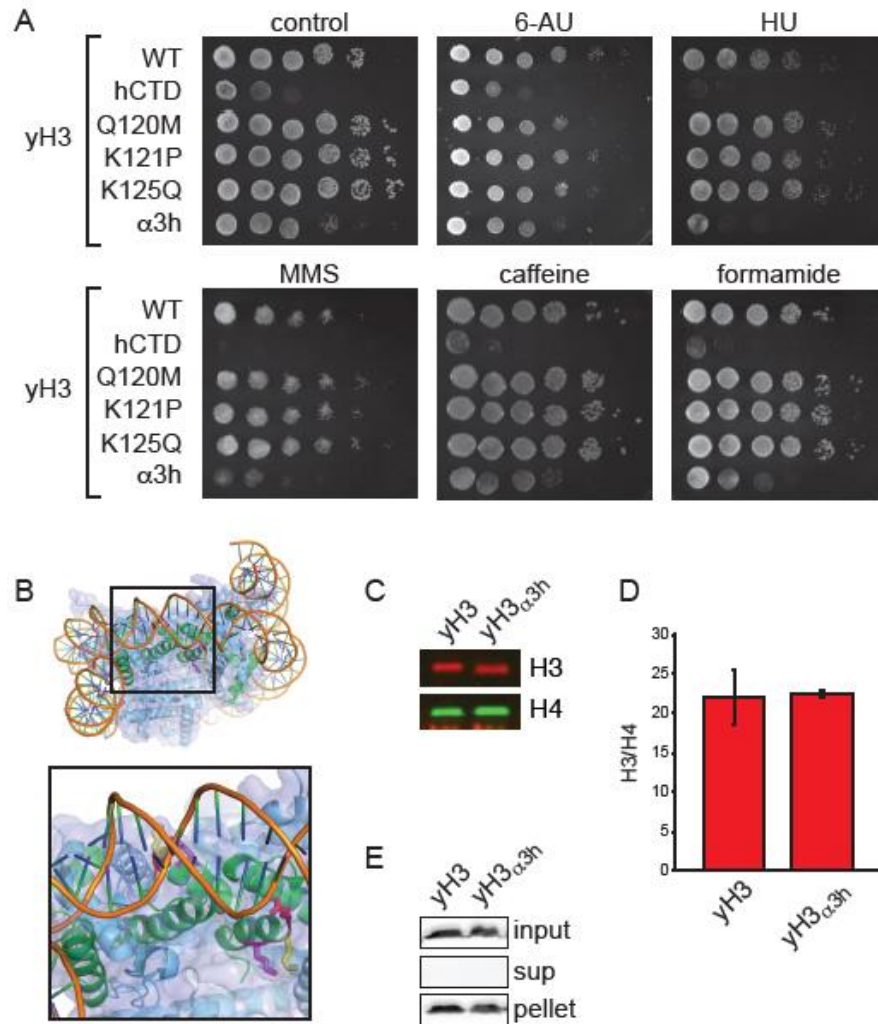


Figure 4.2: Mutation of the histone H3 $\alpha 3$ helix confers a growth defect in yeast that is not due to impaired histone deposition. (A) Yeast expressing wild type histone H3, or histone H3 with yeast-to-human substitutions at the indicated amino acids were plated in five-fold serial dilutions on YPD or media supplemented with 0.015% MMS, 2% formamide, 4 mM caffeine, 75 mM HU, or 100 $\mu\text{g}/\text{mL}$ 6-AU, and incubated at 30°C for 3 days. (B) PyMOL (Schrödinger 2010) structure of a yeast nucleosome (White *et al.* 2001) with both subunits of H3 highlighted in green. Residues Q120 (red), K121 (yellow), and K125 (magenta) of the $\alpha 3$ helix are indicated. (C) Strains expressing wild type H3 or histone H3 with the yeast-to-human substitutions at amino acids 120, 121, and 125 ($yH3_{\alpha 3h}$) were lysed and subjected to immunoblot analysis. (D) Quantitative analysis of H3 over H4 signal in (C) from three biological replicates. (E) Yeast whole cell extracts (input) from the indicated strains were fractionated into soluble (sup) and insoluble (pellet) components and subjected to immunoblot for histone H3.

Newly synthesized histones are deposited on DNA with the aid of histone chaperones and multiple chaperones have been shown to interact with the histone H3 $\alpha 3$ helix, although in the case of the Asf1 histone chaperone, residues critical for interaction are conserved from yeast to human (Antczak et al. 2006; English et al. 2006; Agez et al. 2007). Nevertheless, to rule out the possibility that the growth defect of the $\gamma\text{H3}_{\alpha 3\text{h}}$ mutant is due to a histone deposition defect, we fractionated yeast whole cell extracts into soluble and chromatin-associated fractions. Figure 2E demonstrates equal levels of histone H3 in the chromatin fraction in both the wild type and mutant strains suggesting that the growth defect observed in Figure 2B was not due to less histones associated with DNA.

Although the $\gamma\text{H3}_{\alpha 3\text{h}}$ mutant did not appear to have a defect in nucleosome assembly, it is possible that the nucleosomes were mis-localized relative to the DNA sequence in this strain. To test this, we mapped nucleosome positions by deep sequencing of micrococcal nuclease (MNase) resistant fragments. Our first observation was that replacement of the γH3 $\alpha 3$ helix with the human counterpart resulted in an increase in MNase sensitivity (Figure 3A). Despite the recovery of slightly shorter DNA, the use of “spike-in” control DNA indicated that we did not recover less MNase-resistant DNA from the mutant, again supporting the fact that there are not less nucleosomes in the $\gamma\text{H3}_{\alpha 3\text{h}}$ mutant.

To determine nucleosome positioning in both the wild type and $\gamma\text{H3}_{\alpha 3\text{h}}$ cells, the midpoint of each sequence read was calculated and mapped relative to 5043 transcriptional start sites (TSSs) (van Bakel et al. 2013). Figure 3B shows that wild type cells exhibited a typical nucleosome position pattern with a nucleosome-depleted region (NDR) upstream of the TSS, a well-positioned “plus one” nucleosome and a regular array of nucleosomes across the gene body. The $\gamma\text{H3}_{\alpha 3\text{h}}$ mutant showed a similar NDR, but the peak summits of the nucleosomes were lower and the valleys were shallower, indicative of less regular nucleosome packing. These differences were also observed when mapping full reads and full reads adjusted for read length demonstrating that the altered nucleosome positioning observed in the mutant was not an effect of reduced MNase protection (data not shown). To further confirm that the

nucleosomes were less well positioned in the $\gamma\text{H3}_{\alpha 3\text{h}}$ mutant, we plotted the read midpoints as a phasogram, which displays the average distance between the dyad of each nucleosome and the dyad of adjacent nucleosomes (Figure 3C). Although the phases were similar in wild type and mutant cells (162 bp), indicative of a similar average nucleosome repeat length, the phasogram confirmed that nucleosomes were not as regularly packed relative to each other in the $\gamma\text{H3}_{\alpha 3\text{h}}$ mutant when compared to wild type.

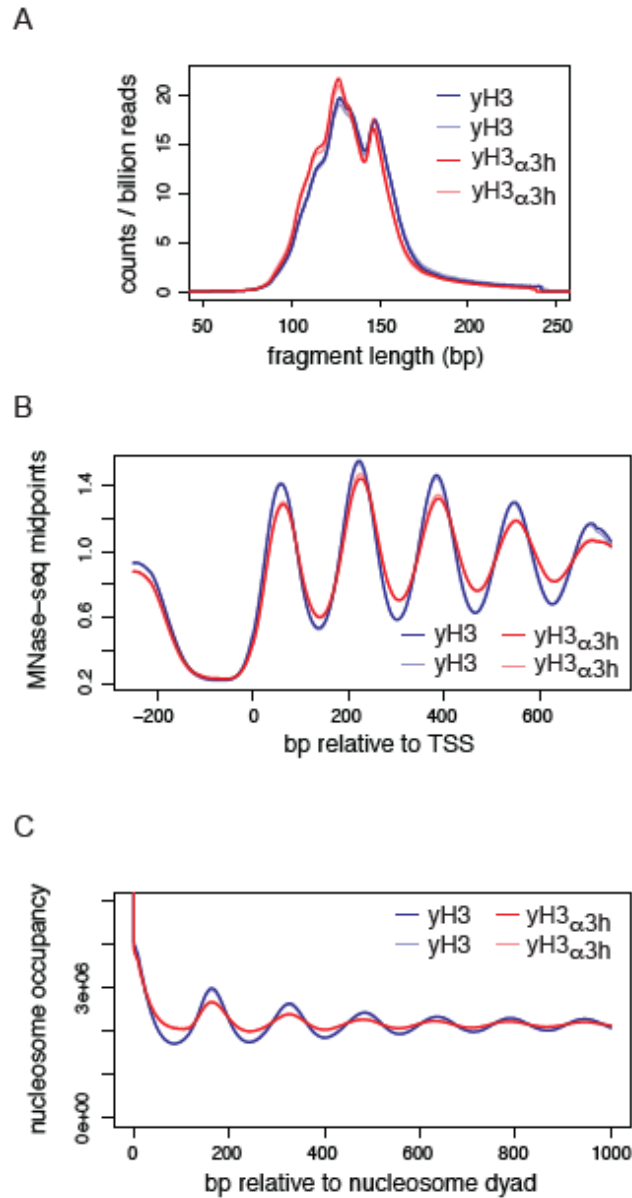


Figure 4.3: The α 3 helix of yeast histone H3 mediates nucleosome positioning. (A) Histogram of read lengths of sequences of micrococcal nuclease digested DNA from yeast expressing wild type histone H3 (yH3) or histone H3 with yeast-to-human substitutions at amino acids 120, 121, and 125 (yH3 α 3h). Note that the replicates were from independent cultures. (B) The average number of read midpoints (ie. Nucleosome dyads) from sequencing of micrococcal nuclease resistant DNA plotted relative to 5042 transcriptional start sites (TSS) (van Bakel *et al.* 2013). (C) A phasogram (distribution of distance between read midpoints) across the yeast genome for yeast expressing the indicated versions of histone H3.

4.3.3 The human histone H3 $\alpha 3$ helix enhances preference for nucleosome positioning sequences in *S. cerevisiae*.

Although nucleosomes will assemble on most sequences, they do show sequence preference. Indeed algorithms have been developed that predict nucleosome occupancy based on sequence alone (Kaplan et al. 2009; Tillo and Hughes 2009). The performance of these algorithms however is modest in predicting positions in vivo, presumably due to cellular activities that mobilize nucleosomes away from their sequence-preferred positions. The atypical nucleosome positioning in the $\gamma\text{H3}_{\alpha 3\text{h}}$ mutant led us to hypothesize that $\gamma\text{H3}_{\alpha 3\text{h}}$ -containing octamers have increased preference for nucleosome favoring sequences. To test this, we called the position of 63,998 nucleosomes in yeast expressing wild type H3 and determined the optimal predicted nucleosome occupancy 125 bp upstream and downstream of the dyad of each nucleosome. Nucleosomes were then sorted based on the distance between the maximum predicted nucleosome occupancy and the actual nucleosome occupancy, and the predicted and actual occupancies plotted as heat maps. Comparison of the left panel (predicted nucleosome occupancy) with the middle panel (actual nucleosome occupancy) in Figure 4A confirmed that the majority of nucleosomes deviate from the site predicted based on DNA sequence. We then calculated the increase in nucleosome occupancy in the $\gamma\text{H3}_{\alpha 3\text{h}}$ mutant across the same nucleosomes. The right panel of Figure 4A shows that changes in nucleosome occupancy in the mutant closely matched the predicted nucleosome position suggesting the nucleosomes were shifting to more preferred sequences in the $\gamma\text{H3}_{\alpha 3\text{h}}$ mutant.

The re-localization of nucleosomes to preferred sequences was documented in another study examining the effects of histone H3 depletion (Gossett and Lieb 2012). Although our data thus far has ruled out a major loss of nucleosomes in the $\gamma\text{H3}_{\alpha 3\text{h}}$ mutant, subtle changes in the occupancy of neighboring nucleosomes could explain the results observed in Figure 4A. To rule this possibility out, we used K-means clustering to divide genes longer than 750 bp (4455 genes) into 6 clusters based on the

pattern of changes in nucleosome occupancy from 250 bp upstream to 750 bp downstream of the TSS in the $\gamma\text{H3}_{\alpha 3\text{h}}$ mutant (Figure 4B, left panel). Again, observed increases in nucleosome occupancy closely mirrored patterns of predicted nucleosome occupancy (Figure 4B, middle panel). We then compared changes in nucleosome occupancy in the $\gamma\text{H3}_{\alpha 3\text{h}}$ mutant to changes due to depletion of histone H3 (Figure 4B, right panel). Clusters that showed increased nucleosome occupancy in the $\gamma\text{H3}_{\alpha 3\text{h}}$ mutant did not exhibit similar increases upon depletion of histone H3 indicating that the changes in nucleosome position in the $\gamma\text{H3}_{\alpha 3\text{h}}$ mutant were not a manifestation of changes in nucleosome occupancy.

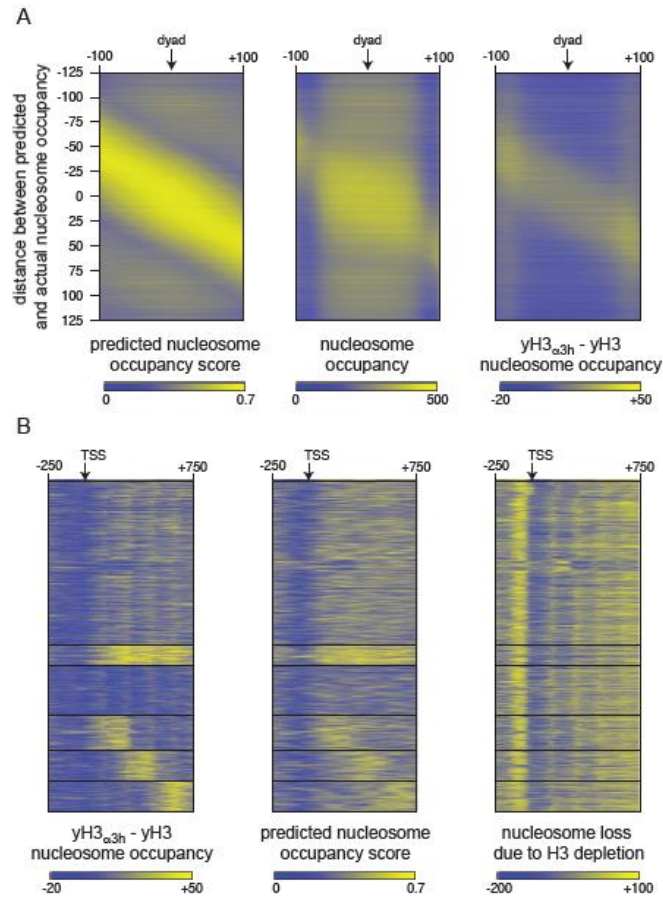


Figure 4.4: The human histone H3 $\alpha 3$ helix enhances preference for nucleosome positioning sequences in *S. cerevisiae*. (A) The position of 63,998 nucleosomes in yeast expressing wild type histone H3 were called using the greedy caller algorithm from the Java Genomics Toolkit, and the nucleosome dyads determined. The predicted nucleosome occupancy (Kaplan *et al.* 2009) 125 bp upstream and downstream of the dyad was determined and the nucleosomes were sorted based on the distance between the maximum predicted occupancy and the actual nucleosome dyad. Predicted nucleosome occupancy, actual nucleosome occupancy, and increase in nucleosome occupancy in the yH3 _{$\alpha 3h$} mutant were plotted as heat maps.(B) K-means clustering was used to divide yeast genes longer than 750bp into six bins based on changes in nucleosome occupancy in the yH3 _{$\alpha 3h$} mutant. Increase in nucleosome occupancy in the yH3 _{$\alpha 3h$} , predicted nucleosome occupancy (Kaplan *et al.* 2009) and nucleosome loss due to histone H3 depletion (Gossett and Lieb 2012) were plotted as heatmaps.

4.3.4 The $\alpha 3$ helix of histone H3 influences nucleosome positioning *in vitro*.

Our data has thus far shown that yeast-to-human changes of amino acids at positions 120, 121 and 125 in the carboxyl-terminus of histone H3 (which reduce positive charge) direct nucleosomes towards predicted positioning sequences *in vivo*. This shift could be the result of altered interactions between histone H3 and the cellular machinery or direct effects on histone-DNA interactions. In support of the latter, it has been shown that neutralization of charge in this area by acetylation of H3 K122 destabilizes the nucleosome *in vitro* (Manohar et al. 2009). To test between these two possibilities we monitored the positioning of recombinant nucleosomes containing yeast H3 and yH3 _{$\alpha 3h$} on DNA *in vitro*. Using the standard salt dialysis method, we loaded histone octamers onto a 25-mer repeat of the 197 bp Widom 601 nucleosome positioning sequencing (Figure 5A). The positioning of nucleosomes on this array can be readily measured by restriction enzyme digestion with *AvaI* and *HhaI*, whose recognition sites are in the linker regions and at the nucleosome dyad axis respectively (Figure 5A, B). As expected and previously observed, we found that recombinant human histone octamers loaded in an ordered fashion onto 601 DNA; almost all *AvaI* sites in these arrays were digested after 60 minutes, but all *HhaI* sites remained protected (Figure 5C, left). By contrast we found that recombinant octamers containing yH3 exhibited an alternative loading behaviour. While all *HhaI* sites were protected, only ~55% of *AvaI* sites were digested, indicating a proportion of nucleosomes in these arrays occlude the linker region (Figure 5C, middle). This positioning difference can be attributed to yeast specific amino acids at positions 120, 121 and 125 in the C-terminus of H3 because yeast nucleosomes bearing yH3 _{$\alpha 3h$} position as human nucleosomes; 94% of these chromatin arrays were reduced to mono-nucleosome species with *AvaI* (Figure 5C, right). Collectively these results suggest that amino acid differences within the $\alpha 3$ helix of histone H3 function to directly dictate organismal-specific chromatin structure.

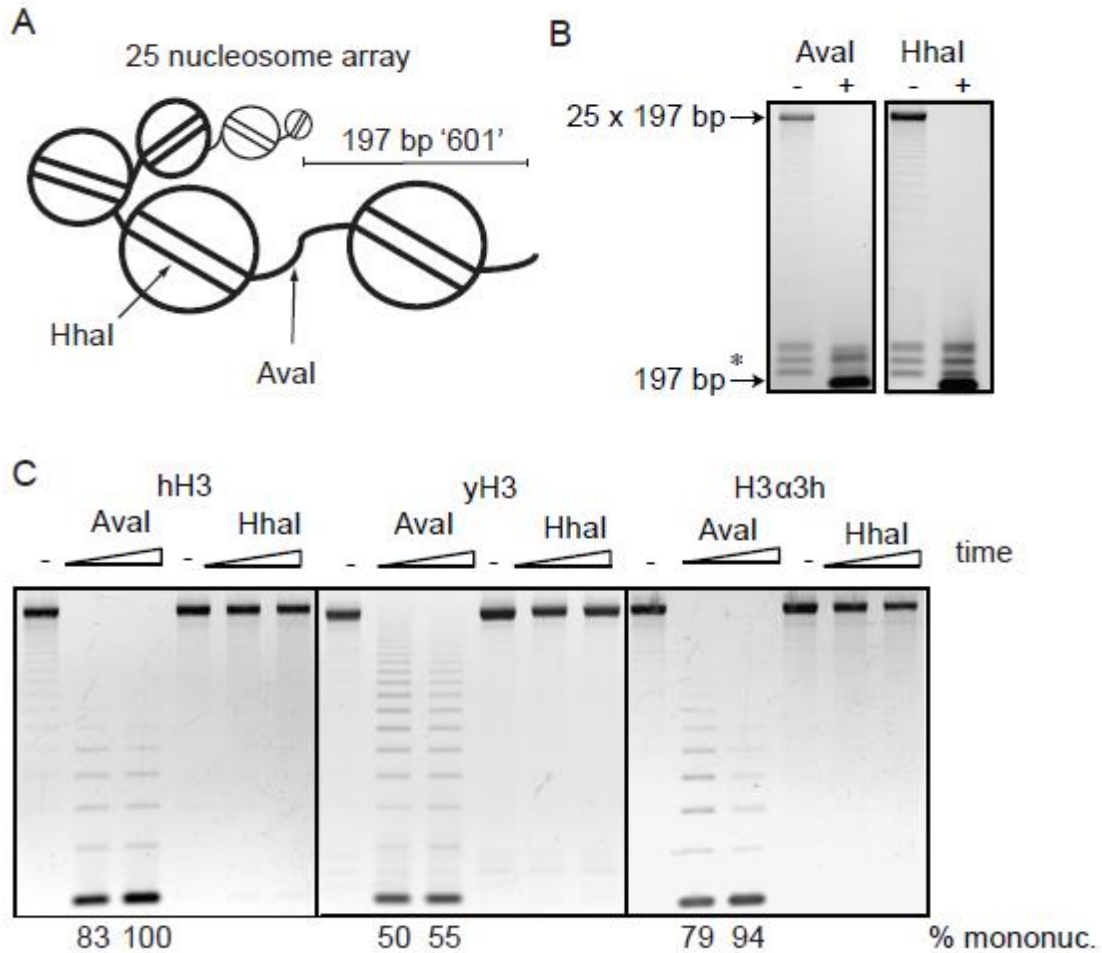


Figure 4.5: The α 3 helix of histone H3 affects nucleosome positioning *in vitro*. (A) Schematic representation of chromatin arrays including restriction enzyme site locations. (B) Fifteen minute Aval or HhaI digestion of naked array DNA liberates a 107 bp mononucleosome fragment. * indicates competitor DNA fragments generated from the array plasmid that are removed upon preparative chromatin array precipitation. (C) Chromatin arrays assembled from recombinant human (hH3), yeast (yH3) or humanized yH3 (yH3 α 3h) were digested with Aval or HhaI for 0, 30, and 60 minutes. DNAs were purified, resolved and visualized by ethidium bromide staining. The proportion of array digested to mono-nucleosome was estimated by the densitometric ration of mononucleosome species to input (undigested) array.

4.4 DISCUSSION

The budding yeast *S. cerevisiae* has been used extensively as a model organism for the study of chromatin structure with the assumption that, due to the high conservation of histones, data generated is relevant to other eukaryotes. Differences in histone sequences do exist between yeast and humans and in this study we examined the contribution that yeast-specific amino acids within histone H3 have on chromatin structure. Through this analysis we demonstrated that replacement of all but the $\alpha 3$ helix of yeast H3, including the residues that differentiate histone H3.1 from H3.3, with the human counterparts fully rescues growth of yeast in multiple conditions. In contrast, replacing residues within the $\alpha 3$ helix of yeast histone H3 with their human counterpart's results in a severe growth defect, increased nuclease sensitivity and altered nucleosome positioning both *in vivo* and *in vitro*. Collectively these results confirm other studies that suggest that minor sequence variations within histones function to establish a unique chromatin structure in *S. cerevisiae* (D'Arcy and Luger 2011).

Despite the differences in sequences of hH3.1 and hH3.3, we found that both equally rescued growth of yeast in numerous conditions suggesting that *S. cerevisiae* did not retain a H3.3-like variant to mediate an open chromatin structure. The full rescue of cell growth with a H3.1-like variant is surprising when one considers that ectopically expressed hH3.3 is incorporated into yeast chromatin via the RI pathway, but hH3.1 is not (Song et al. 2013). It should be noted however that, in contrast to the aforementioned study, the yeast in our study did not have wild type histone H3 available and thus a failure to integrate hH3.1 could be due to competition effects. Alternately, it is possible that growth of yeast is not strongly dependent on RI histone deposition. Indeed, loss of the HIR complex, responsible for RI deposition of H3.3, does not result in a growth defect (Sherwood et al. 1993). It also should be noted our analysis does not rule out the possibility that hH3.1 may not rescue yeast growth in other media or in competitive growth conditions.

In contrast to the minimal impact of replacing the remainder of histone H3, substitution of the $\alpha 3$ helix of yeast histone H3 had significant consequences on chromatin structure including increased micrococcal nuclease sensitivity, defects in nucleosome phasing and an increased preference of octamers for nucleosome-favoring sequences. Altered nucleosome positioning was observed both *in vitro* and *in vivo*, suggesting intrinsic differences in nucleosome structure in the mutant, as opposed to differing susceptibility to cellular factors such as polymerases or ATP-dependent remodelers. One explanation for our observations is that histone octamers with human histone H3 are more sensitive to sequence positioning effects. Interestingly, the algorithm we used for prediction of nucleosome favoring sequences was trained using DNA reconstituted with *Xenopus* histones, which share an identical $\alpha 3$ helix with human H3 (Kaplan et al. 2009). If yeast and human histones show different sequence dependencies, one would expect the algorithm to work better *in vivo* when using the $\gamma H3_{\alpha 3h}$ mutant. However, other approaches that disrupt nucleosome packing, such as transcription inhibition or histone depletion, also increase the ability of the Kaplan score to predict nucleosome position (Weiner et al. 2010; Gossett and Lieb 2012) suggesting that factors that govern nucleosome occupancy of *Xenopus* nucleosomes are relevant to yeast nucleosomes.

A second explanation for our results is that nucleosomes with the human histone H3 $\alpha 3$ helix may be refractory to statistical positioning, and thus relocate to preferred positions as a default. The statistical positioning model suggests that nucleosome position is dictated by the packing of nucleosomes against a strongly positioned nucleosome barrier (Kornberg and Stryer 1988). The +1 nucleosome on protein coding genes is the most well characterized barrier nucleosome, and our data suggests that the position of the NDR and +1 nucleosome is unchanged in the $\gamma H3_{\alpha 3h}$ mutant. We observe the same results when examining other barrier nucleosomes (Hsieh et al. 2015) (data not shown). We therefore propose that it is the packing of nucleosomes that is defective in the $\gamma H3_{\alpha 3h}$ mutant. Humanization of the $\alpha 3$ helix involves loss of two lysine residues and the introduction of a proline, which are expected to alter both the charge

and secondary structure of this motif. The $\alpha 3$ helix is located at the dyad axis of the nucleosome, where it could conceivably alter the trajectory of linker DNA entering and exiting the nucleosome, thus determining the orientation and packing of adjacent nucleosomes in an array. The $\alpha 3$ helix is unlikely to play as critical a role in statistical positioning in human cells as these cells have longer linker DNA and thus the trajectory of DNA exiting the nucleosome would not have such an impact. Further, since linker length is dictated by the abundance of linker histones (Schlegel et al. 1980; Fan et al. 2005), *S. cerevisiae*-specific amino acids within the histone H3 $\alpha 3$ helix may be important due to the sub-stoichiometric amounts of linker histones in this organism (Freidkin and Katcoff 2001; Downs et al. 2003). It will be interesting to determine whether there is a link between $\alpha 3$ helix sequences and linker histone stoichiometry in other organisms.

CHAPTER 5: CONCLUSIONS AND DISCUSSION

5.1 CHAPTER SUMMARY

The regulation of chromatin structure is critical to gene expression, as it controls the accessibility of DNA to the transcriptional machinery. In *S. cerevisiae*, there are three mechanisms by which chromatin structure is regulated: the post-translational modification of histones, the sliding or eviction of nucleosomes by ATP-dependent chromatin remodelers, and the incorporation of histone variants. This thesis enhances our understanding of the regulation of chromatin structure by providing evidence for two mechanisms by which a HAT is recruited to specific regions of the genome. Furthermore, we provide insight into the regulation of chromatin structure by yeast H3, and human 3.1, H3.2, and H3.3. Together, these studies add to our current knowledge of chromatin dynamics.

In Chapter 2, we show that recruitment of the NuA3 HAT complex to specific regions of the genome is dependent on H3K36me₃, and implicate the PWWP domain of Pdp3 in mediating this interaction. Previous studies suggested that recruitment of NuA3 to chromatin is dependent on both H3K4 and H3K36 methylation, leading to the hypothesis that multiple chromatin-targeting domains exist within the complex (Martin *et al.* 2006a). The PHD finger of Yng1 was the first chromatin-targeting domain of NuA3 to be identified, linking HAT activity to H3K4me₃ (Martin *et al.* 2006b; Taverna *et al.* 2006). We introduce a novel subunit of the NuA3 complex, Pdp3, and implicate its PWWP domain in interaction with H3K36me₃. We also present evidence that Sas3 - the catalytic subunit of the NuA3 complex - is found across gene bodies, but enriched at +5 and +6 nucleosomes similar to H3K36me₃. Our findings support a multivalent mechanism of interaction whereby interaction of NuA3 with chromatin is dependent on both H3K4 and K36 methylation and their two readers.

Similar to recent publications, the data in Chapter 3 identifies the YEATS domain of Taf14 as a reader of histone acetylation (Li *et al.* 2014; Shanle *et al.* 2015). We show that this domain interacts specifically with histone H3 tails acetylated at K9, 18, and 27, and go on to demonstrate that these interactions are required for efficient recruitment of NuA3 to chromatin. Since genome-wide localization studies of histone acetylation place it at the promoter and 5' end of genes, this represents a novel mechanism for NuA3 recruitment to this region (Schübeler *et al.* 2004; Kurdistani *et al.* 2004; Pokholok *et al.* 2005; Barski *et al.* 2007; Wang *et al.* 2008). Interestingly, H3K9, 18, and 27 are all targets of the Gcn5 histone acetyltransferase, and we provide evidence here that the interaction between NuA3 and chromatin is dependent on this HAT (Kuo and Andrews 2013). This suggests a mechanism by which acetylation by one HAT targets further acetylation by another, presumably with the intention of facilitating transcription. Finally we demonstrate that H3K14 and K23 are targets of Sas3, providing confirmation of this activity *in vivo*. Taken together, data from this chapter supports a mechanism by which Gcn5-deposited acetylation stimulates acetylation of H3K14 and 23 through recruitment of NuA3.

In Chapter 5 of this thesis, we turned our attention to histone H3 and its variants in higher eukaryotes. Despite histones being some of the most conserved proteins known, differences in sequence do exist between yeast and metazoans. In this study we examined the contribution that divergent amino acids within histone H3 make to cell growth and structure in *S. cerevisiae*. We show that while amino acids that differentiate histone H3.3 from histones H3.1 and H3.2 are dispensable for yeast growth, substitution of residues within the histone H3 α 3 helix with their human counterparts results in a severe growth defect. Furthermore, these mutations result in altered nucleosome positioning, both *in vivo* and *in vitro*, which is accompanied by an increased preference for nucleosome positioning sequences. Taken together, this suggests that divergent residues within the histone H3 α 3 helix play differing roles in chromatin regulation between yeast and metazoans.

5.2 GENERAL DISCUSSION

Chapters 2 and 3 of this thesis concern chromatin-targeting of the NuA3 histone acetyltransferase complex. This work along with previous studies performed by ourselves and others has demonstrated that NuA3 contains three unique chromatin-targeting domains - the PHD finger of Yng1, the PWWP domain of Pdp3, and the YEATS domain of Taf14 - that bind to H3K4me3, H3K36me3, and H3 tail acetylation, respectively (Martin *et al.* 2006b; Taverna *et al.* 2006; Gilbert *et al.* 2014; Shanle *et al.* 2015). Furthermore, our genome-wide localization studies of Sas3 place the HAT across the entirety of transcribed genes, with a peak in occupancy at +5 and +6 nucleosomes. Interestingly, unlike Gcn5 – the other major H3 HAT within yeast – Sas3 occupancy is restricted to the transcribed region, and is depleted at promoters (Robert *et al.* 2004; Taverna *et al.* 2006; Xue-Franzén *et al.* 2010; Vicente-Muñoz *et al.* 2014). This raises the question of how the three chromatin-targeting domains within NuA3 function together to recruit NuA3 to these specific regions of the genome.

Unlike H3K36 methylation, H3K4 methylation and H3 acetylation co-localize to the 5' ends of actively transcribed genes (Schübeler *et al.* 2004; Kurdistanian *et al.* 2004; Bernstein *et al.* 2005; Pokholok *et al.* 2005; Barski *et al.* 2007; Wang *et al.* 2008). This raises the possibility that the PHD finger of Yng1 and the YEATS domain of Taf14 function to recruit NuA3 to this region in either an additive or all-or-nothing manner. However, unlike NuA3 and H3K4 methylation, H3 acetylation is also enriched in promoter regions. This suggests a mechanism by which binding of the YEATS domain to acetylated H3 tails requires the concomitant binding of the PHD finger of Yng1 to H3K4me3 histones. Indeed, the K_d for the interaction between the YEATS domain of Taf14 and acetylated H3K9 was estimated to be 150 μ M, which is 50 fold higher than that of the YEATS domain of AF9 for H3K9ac (Li *et al.* 2014; Shanle *et al.* 2015). The YEATS domain of Taf14 may therefore require additional binding by the PHD finger of Yng1 in order to stabilize its interaction. Nonetheless, H3K4me3 was not required for interaction of recombinant Taf14 with the

acetylated H3 tail *in vitro*. Certainly, more work needs to be done to determine whether this is the case *in vivo*. If the YEATS domain does in fact play a role in stabilizing the interaction between NuA3 and H3K4me3, this would provide one of the first examples of the requirement for concomitant all-or-nothing binding by chromatin-targeting domains within separate subunits of the same chromatin regulatory complex. Previously, tandem domains within the same protein have been shown to function in combination to recruit or stimulate the activity of a chromatin-associated complex. For example, mouse Brdt, a homolog of the TFIID subunit Taf1, binds strongly to H4K5ac/K8ac peptides, but shows no affinity for either individually modified peptide (Morinière *et al.* 2009). Additive interactions between the domains of two proteins within a complex have also been identified. Localization of the human transcriptional regulator ATRX to heterochromatin is dependent not only on its dual PHD finger and zinc finger domains, which interact with a combination of H3K4me0 and H3K9me2/3, but also on the chromodomain of HP1 which associates with ARTX and binds directly to H3K9me3 (Eustermann *et al.* 2011). Loss of any of these PTMs or individual reader domains reduces localization of ATRX to heterochromatin, but doesn't abolish recruitment entirely, suggesting an additive effect (Eustermann *et al.* 2011). However, the strong depletion of Sas3 at promoters despite the enrichment of H3 acetylation in this region suggests the possibility of the first example of an all-or-nothing combinatorial readout from domains within separate subunits of a complex. This supports the histone code hypothesis which posits that histone PTMs act in combination or sequential order to elicit specific downstream functions (Strahl and Allis 2000).

Another interesting outcome of our genome-wide localization study of Sas3 is the finding that the HAT preferentially interacts with di-nucleosomes over mononucleosomes. This is particularly interesting considering that NuA3 contains three chromatin-targeting domains, as it suggests that these domains may interact with modifications on neighbouring nucleosomes. Although the structural composition of NuA3 has not been extensively studied, the possession of three chromatin-targeting domains within three

different subunits of the complex increases the likelihood that at least one of these domains would be distant enough from the others to interact with a neighbouring nucleosome. The recognition of dinucleosomes through multivalent modes of interaction is even more likely when considering the steric hindrance that would likely result from the interaction of three chromatin-targeting subunits and a catalytic subunit with one or both of the H3 tails within a single nucleosome. It also suggests the possibility that the active site of Sas3 may function on neighbouring nucleosomes lacking one or more of these targeting signals, providing fuller coverage of H3K14 and H3K23 acetylation at less frequently transcribed genes where not all nucleosomes possess these modifications. This has previously been observed for the Rpd3S histone deacetylase complex, which makes H3K36me3-dependent and histone PTM-independent contacts on adjoining nucleosomes (Huh *et al.* 2012). This allows the complex to bind methylated nucleosomes and de-acetylate un-methylated neighbouring nucleosomes which is essential in regulating aberrant transcription at less frequently transcribed genes where not all nucleosomes possess H3K36 methylation (Lee *et al.* 2013).

NuA3 is closely related to mammalian MOZ/MORF. In humans, these complexes are composed of a MYST family HAT homologous to Sas3 (MOZ or MORF), an ING protein homologous to Yng1 (ING5), human EAF6, and a protein known as BRPF1 (Yang 2015). BRPF1 has been shown to act as a molecular scaffold for proteins within the MOZ/MORF complex, bridging the association of ING5 and EAF6 with the catalytic HAT (Ullah *et al.* 2008). The NuA3 subunit Nto1 is also important for complex stability (unpublished data from our lab), and shows structural similarity to BRPF1 including the possession of two conserved tandem PHD fingers. Interestingly, BRPF1 also contains a PWWP domain and bromodomain that have been shown to interact with H3K36me3 and acetylated histone tails, respectively (Vezzoli *et al.* 2010; Poplawski *et al.* 2014). Considering that the PWWP protein Pdp3 and the YEATS domain protein Taf14 are missing from MOZ/MORF, this suggests the intriguing possibility that human BRPF1 may play the role of Nto1, Pdp3, and Taf14 in mammals. Genome-wide localization studies of MOZ/MORF will be

required to determine whether possession of these domains results in a similar pattern of recruitment across genes as the NuA3 complex.

In our final study, we show that differences between human H3.1 and H3.3 are inconsequential to cell growth in yeast. This is surprising considering that human H3.3 has long been considered to be the human H3 variant most closely related to yeast H3. Although this is based in part on sequence, several other similarities also contribute to this line of thinking. In humans, H3.3 is localized to actively transcribed regions of the genome unlike the variants H3.1 and H3.2, and is thus more likely to be similar to the H3 used by the much more transcriptionally active yeast genome (Schwartz and Ahmad 2005; Mito *et al.* 2005). Furthermore, while H3.1 and H3.2 are deposited by the RC pathway, yeast H3 is also able to undergo RI histone deposition similar to H3.3. It should be noted, however, that while differences between these human variants resulted in no observable growth defect in yeast, differences in function may still exist and be observable upon growth in other media or in competitive growth conditions.

Unlike replacement of the remainder of histone H3, substitution of the three diverging residues within the $\alpha 3$ helix of yeast H3 resulted in a severe growth defect. It also had significant consequences on chromatin structure, including increased micrococcal nuclease sensitivity, defects in nucleosome phasing, and an increased preference of octamers for nucleosome-favouring sequences. These changes appear to be the result of intrinsic changes in nucleosome structure rather than differing susceptibility to cellular factors such as chromatin remodelers, as altered nucleosome positioning in the mutant was observed *in vitro* as well as *in vivo*; however it should be noted that this doesn't negate the possibility that these residues may also be required for histone chaperone or chromatin remodeler activity *in vivo*. The $\alpha 3$ helix of histone H3 is located in close proximity to the nucleosome dyad, allowing for Q120 to interact directly with the backbone of the nucleosomal DNA through hydrogen bonding (White *et al.* 2001). As methionine is a far weaker hydrogen bond acceptor than glutamine, substitution of Q120 with its human counterpart

likely abolishes this interaction, reducing the stability of the nucleosome (Luscombe *et al.* 2001). This could explain the increased sensitivity to MNase observed in the γ H3 _{α 3h} mutant, and likely contributes to changes in nucleosome positioning. Although K121 and K125 do not make direct contact with DNA, K125 contributes to H3-H4 tetramer formation by interaction of its amino group with the carboxyl group of E53 on histone H4. As glutamine doesn't possess the charged amino group of a lysine, substitution of K125 to its human counterpart would abolish this interaction, decreasing the stability of the nucleosome. Finally, while K121 makes no significant contacts with DNA or neighbouring histones, mutation to proline would insert a kink in the α 3 helix, resulting in a rearrangement in the positioning of all neighbouring residues. Taken together, substitution of divergent residues within the α 3 helix of yeast H3 disrupt histone-DNA and histone-histone contacts within the nucleosome, resulting in altered nucleosome positioning.

5.3 FUTURE DIRECTIONS

In this thesis we show that the YEATS domain of Taf14 is able to bind acetylated H3K9 and 18 peptides *in vitro*, and to a lesser degree acetylated H3K27 peptides. Furthermore we show that acetylation of these residues correlates with Sas3 occupancy, and that loss of *GCN5* – the histone acetyltransferase responsible for acetylation of H3K9, 18, and 27 – impairs the interaction of Sas3 with chromatin. Nonetheless, the extent to which each of these individual acetylated lysines contributes to NuA3 recruitment *in vivo* remains to be shown. ChIP-qPCR of Sas3 from strains expressing histone H3 in which K9, 18, or 27 are mutated to arginine will help determine which of these acetylated residues, if any, plays a dominant role in NuA3 recruitment. It will also be interesting to determine the extent to which Gcn5-deposited acetylation contributes to the genome-wide localization of NuA3 by performing a ChIP-seq of Sas3 in a *gcn5 Δ* strain. Finally, since Taf14 is a component of multiple chromatin-related complexes in addition to NuA3, including INO80, SWI/SNF, TFIID, and TFIIF, it would be interesting to determine the

effect that mutation of the YEATS domain or loss of Gcn5 function has on recruitment of these complexes to specific regions of the genome.

In addition to the YEATS domain of Taf14, the PWWP domain of Pdp3 and the PHD finger of Yng1 also function in recruiting NuA3 to chromatin through association with H3K36me3 and H3K4me3, respectively. The presence of three functioning chromatin-targeting domains is not surprising considering that neither combined loss of *SET1* and *SET2*, nor combined mutation of H3K4 and K36 to arginine, completely abolished binding of Sas3 to chromatin by ChIP. This suggests that all three domains are required for efficient recruitment of NuA3 across the genome. The co-localization of H3K4me3 and H3K9, 18, and 27 acetylation also raises the possibility that the PHD finger of Yng1 and the YEATS domain of Taf14 may function in combination rather than independently to recruit NuA3 to the 5' end of transcribed genes. In order to determine the relative contribution of each domain individually as well as in combination with others, ChIP-qPCR of Sas3 in strains carrying point mutations of residues critical for chromatin-targeting in the YEATS domain, PWWP domain, or PHD finger could be performed. This should provide insight into the extent to which each domain functions in chromatin-recruitment at the 5' and 3' ends of genes.

To date, all chromatin-targeting domains within the NuA3 complex have been characterized as genuine readers of histone modifications with the exception of the tandem PHD fingers of Nto1. BRPF1, the likely homolog of Nto1 in mammalian MOZ/MORF, contains two PHD fingers which have been implicated in complex recruitment. While the first PHD finger of BRPF1 binds unmodified H3 tails, the second PHD finger associates with DNA (Qin *et al.* 2011; Liu *et al.* 2012). Considering the structural similarities between BRPF1 and Nto1, this begs the question of whether the tandem PHD fingers of Nto1 are also able to function in complex recruitment. Alternately, as binding to histones and DNA is non-

specific in BRPF1, these domains may play a role in stabilizing the interaction with chromatin rather than recruiting the complex to specific regions of the genome.

In addition to our studies on recruitment of the NuA3 complex, we have also determined the contribution that divergent residues within the $\alpha 3$ helix of histone H3 make to cell growth and chromatin structure in *S. cerevisiae*. As these residues are in close proximity to the nucleosome dyad, mutation to their human counterparts could potentially alter the trajectory of linker DNA entering and exiting the nucleosome which could have effects on the packing of adjacent nucleosomes in an array. This would have a larger effect in yeast, where linker DNA is shorter than in humans, perhaps resulting in the defects in nucleosome phasing and increased preference of octamers for nucleosome-favouring sequences observed in our study. Furthermore, since linker length is dependent on the concentration of linker histone present in the cell, divergent residues within the $\alpha 3$ helix of human H3 variants may be less critical than in yeast due to the abundance of linker histones in humans (Freidkin and Katcoff 2001; Fan *et al.* 2005). It will be interesting to determine whether there is a link between $\alpha 3$ helix sequences and linker histone stoichiometry in other organisms. Finally, the $\gamma H3_{\alpha 3h}$ mutant displays a slight sensitivity to HU suggesting a functional link to replication. As such, determining how the alterations in chromatin structure that occur upon mutation of residues within the $\alpha 3$ helix of yeast H3 to their human counterparts affect DNA processes such as replication and transcription is also of great interest.

REFERENCES

- Abshiru N., Ippersiel K., Tang Y., Yuan H., Marmorstein R., Verreault A., Thibault P., 2013 Chaperone-mediated acetylation of histones by Rtt109 identified by quantitative proteomics. *J. Proteomics* **81**: 80–90.
- ALLFREY V. G., FAULKNER R., MIRSKY A. E., 1964 ACETYLATION AND METHYLATION OF HISTONES AND THEIR POSSIBLE ROLE IN THE REGULATION OF RNA SYNTHESIS. *Proc. Natl. Acad. Sci. U. S. A.* **51**: 786–94.
- Angell R. R., Jacobs P. A., 1975 Lateral asymmetry in human constitutive heterochromatin. *Chromosoma* **51**: 301–10.
- Attikum H. van, Fritsch O., Hohn B., Gasser S. M., 2004 Recruitment of the INO80 complex by H2A phosphorylation links ATP-dependent chromatin remodeling with DNA double-strand break repair. *Cell* **119**: 777–88.
- Ausubel FM, Brent R, Kingston RE, Moore DD, Seidman JG, Smith JA S. K., 1987 *Current Protocols in Molecular Biology*.
- Avvakumov N., Côté J., 2007a Functions of myst family histone acetyltransferases and their link to disease. *Subcell. Biochem.* **41**: 295–317.
- Avvakumov N., Côté J., 2007b The MYST family of histone acetyltransferases and their intimate links to cancer. *Oncogene* **26**: 5395–5407.
- Bakel H. van, Tsui K., Gebbia M., Mnaimneh S., Hughes T. R., Nislow C., 2013 A compendium of nucleosome and transcript profiles reveals determinants of chromatin architecture and transcription. *PLoS Genet.* **9**: e1003479.
- Barski A., Cuddapah S., Cui K., Roh T.-Y., Schones D. E., Wang Z., Wei G., Chepelev I., Zhao K., 2007 High-resolution profiling of histone methylations in the human genome. *Cell* **129**: 823–37.
- Bernstein B. E., Kamal M., Lindblad-Toh K., Bekiranov S., Bailey D. K., Huebert D. J., McMahon S., Karlsson E. K., Kulbokas E. J., Gingeras T. R., Schreiber S. L., Lander E. S., 2005 Genomic maps and comparative analysis of histone modifications in human and mouse. *Cell* **120**: 169–81.
- Bhaumik S. R., Green M. R., 2002 Differential requirement of SAGA components for recruitment of TATA-box-binding protein to promoters in vivo. *Mol. Cell. Biol.* **22**: 7365–71.
- Bian C., Xu C., Ruan J., Lee K. K., Burke T. L., Tempel W., Barsyte D., Li J., Wu M., Zhou B. O., Fleharty B. E., Paulson A., Allali-Hassani A., Zhou J.-Q., Mer G., Grant P. A., Workman J. L., Zang J., Min J., 2011 Sgf29 binds histone H3K4me2/3 and is required for SAGA complex recruitment and histone H3 acetylation. *EMBO J.* **30**: 2829–2842.
- Bird A., Macleod D., 2004 Reading the DNA methylation signal. *Cold Spring Harb. Symp. Quant. Biol.* **69**: 113–8.

- Biterge B., Schneider R., 2014 Histone variants: key players of chromatin. *Cell Tissue Res.* **356**: 457–66.
- Boeke J. D., LaCroute F., Fink G. R., 1984 A positive selection for mutants lacking orotidine-5'-phosphate decarboxylase activity in yeast: 5-fluoro-orotic acid resistance. *Mol. Gen. Genet.* **197**: 345–6.
- Botstein D., Chervitz S. A., Cherry J. M., 1997 Yeast as a model organism. *Science* **277**: 1259–60.
- Briggs S. D., Bryk M., Strahl B. D., Cheung W. L., Davie J. K., Dent S. Y., Winston F., Allis C. D., 2001 Histone H3 lysine 4 methylation is mediated by Set1 and required for cell growth and rDNA silencing in *Saccharomyces cerevisiae*. *Genes Dev.* **15**: 3286–95.
- Brown J. A., Sherlock G., Myers C. L., Burrows N. M., Deng C., Wu H. I., McCann K. E., Troyanskaya O. G., Brown J. M., 2006 Global analysis of gene function in yeast by quantitative phenotypic profiling. *Mol. Syst. Biol.* **2**: 2006.0001.
- Brownell J. E., Zhou J., Ranalli T., Kobayashi R., Edmondson D. G., Roth S. Y., Allis C. D., 1996 *Tetrahymena* histone acetyltransferase A: a homolog to yeast Gcn5p linking histone acetylation to gene activation. *Cell* **84**: 843–51.
- Carlson M., Osmond B. C., Botstein D., 1981 Mutants of yeast defective in sucrose utilization. *Genetics* **98**: 25–40.
- Carrozza M. J., Li B., Florens L., Sukanuma T., Swanson S. K., Lee K. K., Shia W.-J., Anderson S., Yates J., Washburn M. P., Workman J. L., 2005 Histone H3 methylation by Set2 directs deacetylation of coding regions by Rpd3S to suppress spurious intragenic transcription. *Cell* **123**: 581–92.
- Chen P., Zhao J., Wang Y., Wang M., Long H., Liang D., Huang L., Wen Z., Li W., Li X., Feng H., Zhao H., Zhu P., Li M., Wang Q., Li G., 2013 H3.3 actively marks enhancers and primes gene transcription via opening higher-ordered chromatin. *Genes Dev.* **27**: 2109–24.
- Chereji R. V., Kan T.-W., Grudniewska M. K., Romashchenko A. V., Berezikov E., Zhimulev I. F., Guryev V., Morozov A. V., Moshkin Y. M., 2015 Genome-wide profiling of nucleosome sensitivity and chromatin accessibility in *Drosophila melanogaster*. *Nucleic Acids Res.*: gkv978–.
- Cho E. J., Kobor M. S., Kim M., Greenblatt J., Buratowski S., 2001 Opposing effects of Ctk1 kinase and Fcp1 phosphatase at Ser 2 of the RNA polymerase II C-terminal domain. *Genes Dev.* **15**: 3319–29.
- Choi J. K., Grimes D. E., Rowe K. M., Howe L. J., 2008 Acetylation of Rsc4p by Gcn5p is essential in the absence of histone H3 acetylation. *Mol. Cell. Biol.* **28**: 6967–72.
- Corradi N., Pombert J.-F., Farinelli L., Didier E. S., Keeling P. J., 2010 The complete sequence of the smallest known nuclear genome from the microsporidian *Encephalitozoon intestinalis*. *Nat. Commun.* **1**: 77.
- Dai J., Hyland E. M., Yuan D. S., Huang H., Bader J. S., Boeke J. D., 2008 Probing nucleosome function: a highly versatile library of synthetic histone H3 and H4 mutants. *Cell* **134**: 1066–78.

- Dhalluin C., Carlson J. E., Zeng L., He C., Aggarwal A. K., Zhou M. M., 1999 Structure and ligand of a histone acetyltransferase bromodomain. *Nature* **399**: 491–6.
- Dhayalan A., Rajavelu A., Rathert P., Tamas R., Jurkowska R. Z., Ragozin S., Jeltsch A., 2010 The Dnmt3a PWWP Domain Reads Histone 3 Lysine 36 Trimethylation and Guides DNA Methylation. *J. Biol. Chem.* **285**: 26114–26120.
- Dion M. F., Altschuler S. J., Wu L. F., Rando O. J., 2005 Genomic characterization reveals a simple histone H4 acetylation code. *Proc. Natl. Acad. Sci.* **102**: 5501–5506.
- Dorigo B., Schalch T., Bystricky K., Richmond T. J., 2003 Chromatin fiber folding: requirement for the histone H4 N-terminal tail. *J. Mol. Biol.* **327**: 85–96.
- Drouin S., Laramée L., Jacques P.-É., Forest A., Bergeron M., Robert F., 2010 DSIF and RNA polymerase II CTD phosphorylation coordinate the recruitment of Rpd3S to actively transcribed genes. *PLoS Genet.* **6**: e1001173.
- Duina A. A., Winston F., 2004 Analysis of a mutant histone H3 that perturbs the association of Swi/Snf with chromatin. *Mol. Cell. Biol.* **24**: 561–72.
- Eberharter A., Sterner D. E., Schieltz D., Hassan A., Yates J. R., Berger S. L., Workman J. L., 1999 The ADA complex is a distinct histone acetyltransferase complex in *Saccharomyces cerevisiae*. *Mol. Cell. Biol.* **19**: 6621–31.
- Eustermann S., Yang J.-C., Law M. J., Amos R., Chapman L. M., Jelinska C., Garrick D., Clynes D., Gibbons R. J., Rhodes D., Higgs D. R., Neuhaus D., 2011 Combinatorial readout of histone H3 modifications specifies localization of ATRX to heterochromatin. *Nat. Struct. Mol. Biol.* **18**: 777–82.
- Fan Y., Nikitina T., Zhao J., Fleury T. J., Bhattacharyya R., Bouhassira E. E., Stein A., Woodcock C. L., Skoultchi A. I., 2005 Histone H1 depletion in mammals alters global chromatin structure but causes specific changes in gene regulation. *Cell* **123**: 1199–212.
- Fan X., Lamarre-Vincent N., Wang Q., Struhl K., 2008 Extensive chromatin fragmentation improves enrichment of protein binding sites in chromatin immunoprecipitation experiments. *Nucleic Acids Res.* **36**: e125.
- Ferreira H., Flaus A., Owen-Hughes T., 2007 Histone Modifications Influence the Action of Snf2 Family Remodelling Enzymes by Different Mechanisms. *J. Mol. Biol.* **374**: 563–579.
- Finch J. T., Klug A., 1976 Solenoidal model for superstructure in chromatin. *Proc. Natl. Acad. Sci. U. S. A.* **73**: 1897–901.
- Freidkin I., Katcoff D. J., 2001 Specific distribution of the *Saccharomyces cerevisiae* linker histone homolog HHO1p in the chromatin. *Nucleic Acids Res.* **29**: 4043–51.

- Fuchs S. M., Kizer K. O., Braberg H., Krogan N. J., Strahl B. D., 2012 RNA polymerase II carboxyl-terminal domain phosphorylation regulates protein stability of the Set2 methyltransferase and histone H3 di- and trimethylation at lysine 36. *J. Biol. Chem.* **287**: 3249–56.
- Garcia-Ramirez M., Rocchini C., Ausio J., 1995 Modulation of chromatin folding by histone acetylation. *J. Biol. Chem.* **270**: 17923–8.
- Gilbert T. M., McDaniel S. L., Byrum S. D., Cades J. A., Dancy B. C. R., Wade H., Tackett A. J., Strahl B. D., Taverna S. D., 2014 A PWWP domain-containing protein targets the NuA3 acetyltransferase complex via histone H3 lysine 36 trimethylation to coordinate transcriptional elongation at coding regions. *Mol. Cell. Proteomics* **13**: 2883–95.
- Gillam S., Smith M., 1979 Site-specific mutagenesis using synthetic oligodeoxyribonucleotide primers: I. Optimum conditions and minimum oligodeoxyribonucleotide length. *Gene* **8**: 81–97.
- Ginsburg D. S., Govind C. K., Hinnebusch A. G., 2009 NuA4 Lysine Acetyltransferase Esa1 Is Targeted to Coding Regions and Stimulates Transcription Elongation with Gcn5. *Mol. Cell. Biol.* **29**: 6473–6487.
- Goldberg A. D., Banaszynski L. A., Noh K.-M., Lewis P. W., Elsaesser S. J., Stadler S., Dewell S., Law M., Guo X., Li X., Wen D., Chappier A., DeKolver R. C., Miller J. C., Lee Y.-L., Boydston E. A., Holmes M. C., Gregory P. D., Greally J. M., Rafii S., Yang C., Scambler P. J., Garrick D., Gibbons R. J., Higgs D. R., Cristea I. M., Urnov F. D., Zheng D., Allis C. D., 2010 Distinct factors control histone variant H3.3 localization at specific genomic regions. *Cell* **140**: 678–91.
- Goldknopf I. L., Busch H., 1977 Isopeptide linkage between nonhistone and histone 2A polypeptides of chromosomal conjugate-protein A24. *Proc. Natl. Acad. Sci. U. S. A.* **74**: 864–8.
- Gossett A. J., Lieb J. D., 2012 In vivo effects of histone H3 depletion on nucleosome occupancy and position in *Saccharomyces cerevisiae*. *PLoS Genet.* **8**: e1002771.
- Goutte-Gattat D., Shuaib M., Ouararhni K., Gautier T., Skoufias D. A., Hamiche A., Dimitrov S., 2013 Phosphorylation of the CENP-A amino-terminus in mitotic centromeric chromatin is required for kinetochore function. *Proc. Natl. Acad. Sci.* **110**: 8579–8584.
- Govind C. K., Zhang F., Qiu H., Hofmeyer K., Hinnebusch A. G., 2007 Gcn5 Promotes Acetylation, Eviction, and Methylation of Nucleosomes in Transcribed Coding Regions. *Mol. Cell* **25**: 31–42.
- Grant P. A., Duggan L., Côté J., Roberts S. M., Brownell J. E., Candau R., Ohba R., Owen-Hughes T., Allis C. D., Winston F., Berger S. L., Workman J. L., 1997 Yeast Gcn5 functions in two multisubunit complexes to acetylate nucleosomal histones: characterization of an Ada complex and the SAGA (Spt/Ada) complex. *Genes Dev.* **11**: 1640–50.
- Guillemette B., Drogaris P., Lin H.-H. S., Armstrong H., Hiragami-Hamada K., Imhof A., Bonneil E., Thibault P., Verreault A., Festenstein R. J., 2011 H3 lysine 4 is acetylated at active gene promoters and is regulated by H3 lysine 4 methylation. *PLoS Genet.* **7**: e1001354.

- Hake S. B., Garcia B. A., Duncan E. M., Kauer M., Dellaire G., Shabanowitz J., Bazett-Jones D. P., Allis C. D., Hunt D. F., 2005 Expression Patterns and Post-translational Modifications Associated with Mammalian Histone H3 Variants. *J. Biol. Chem.* **281**: 559–568.
- Han J., Zhou H., Li Z., Xu R.-M., Zhang Z., 2007 Acetylation of lysine 56 of histone H3 catalyzed by RTT109 and regulated by ASF1 is required for replisome integrity. *J. Biol. Chem.* **282**: 28587–96.
- Hargreaves D. C., Crabtree G. R., 2011 ATP-dependent chromatin remodeling: genetics, genomics and mechanisms. *Cell Res.* **21**: 396–420.
- He N., Chan C. K., Sobhian B., Chou S., Xue Y., Liu M., Alber T., Benkirane M., Zhou Q., 2011 Human Polymerase-Associated Factor complex (PAF_c) connects the Super Elongation Complex (SEC) to RNA polymerase II on chromatin. *Proc. Natl. Acad. Sci. U. S. A.* **108**: E636–45.
- Hebbes T. R., Clayton A. L., Thorne A. W., Crane-Robinson C., 1994 Core histone hyperacetylation co-maps with generalized DNase I sensitivity in the chicken beta-globin chromosomal domain. *EMBO J.* **13**: 1823–30.
- Ho J. W. K., Bishop E., Karchenko P. V., Nègre N., White K. P., Park P. J., 2011 ChIP-chip versus ChIP-seq: lessons for experimental design and data analysis. *BMC Genomics* **12**: 134.
- Hong L., Schroth G. P., Matthews H. R., Yau P., Bradbury E. M., 1993 Studies of the DNA binding properties of histone H4 amino terminus. Thermal denaturation studies reveal that acetylation markedly reduces the binding constant of the H4 “tail” to DNA. *J. Biol. Chem.* **268**: 305–14.
- Howe L., Auston D., Grant P., John S., Cook R. G., Workman J. L., Pillus L., 2001 Histone H3 specific acetyltransferases are essential for cell cycle progression. *Genes Dev.* **15**: 3144–54.
- Howe L., Kusch T., Muster N., Chaterji R., Yates J. R., Workman J. L., 2002 Yng1p modulates the activity of Sas3p as a component of the yeast NuA3 Hhistone acetyltransferase complex. *Mol. Cell. Biol.* **22**: 5047–53.
- Hughes A. L., Rando O. J., 2014 Mechanisms underlying nucleosome positioning in vivo. *Annu. Rev. Biophys.* **43**: 41–63.
- Huh J.-W., Wu J., Lee C.-H., Yun M., Gilada D., Brautigam C. A., Li B., 2012 Multivalent di-nucleosome recognition enables the Rpd3S histone deacetylase complex to tolerate decreased H3K36 methylation levels. *EMBO J.* **31**: 3564–3574.
- Huynh V. A. T., Robinson P. J. J., Rhodes D., 2005 A method for the in vitro reconstitution of a defined “30 nm” chromatin fibre containing stoichiometric amounts of the linker histone. *J. Mol. Biol.* **345**: 957–68.
- Jin C., Felsenfeld G., 2007 Nucleosome stability mediated by histone variants H3.3 and H2A.Z. *Genes Dev.* **21**: 1519–29.

- Jin C., Zang C., Wei G., Cui K., Peng W., Zhao K., Felsenfeld G., 2009 H3.3/H2A.Z double variant-containing nucleosomes mark “nucleosome-free regions” of active promoters and other regulatory regions. *Nat. Genet.* **41**: 941–5.
- John S., Howe L., Tafrov S. T., Grant P. A., Sternglanz R., Workman J. L., 2000 The something about silencing protein, Sas3, is the catalytic subunit of NuA3, a γ TAF(II)30-containing HAT complex that interacts with the Spt16 subunit of the yeast CP (Cdc68/Pob3)-FACT complex. *Genes Dev.* **14**: 1196–208.
- Joshi A. A., Struhl K., 2005 Eaf3 chromodomain interaction with methylated H3-K36 links histone deacetylation to Pol II elongation. *Mol. Cell* **20**: 971–8.
- Kadosh D., Struhl K., 1998 Targeted recruitment of the Sin3-Rpd3 histone deacetylase complex generates a highly localized domain of repressed chromatin in vivo. *Mol. Cell. Biol.* **18**: 5121–7.
- Kan P.-Y., Caterino T. L., Hayes J. J., 2009 The H4 tail domain participates in intra- and internucleosome interactions with protein and DNA during folding and oligomerization of nucleosome arrays. *Mol. Cell. Biol.* **29**: 538–46.
- Kaplan N., Moore I. K., Fondufe-Mittendorf Y., Gossett A. J., Tillo D., Field Y., LeProust E. M., Hughes T. R., Lieb J. D., Widom J., Segal E., 2009 The DNA-encoded nucleosome organization of a eukaryotic genome. *Nature* **458**: 362–6.
- Kemmeren P., Sameith K., Pasch L. A. L. van de, Benschop J. J., Lenstra T. L., Margaritis T., O’Duibhir E., Apweiler E., Wageningen S. van, Ko C. W., Heesch S. van, Kashani M. M., Ampatziadis-Michailidis G., Brok M. O., Brabers N. A. C. H., Miles A. J., Bouwmeester D., Hooff S. R. van, Bakel H. van, Sluiters E., Bakker L. V, Snel B., Lijnzaad P., Leenen D. van, Groot Koerkamp M. J. A., Holstege F. C. P., 2014 Large-scale genetic perturbations reveal regulatory networks and an abundance of gene-specific repressors. *Cell* **157**: 740–52.
- Keogh M.-C., Kurdistani S. K., Morris S. A., Ahn S. H., Podolny V., Collins S. R., Schuldiner M., Chin K., Punna T., Thompson N. J., Boone C., Emili A., Weissman J. S., Hughes T. R., Strahl B. D., Grunstein M., Greenblatt J. F., Buratowski S., Krogan N. J., 2005 Cotranscriptional set2 methylation of histone H3 lysine 36 recruits a repressive Rpd3 complex. *Cell* **123**: 593–605.
- Kornberg R. D., Stryer L., 1988 Statistical distributions of nucleosomes: nonrandom locations by a stochastic mechanism. *Nucleic Acids Res.* **16**: 6677–90.
- Kornberg R. D., Lorch Y., 1999 Twenty-five years of the nucleosome, fundamental particle of the eukaryote chromosome. *Cell* **98**: 285–94.
- Krajewski W. A., Becker P. B., 1998 Reconstitution of hyperacetylated, DNase I-sensitive chromatin characterized by high conformational flexibility of nucleosomal DNA. *Proc. Natl. Acad. Sci. U. S. A.* **95**: 1540–5.

- Kristjuhan A., Walker J., Suka N., Grunstein M., Roberts D., Cairns B. R., Svejstrup J. Q., 2002
Transcriptional inhibition of genes with severe histone H3 hypoacetylation in the coding region.
Mol. Cell **10**: 925–33.
- Krogan N. J., Dover J., Khorrami S., Greenblatt J. F., Schneider J., Johnston M., Shilatifard A., 2002
COMPASS, a histone H3 (Lysine 4) methyltransferase required for telomeric silencing of gene
expression. *J. Biol. Chem.* **277**: 10753–5.
- Krogan N. J., Dover J., Wood A., Schneider J., Heidt J., Boateng M. A., Dean K., Ryan O. W., Golshani A.,
Johnston M., Greenblatt J. F., Shilatifard A., 2003a The Paf1 Complex Is Required for Histone H3
Methylation by COMPASS and Dot1p: Linking Transcriptional Elongation to Histone Methylation.
Mol. Cell **11**: 721–729.
- Krogan N. J., Dover J., Wood A., Schneider J., Heidt J., Boateng M. A., Dean K., Ryan O. W., Golshani A.,
Johnston M., Greenblatt J. F., Shilatifard A., 2003b The Paf1 complex is required for histone H3
methylation by COMPASS and Dot1p: linking transcriptional elongation to histone methylation.
Mol. Cell **11**: 721–9.
- Krogan N. J., Cagney G., Yu H., Zhong G., Guo X., Ignatchenko A., Li J., Pu S., Datta N., Tikuisis A. P., Punna
T., Peregrín-Alvarez J. M., Shales M., Zhang X., Davey M., Robinson M. D., Paccanaro A., Bray J. E.,
Sheung A., Beattie B., Richards D. P., Canadien V., Lalev A., Mena F., Wong P., Starostine A., Canete
M. M., Vlasblom J., Wu S., Orsi C., Collins S. R., Chandran S., Haw R., Rilstone J. J., Gandi K.,
Thompson N. J., Musso G., St Onge P., Ghanny S., Lam M. H. Y., Butland G., Altaf-Ul A. M., Kanaya
S., Shilatifard A., O'Shea E., Weissman J. S., Ingles C. J., Hughes T. R., Parkinson J., Gerstein M.,
Wodak S. J., Emili A., Greenblatt J. F., 2006 Global landscape of protein complexes in the yeast
Saccharomyces cerevisiae. *Nature* **440**: 637–43.
- Kuo M. H., Brownell J. E., Sobel R. E., Ranalli T. A., Cook R. G., Edmondson D. G., Roth S. Y., Allis C. D.,
1996 Transcription-linked acetylation by Gcn5p of histones H3 and H4 at specific lysines. *Nature*
383: 269–72.
- Kuo M. H., Zhou J., Jambeck P., Churchill M. E., Allis C. D., 1998 Histone acetyltransferase activity of
yeast Gcn5p is required for the activation of target genes in vivo. *Genes Dev.* **12**: 627–39.
- Kuo M. H., Baur E. vom, Struhl K., Allis C. D., 2000 Gcn4 activator targets Gcn5 histone acetyltransferase
to specific promoters independently of transcription. *Mol. Cell* **6**: 1309–20.
- Kuo Y. M., Andrews A. J., 2013 Quantitating the Specificity and Selectivity of Gcn5-Mediated Acetylation
of Histone H3. *PLoS One* **8**.
- Kurdistani S. K., Grunstein M., 2003 Histone acetylation and deacetylation in yeast. *Nat. Rev. Mol. Cell
Biol.* **4**: 276–84.
- Kurdistani S. K., Tavazoie S., Grunstein M., 2004 Mapping global histone acetylation patterns to gene
expression. *Cell* **117**: 721–33.
- Kushnirov V. V., 2000 Rapid and reliable protein extraction from yeast. *Yeast* **16**: 857–60.

- Lafon A., Chang C. S., Scott E. M., Jacobson S. J., Pillus L., 2007 MYST opportunities for growth control: yeast genes illuminate human cancer gene functions. *Oncogene* **26**: 5373–84.
- Lambert J.-P., Mitchell L., Rudner A., Baetz K., Figeys D., 2009 A novel proteomics approach for the discovery of chromatin-associated protein networks. *Mol. Cell. Proteomics* **8**: 870–82.
- Lee D. Y., Hayes J. J., Pruss D., Wolffe A. P., 1993 A positive role for histone acetylation in transcription factor access to nucleosomal DNA. *Cell* **72**: 73–84.
- Lee C.-H., Wu J., Li B., 2013 Chromatin remodelers fine-tune H3K36me-directed deacetylation of neighbor nucleosomes by Rpd3S. *Mol. Cell* **52**: 255–63.
- Lenstra T. L., Benschop J. J., Kim T., Schulze J. M., Brabers N. A. C. H., Margaritis T., Pasch L. A. L. van de, Heesch S. A. A. C. van, Brok M. O., Groot Koerkamp M. J. A., Ko C. W., Leenen D. van, Sameith K., Hooff S. R. van, Lijnzaad P., Kemmeren P., Hentrich T., Kobor M. S., Buratowski S., Holstege F. C. P., 2011 The specificity and topology of chromatin interaction pathways in yeast. *Mol. Cell* **42**: 536–49.
- Lewis P. W., Elsaesser S. J., Noh K.-M., Stadler S. C., Allis C. D., 2010 Daxx is an H3.3-specific histone chaperone and cooperates with ATRX in replication-independent chromatin assembly at telomeres. *Proc. Natl. Acad. Sci. U. S. A.* **107**: 14075–80.
- Li H., Ilin S., Wang W., Duncan E. M., Wysocka J., Allis C. D., Patel D. J., 2006 Molecular basis for site-specific read-out of histone H3K4me3 by the BPTF PHD finger of NURF. *Nature* **442**: 91–5.
- Li B., Jackson J., Simon M. D., Fleharty B., Gogol M., Seidel C., Workman J. L., Shilatifard A., 2009a Histone H3 lysine 36 dimethylation (H3K36me₂) is sufficient to recruit the Rpd3s histone deacetylase complex and to repress spurious transcription. *J. Biol. Chem.* **284**: 7970–6.
- Li H., Durbin R., 2009 Fast and accurate short read alignment with Burrows-Wheeler transform. *Bioinformatics* **25**: 1754–60.
- Li H., Handsaker B., Wysoker A., Fennell T., Ruan J., Homer N., Marth G., Abecasis G., Durbin R., 2009b The Sequence Alignment/Map format and SAMtools. *Bioinformatics* **25**: 2078–9.
- Li H., Durbin R., 2010 Fast and accurate long-read alignment with Burrows-Wheeler transform. *Bioinformatics* **26**: 589–95.
- Li M., Valsakumar V., Poorey K., Bekiranov S., Smith J. S., 2013a Genome-wide analysis of functional sirtuin chromatin targets in yeast. *Genome Biol.* **14**: R48.
- Li F., Mao G., Tong D., Huang J., Gu L., Yang W., Li G.-M., 2013b The histone mark H3K36me₃ regulates human DNA mismatch repair through its interaction with MutS α . *Cell* **153**: 590–600.
- Li Y., Wen H., Xi Y., Tanaka K., Wang H., Peng D., Ren Y., Jin Q., Dent S. Y. R., Li W., Li H., Shi X., 2014 AF9 YEATS Domain Links Histone Acetylation to DOT1L-Mediated H3K79 Methylation. *Cell* **159**: 558–571.

- Liang G., Kloise R. J., Gardner K. E., Zhang Y., 2007 Yeast Jhd2p is a histone H3 Lys4 trimethyl demethylase. *Nat. Struct. Mol. Biol.* **14**: 243–245.
- Lindroth A. M., Shultis D., Jasencakova Z., Fuchs J., Johnson L., Schubert D., Patnaik D., Pradhan S., Goodrich J., Schubert I., Jenuwein T., Khorasanizadeh S., Jacobsen S. E., 2004 Dual histone H3 methylation marks at lysines 9 and 27 required for interaction with CHROMOMETHYLASE3. *EMBO J.* **23**: 4286–96.
- Lindstrom K. C., Vary J. C., Parthun M. R., Delrow J., Tsukiyama T., 2006 Isw1 Functions in Parallel with the NuA4 and Swr1 Complexes in Stress-Induced Gene Repression. *Mol. Cell. Biol.* **26**: 6117–6129.
- Liu L., Qin S., Zhang J., Ji P., Shi Y., Wu J., 2012 Solution structure of an atypical PHD finger in BRPF2 and its interaction with DNA. *J. Struct. Biol.* **180**: 165–173.
- Luger K., Mäder A. W., Richmond R. K., Sargent D. F., Richmond T. J., 1997 Crystal structure of the nucleosome core particle at 2.8 Å resolution. *Nature* **389**: 251–60.
- Luscombe N. M., Laskowski R. A., Thornton J. M., 2001 Amino acid-base interactions: a three-dimensional analysis of protein-DNA interactions at an atomic level. *Nucleic Acids Res.* **29**: 2860–74.
- MacDonald V. E., Howe L. J., 2009 Histone acetylation: where to go and how to get there. *Epigenetics* **4**: 139–43.
- Maeshima K., Hihara S., Eltsov M., 2010 Chromatin structure: does the 30-nm fibre exist in vivo? *Curr. Opin. Cell Biol.* **22**: 291–7.
- Mahadevan L. C., Willis A. C., Barratt M. J., 1991 Rapid histone H3 phosphorylation in response to growth factors, phorbol esters, okadaic acid, and protein synthesis inhibitors. *Cell* **65**: 775–783.
- Maltby V. E., Martin B. J. E., Schulze J. M., Johnson I., Hentrich T., Sharma A., Kobor M. S., Howe L., 2012a Histone H3 lysine 36 methylation targets the Isw1b remodeling complex to chromatin. *Mol. Cell. Biol.* **32**: 3479–85.
- Maltby V. E., Martin B. J. E., Brind'Amour J., Chruscicki A. T., McBurney K. L., Schulze J. M., Johnson I. J., Hills M., Hentrich T., Kobor M. S., Lorincz M. C., Howe L. J., 2012b Histone H3K4 demethylation is negatively regulated by histone H3 acetylation in *Saccharomyces cerevisiae*. *Proc. Natl. Acad. Sci. U. S. A.* **109**: 18505–10.
- Martin A. M., 2004 Redundant Roles for Histone H3 N-Terminal Lysine Residues in Subtelomeric Gene Repression in *Saccharomyces cerevisiae*. *Genetics* **167**: 1123–1132.
- Martin D. G. E., Grimes D. E., Baetz K., Howe L., 2006a Methylation of histone H3 mediates the association of the NuA3 histone acetyltransferase with chromatin. *Mol. Cell. Biol.* **26**: 3018–28.

- Martin D. G. E., Baetz K., Shi X., Walter K. L., MacDonald V. E., Wlodarski M. J., Gozani O., Hieter P., Howe L., 2006b The Yng1p plant homeodomain finger is a methyl-histone binding module that recognizes lysine 4-methylated histone H3. *Mol. Cell. Biol.* **26**: 7871–9.
- Miller T., Krogan N. J., Dover J., Erdjument-Bromage H., Tempst P., Johnston M., Greenblatt J. F., Shilatifard A., 2001 COMPASS: a complex of proteins associated with a trithorax-related SET domain protein. *Proc. Natl. Acad. Sci. U. S. A.* **98**: 12902–7.
- Mito Y., Henikoff J. G., Henikoff S., 2005 Genome-scale profiling of histone H3.3 replacement patterns. *Nat. Genet.* **37**: 1090–7.
- Morinière J., Rousseaux S., Steuerwald U., Soler-López M., Curtet S., Vitte A.-L., Govin J., Gaucher J., Sadoul K., Hart D. J., Krijgsveld J., Khochbin S., Müller C. W., Petosa C., 2009 Cooperative binding of two acetylation marks on a histone tail by a single bromodomain. *Nature* **461**: 664–668.
- Morris S. A., Rao B., Garcia B. A., Hake S. B., Diaz R. L., Shabanowitz J., Hunt D. F., Allis C. D., Lieb J. D., Strahl B. D., 2007 Identification of histone H3 lysine 36 acetylation as a highly conserved histone modification. *J. Biol. Chem.* **282**: 7632–40.
- Morrison A. J., Highland J., Krogan N. J., Arbel-Eden A., Greenblatt J. F., Haber J. E., Shen X., 2004 INO80 and γ -H2AX Interaction Links ATP-Dependent Chromatin Remodeling to DNA Damage Repair. *Cell* **119**: 767–775.
- Mosley A. L., Pattenden S. G., Carey M., Venkatesh S., Gilmore J. M., Florens L., Workman J. L., Washburn M. P., 2009 Rtr1 is a CTD phosphatase that regulates RNA polymerase II during the transition from serine 5 to serine 2 phosphorylation. *Mol. Cell* **34**: 168–78.
- Mumberg D., Müller R., Funk M., 1994 Regulatable promoters of *Saccharomyces cerevisiae*: comparison of transcriptional activity and their use for heterologous expression. *Nucleic Acids Res.* **22**: 5767–8.
- Musselman C. A., Lalonde M.-E., Côté J., Kutateladze T. G., 2012 Perceiving the epigenetic landscape through histone readers. *Nat. Struct. Mol. Biol.* **19**: 1218–27.
- Neely K. E., Hassan A. H., Brown C. E., Howe L., Workman J. L., 2002 Transcription activator interactions with multiple SWI/SNF subunits. *Mol. Cell. Biol.* **22**: 1615–25.
- Nelson J. D., Denisenko O., Bomsztyk K., 2006 Protocol for the fast chromatin immunoprecipitation (ChIP) method. *Nat. Protoc.* **1**: 179–85.
- Ng H. H., Robert F., Young R. A., Struhl K., 2003 Targeted recruitment of Set1 histone methylase by elongating Pol II provides a localized mark and memory of recent transcriptional activity. *Mol. Cell* **11**: 709–19.
- Nuland R. van, Schaik F. M. van, Simonis M., Heesch S. van, Cuppen E., Boelens R., Timmers H. M., Ingen H. van, 2013 Nucleosomal DNA binding drives the recognition of H3K36-methylated nucleosomes by the PSIP1-PWWP domain. *Epigenetics Chromatin* **6**: 12.

- Obrdlik A., Kukalev A., Louvet E., Farrants A.-K. O., Caputo L., Percipalle P., 2008 The histone acetyltransferase PCAF associates with actin and hnRNP U for RNA polymerase II transcription. *Mol. Cell. Biol.* **28**: 6342–57.
- Ohtsuki K., Kasahara K., Shirahige K., Kokubo T., 2009 Genome-wide localization analysis of a complete set of Tafs reveals a specific effect of the taf1 mutation on Taf2 occupancy and provides indirect evidence for different TFIID conformations at different promoters. *Nucleic Acids Res.* **38**: 1805–1820.
- Park Y.-J., Dyer P. N., Tremethick D. J., Luger K., 2004 A New Fluorescence Resonance Energy Transfer Approach Demonstrates That the Histone Variant H2AZ Stabilizes the Histone Octamer within the Nucleosome. *J. Biol. Chem.* **279**: 24274–24282.
- Park D., Morris A. R., Battenhouse A., Iyer V. R., 2014 Simultaneous mapping of transcript ends at single-nucleotide resolution and identification of widespread promoter-associated non-coding RNA governed by TATA elements. *Nucleic Acids Res.* **42**: 3736–49.
- Pavlidis P., Noble W. S., 2003 Matrix2png: a utility for visualizing matrix data. *Bioinformatics* **19**: 295–6.
- Peterson C. L., Laniel M.-A., 2004 Histones and histone modifications. *Curr. Biol.* **14**: R546–51.
- Pokholok D. K., Harbison C. T., Levine S., Cole M., Hannett N. M., Lee T. I., Bell G. W., Walker K., Rolfe P. A., Herbolsheimer E., Zeitlinger J., Lewitter F., Gifford D. K., Young R. A., 2005 Genome-wide map of nucleosome acetylation and methylation in yeast. *Cell* **122**: 517–27.
- Poplawski A., Hu K., Lee W., Natesan S., Peng D., Carlson S., Shi X., Balaz S., Markley J. L., Glass K. C., 2014 Molecular insights into the recognition of N-terminal histone modifications by the BRPF1 bromodomain. *J. Mol. Biol.* **426**: 1661–76.
- Pray-Grant M. G., Schieltz D., McMahon S. J., Wood J. M., Kennedy E. L., Cook R. G., Workman J. L., Yates J. R., Grant P. A., 2002 The novel SLIK histone acetyltransferase complex functions in the yeast retrograde response pathway. *Mol. Cell. Biol.* **22**: 8774–86.
- Qian W., Ma D., Xiao C., Wang Z., Zhang J., 2012 The genomic landscape and evolutionary resolution of antagonistic pleiotropy in yeast. *Cell Rep.* **2**: 1399–410.
- Qin S., Jin L., Zhang J., Liu L., Ji P., Wu M., Wu J., Shi Y., 2011 Recognition of unmodified histone H3 by the first PHD finger of bromodomain-PHD finger protein 2 provides insights into the regulation of histone acetyltransferases monocytic leukemic zinc-finger protein (MOZ) and MOZ-related factor (MORF). *J. Biol. Chem.* **286**: 36944–55.
- Qiu H., Hu C., Yoon S., Natarajan K., Swanson M. J., Hinnebusch A. G., 2004 An array of coactivators is required for optimal recruitment of TATA binding protein and RNA polymerase II by promoter-bound Gcn4p. *Mol. Cell. Biol.* **24**: 4104–17.
- Quinlan A. R., Hall I. M., 2010 BEDTools: a flexible suite of utilities for comparing genomic features. *Bioinformatics* **26**: 841–2.

- Rando O. J., Winston F., 2012 Chromatin and transcription in yeast. *Genetics* **190**: 351–87.
- Rando O. J., 2012 Combinatorial complexity in chromatin structure and function: revisiting the histone code. *Curr. Opin. Genet. Dev.* **22**: 148–55.
- Reifsnnyder C., Lowell J., Clarke A., Pillus L., 1996 Yeast SAS silencing genes and human genes associated with AML and HIV-1 Tat interactions are homologous with acetyltransferases. *Nat. Genet.* **14**: 42–9.
- Robert F., Pokholok D. K., Hannett N. M., Rinaldi N. J., Chandy M., Rolfe A., Workman J. L., Gifford D. K., Young R. A., 2004 Global Position and Recruitment of HATs and HDACs in the Yeast Genome. *Mol. Cell* **16**: 199–209.
- Rodriguez C. R., Cho E. J., Keogh M. C., Moore C. L., Greenleaf A. L., Buratowski S., 2000 Kin28, the TFIIF-associated carboxy-terminal domain kinase, facilitates the recruitment of mRNA processing machinery to RNA polymerase II. *Mol. Cell. Biol.* **20**: 104–12.
- Roguev A., 2001 The *Saccharomyces cerevisiae* Set1 complex includes an Ash2 homologue and methylates histone 3 lysine 4. *EMBO J.* **20**: 7137–7148.
- Rosaleny L. E., Ruiz-García A. B., García-Martínez J., Pérez-Ortín J. E., Tordera V., 2007 The Sas3p and Gcn5p histone acetyltransferases are recruited to similar genes. *Genome Biol.* **8**: R119.
- Rufiange A., Jacques P.-É., Bhat W., Robert F., Nourani A., 2007 Genome-Wide Replication-Independent Histone H3 Exchange Occurs Predominantly at Promoters and Implicates H3 K56 Acetylation and Asf1. *Mol. Cell* **27**: 393–405.
- Rundlett S. E., Carmen A. A., Suka N., Turner B. M., Grunstein M., 1998 Transcriptional repression by UME6 involves deacetylation of lysine 5 of histone H4 by RPD3. *Nature* **392**: 831–5.
- Rusche L. N., Kirchmaier A. L., Rine J., 2003 The establishment, inheritance, and function of silenced chromatin in *Saccharomyces cerevisiae*. *Annu. Rev. Biochem.* **72**: 481–516.
- Ruthenburg A. J., Li H., Milne T. A., Dewell S., McGinty R. K., Yuen M., Ueberheide B., Dou Y., Muir T. W., Patel D. J., Allis C. D., 2011 Recognition of a mononucleosomal histone modification pattern by BPTF via multivalent interactions. *Cell* **145**: 692–706.
- Sanchez R., Zhou M.-M., 2011 The PHD finger: a versatile epigenome reader. *Trends Biochem. Sci.* **36**: 364–72.
- Schneider J., Wood A., Lee J.-S., Schuster R., Dueker J., Maguire C., Swanson S. K., Florens L., Washburn M. P., Shilatifard A., 2005 Molecular regulation of histone H3 trimethylation by COMPASS and the regulation of gene expression. *Mol. Cell* **19**: 849–56.
- Schrödinger, 2010 The {PyMOL} Molecular Graphics System, Version~1.3r1.

- Schübeler D., MacAlpine D. M., Scalzo D., Wirbelauer C., Kooperberg C., Leeuwen F. van, Gottschling D. E., O'Neill L. P., Turner B. M., Delrow J., Bell S. P., Groudine M., 2004 The histone modification pattern of active genes revealed through genome-wide chromatin analysis of a higher eukaryote. *Genes Dev.* **18**: 1263–71.
- Schulze J. M., Wang A. Y., Kobor M. S., 2009 YEATS domain proteins: a diverse family with many links to chromatin modification and transcription. *Biochem. Cell Biol.* **87**: 65–75.
- Schwartz B. E., Ahmad K., 2005 Transcriptional activation triggers deposition and removal of the histone variant H3.3. *Genes Dev.* **19**: 804–14.
- Seward D. J., Cubberley G., Kim S., Schonewald M., Zhang L., Tripet B., Bentley D. L., 2007 Demethylation of trimethylated histone H3 Lys4 in vivo by JARID1 MjC proteins. *Nat. Struct. Mol. Biol.* **14**: 240–2.
- Shanle E. K., Andrews F. H., Meriesh H., McDaniel S. L., Dronamraju R., DiFiore J. V., Jha D., Wozniak G. G., Bridgers J. B., Kerschner J. L., Krajewski K., Martín G. M., Morrison A. J., Kutateladze T. G., Strahl B. D., 2015 Association of Taf14 with acetylated histone H3 directs gene transcription and the DNA damage response. *Genes Dev.* **29**: 1795–800.
- Shi X., Hong T., Walter K. L., Ewalt M., Michishita E., Hung T., Carney D., Peña P., Lan F., Kaadige M. R., Lacoste N., Cayrou C., Davrazou F., Saha A., Cairns B. R., Ayer D. E., Kutateladze T. G., Shi Y., Côté J., Chua K. F., Gozani O., 2006a ING2 PHD domain links histone H3 lysine 4 methylation to active gene repression. *Nature* **442**: 96–9.
- Shi X., Kachirskaja I., Walter K. L., Kuo J.-H. A., Lake A., Davrazou F., Chan S. M., Martin D. G. E., Fingerman I. M., Briggs S. D., Howe L., Utz P. J., Kutateladze T. G., Lugovskoy A. A., Bedford M. T., Gozani O., 2006b Proteome-wide Analysis in *Saccharomyces cerevisiae* Identifies Several PHD Fingers as Novel Direct and Selective Binding Modules of Histone H3 Methylated at Either Lysine 4 or Lysine 36. *J. Biol. Chem.* **282**: 2450–2455.
- Shiio Y., Eisenman R. N., 2003 Histone sumoylation is associated with transcriptional repression. *Proc. Natl. Acad. Sci. U. S. A.* **100**: 13225–30.
- Sikorski R. S., Hieter P., 1989 A system of shuttle vectors and yeast host strains designed for efficient manipulation of DNA in *Saccharomyces cerevisiae*. *Genetics* **122**: 19–27.
- Sinha D., Shogren-Knaak M. A., 2010 Role of direct interactions between the histone H4 Tail and the H2A core in long range nucleosome contacts. *J. Biol. Chem.* **285**: 16572–81.
- Smith S., Stillman B., 1989 Purification and characterization of CAF-I, a human cell factor required for chromatin assembly during DNA replication in vitro. *Cell* **58**: 15–25.
- Smith S. B., Cui Y., Bustamante C., 1996 Overstretching B-DNA: the elastic response of individual double-stranded and single-stranded DNA molecules. *Science* **271**: 795–9.
- Stern M., Jensen R., Herskowitz I., 1984 Five SWI genes are required for expression of the HO gene in yeast. *J. Mol. Biol.* **178**: 853–68.

- Sterner D. E., Belotserkovskaya R., Berger S. L., 2002 SALSA, a variant of yeast SAGA, contains truncated Spt7, which correlates with activated transcription. *Proc. Natl. Acad. Sci. U. S. A.* **99**: 11622–7.
- Strahl B. D., Allis C. D., 2000 The language of covalent histone modifications. *Nature* **403**: 41–5.
- Strahl B. D., Grant P. A., Briggs S. D., Sun Z.-W., Bone J. R., Caldwell J. A., Mollah S., Cook R. G., Shabanowitz J., Hunt D. F., Allis C. D., 2002 Set2 is a nucleosomal histone H3-selective methyltransferase that mediates transcriptional repression. *Mol. Cell. Biol.* **22**: 1298–306.
- Su D., Hu Q., Li Q., Thompson J. R., Cui G., Fazly A., Davies B. A., Botuyan M. V., Zhang Z., Mer G., 2012 Structural basis for recognition of H3K56-acetylated histone H3-H4 by the chaperone Rtt106. *Nature* **483**: 104–7.
- Suto R. K., Clarkson M. J., Tremethick D. J., Luger K., 2000 Crystal structure of a nucleosome core particle containing the variant histone H2A.Z. *Nat. Struct. Biol.* **7**: 1121–4.
- Szenker E., Ray-Gallet D., Almouzni G., 2011 The double face of the histone variant H3.3. *Cell Res.* **21**: 421–434.
- Takechi S., Nakayama T., 1999 Sas3 is a histone acetyltransferase and requires a zinc finger motif. *Biochem. Biophys. Res. Commun.* **266**: 405–10.
- Taunton J., Hassig C. A., Schreiber S. L., 1996 A mammalian histone deacetylase related to the yeast transcriptional regulator Rpd3p. *Science* **272**: 408–11.
- Taverna S. D., Ilin S., Rogers R. S., Tanny J. C., Lavender H., Li H., Baker L., Boyle J., Blair L. P., Chait B. T., Patel D. J., Aitchison J. D., Tackett A. J., Allis C. D., 2006 Yng1 PHD finger binding to H3 trimethylated at K4 promotes NuA3 HAT activity at K14 of H3 and transcription at a subset of targeted ORFs. *Mol. Cell* **24**: 785–96.
- Thakar A., Gupta P., Ishibashi T., Finn R., Silva-Moreno B., Uchiyama S., Fukui K., Tomschik M., Ausio J., Zlatanova J., 2009 H2A.Z and H3.3 histone variants affect nucleosome structure: biochemical and biophysical studies. *Biochemistry* **48**: 10852–7.
- Thompson P. R., Fast W., 2006 Histone citrullination by protein arginine deiminase: is arginine methylation a green light or a roadblock? *ACS Chem. Biol.* **1**: 433–41.
- Tse C., Sera T., Wolffe A. P., Hansen J. C., 1998 Disruption of higher-order folding by core histone acetylation dramatically enhances transcription of nucleosomal arrays by RNA polymerase III. *Mol. Cell. Biol.* **18**: 4629–38.
- Ullah M., Pelletier N., Xiao L., Zhao S. P., Wang K., Degerny C., Tahmasebi S., Cayrou C., Doyon Y., Goh S.-L., Champagne N., Cote J., Yang X.-J., 2008 Molecular Architecture of Quartet MOZ/MORF Histone Acetyltransferase Complexes. *Mol. Cell. Biol.* **28**: 6828–6843.
- Utleay R. T., Côté J., 2003 The MYST family of histone acetyltransferases. *Curr. Top. Microbiol. Immunol.* **274**: 203–36.

- Vezzoli A., Bonadies N., Allen M. D., Freund S. M. V., Santiveri C. M., Kvinlaug B. T., Huntly B. J. P., Göttgens B., Bycroft M., 2010 Molecular basis of histone H3K36me3 recognition by the PWWP domain of Brpf1. *Nat. Struct. Mol. Biol.* **17**: 617–619.
- Vicente-Muñoz S., Romero P., Magraner-Pardo L., Martinez-Jimenez C. P., Tordera V., Pamblanco M., 2014 Comprehensive analysis of interacting proteins and genome-wide location studies of the Sas3-dependent NuA3 histone acetyltransferase complex. *FEBS Open Bio* **4**: 996–1006.
- Villa-García M. J., Choi M. S., Hinz F. I., Gaspar M. L., Jesch S. A., Henry S. A., 2011 Genome-wide screen for inositol auxotrophy in *Saccharomyces cerevisiae* implicates lipid metabolism in stress response signaling. *Mol. Genet. Genomics* **285**: 125–49.
- Vivarès C. P., Méténier G., 2000 Towards the minimal eukaryotic parasitic genome. *Curr. Opin. Microbiol.* **3**: 463–7.
- Wang W., Xue Y., Zhou S., Kuo A., Cairns B. R., Crabtree G. R., 1996 Diversity and specialization of mammalian SWI/SNF complexes. *Genes Dev.* **10**: 2117–30.
- Wang Z., Zang C., Rosenfeld J. A., Schones D. E., Barski A., Cuddapah S., Cui K., Roh T.-Y., Peng W., Zhang M. Q., Zhao K., 2008 Combinatorial patterns of histone acetylations and methylations in the human genome. *Nat. Genet.* **40**: 897–903.
- Wang A. Y., Schulze J. M., Skordalakes E., Gin J. W., Berger J. M., Rine J., Kobor M. S., 2009 Asf1-like structure of the conserved Yaf9 YEATS domain and role in H2A.Z deposition and acetylation. *Proc. Natl. Acad. Sci. U. S. A.* **106**: 21573–8.
- Weber C. M., Henikoff S., 2014 Histone variants: dynamic punctuation in transcription. *Genes Dev.* **28**: 672–82.
- Weiner A., Hughes A., Yassour M., Rando O. J., Friedman N., 2010 High-resolution nucleosome mapping reveals transcription-dependent promoter packaging. *Genome Res.* **20**: 90–100.
- Weiner A., Hsieh T.-H. S., Appleboim A., Chen H. V., Rahat A., Amit I., Rando O. J., Friedman N., 2015 High-Resolution Chromatin Dynamics during a Yeast Stress Response. *Mol. Cell.*
- White C. L., Suto R. K., Luger K., 2001 Structure of the yeast nucleosome core particle reveals fundamental changes in internucleosome interactions. *EMBO J.* **20**: 5207–18.
- Williams A. F., Barclay A. N., 1988 The immunoglobulin superfamily--domains for cell surface recognition. *Annu. Rev. Immunol.* **6**: 381–405.
- Winkler G. S., Kristjuhan A., Erdjument-Bromage H., Tempst P., Svejstrup J. Q., 2002 Elongator is a histone H3 and H4 acetyltransferase important for normal histone acetylation levels in vivo. *Proc. Natl. Acad. Sci.* **99**: 3517–3522.
- Wong K. H., Jin Y., Struhl K., 2014 TFIIH phosphorylation of the Pol II CTD stimulates mediator dissociation from the preinitiation complex and promoter escape. *Mol. Cell* **54**: 601–12.

- Woodcock C. L., Ghosh R. P., 2010 Chromatin higher-order structure and dynamics. *Cold Spring Harb. Perspect. Biol.* **2**: a000596.
- Wu H., Zeng H., Lam R., Tempel W., Amaya M. F., Xu C., Dombrowski L., Qiu W., Wang Y., Min J., 2011 Structural and Histone Binding Ability Characterizations of Human PWWP Domains (P Kursula, Ed.). *PLoS One* **6**: e18919.
- Xue-Franzén Y., Johnsson A., Brodin D., Henriksson J., Bürglin T. R., Wright A. P. H., 2010 Genome-wide characterisation of the Gcn5 histone acetyltransferase in budding yeast during stress adaptation reveals evolutionarily conserved and diverged roles. *BMC Genomics* **11**: 200.
- Yang X.-J., 2015 MOZ and MORF acetyltransferases: Molecular interaction, animal development and human disease. *Biochim. Biophys. Acta - Mol. Cell Res.* **1853**: 1818–1826.
- Yen K., Vinayachandran V., Batta K., Koerber R. T., Pugh B. F., 2012 Genome-wide nucleosome specificity and directionality of chromatin remodelers. *Cell* **149**: 1461–73.
- Zdobnov E. M., Apweiler R., 2001 InterProScan--an integration platform for the signature-recognition methods in InterPro. *Bioinformatics* **17**: 847–8.
- Zeisig D. T., Bittner C. B., Zeisig B. B., García-Cuellar M.-P., Hess J. L., Slany R. K., 2005 The eleven-nineteen-leukemia protein ENL connects nuclear MLL fusion partners with chromatin. *Oncogene* **24**: 5525–32.
- Zeng L., Zhang Q., Li S., Plotnikov A. N., Walsh M. J., Zhou M.-M., 2010 Mechanism and regulation of acetylated histone binding by the tandem PHD finger of DPF3b. *Nature* **466**: 258–62.
- Zhang H., Richardson D. O., Roberts D. N., Utlely R., Erdjument-Bromage H., Tempst P., Côté J., Cairns B. R., 2004 The Yaf9 component of the SWR1 and NuA4 complexes is required for proper gene expression, histone H4 acetylation, and Htz1 replacement near telomeres. *Mol. Cell. Biol.* **24**: 9424–36.
- Zhang H., Roberts D. N., Cairns B. R., 2005 Genome-wide dynamics of Htz1, a histone H2A variant that poises repressed/basal promoters for activation through histone loss. *Cell* **123**: 219–31.
- Zhang W., Zhang J., Zhang X., Xu C., Tu X., 2011 Solution structure of the Taf14 YEATS domain and its roles in cell growth of *Saccharomyces cerevisiae*. *Biochem. J.* **436**: 83–90.
- Zhou Y. B., Gerchman S. E., Ramakrishnan V., Travers A., Muyldermans S., 1998 Position and orientation of the globular domain of linker histone H5 on the nucleosome. *Nature* **395**: 402–5.